University of Stavanger

Faculty of Science and Technology

MASTER'S THESIS

Study program: MSc in Petroleum Engineering Specialization: Reservoir Engineering	Spring semester, 2015 Open
Writer: Jaspreet Singh Sachdeva	…… (Writer's signature)

Faculty supervisor: Dimitrios Georgios Hatzignatiou

External supervisor(s):

Thesis title:
Evaluation of Silicate and Polymer Systems for Disproportionate Permeability Reduction in Oil Reservoirs

Credits (ECTS): 30

Key words: Water production Disproportionate Permeability Reduction Sodium silicate Potassium silicate Gelation time Associative polymers Polyacrylamides Crosslinkers Core Flooding	Pages: 159 Stavanger, June 15, 2015

ABSTRACT

The main objective of this work is to screen and evaluate various commercially existing polymers and silicate systems mixed with crosslinkers and/or activators for their gel-forming capabilities for the water management purposes in high water cut producing wells in the matured fields. A thorough evaluation has been done for these chemicals to evaluate their behaviour before, during and after gelation. The properties measured and monitored include gelant system's viscosity and pH, gelation time and kinetics of the gelation process, gel stability, gel strength from Maximum Compressional Pressure (MCP) tests, gel shrinkage and post-gelation time behaviour.

Traditional tube testing, also known as bottle testing, was done for the different polymer systems mixed with various crosslinkers wherein the mixtures were prepared and kept in the oven at temperatures of 40°C, 60°C and 80°C. Associative polymers were found to be very effective in forming gels with zirconium (III) crosslinker at high temperatures.

For the rheology measurements, dynamic oscillatory tests were performed for the different silicate systems mixed with activators to determine the onset of gelation (sol-gel transition point or gel point) and the viscosity increase as a function of time at different temperatures. Gel point plays an important role in the designing of successful water-shutoff treatments since it is needed to determine the time required for the injected gelant system to gel so that the time gap is sufficient for the successful placement of the prepared system. The effects of the different factors, such as silicate and activator concentrations, temperature, the concentration of divalent ions (Ca^{2+}) etc., are investigated. The sodium silicate system was found to gel faster at lower temperatures compared to the potassium silicate system while at high temperatures the potassium silicate system gels faster than the sodium silicate system. Therefore, an appropriate silicate system can be chosen for conformance-improvement treatment depending on the important parameters like gelation time required, time required to inject and place the gelant system at the designated areas, available activator systems, depth of the reservoir, reservoir temperatures and maximum injection rates that can be achieved without damaging the reservoir among other factors.

In addition to bulk measurements and dynamic oscillatory tests, one core flood experiment was performed with associative polymer on the water-wet Berea sandstone core to investigate the effect of Disproportionate Permeability Reduction (DPR). The Berea core has shown a significant drop in the effective permeability to water and potential DPR effects after polymer injection.

ACKNOWLEDGEMENT

I would like to express my gratitude to everyone who helped and encouraged me in various ways in carrying out my Master Thesis work. Their contributions are sincerely appreciated and gratefully acknowledged.

First and foremost, I would like to thank Dr. Dimitrios G. Hatzignatiou for his guidance, advice and suggestions throughout the term of my thesis work. Without his valuable support, always given generously and unstintingly, the completion of this work would have been immeasurably more difficult.

I am also indebted to the Department of Petroleum Engineering staff, University of Stavanger, and the employees at the International Research Institute of Stavanger (IRIS) for their support and cooperation during the course of my thesis.

I would like to give my special thanks to Mr. Reza Askarinezhad for his invaluable help in carrying out the experimental work and discussing the results. During the course of this work, the continuous help and indispensable suggestions provided by Mr. Arne Stavland and Mr. Nils Harald Giske are highly appreciated.

I would also like to express my sincere gratitude to my father Mr. Amarjeet Singh Sachdeva and my dear friend Ms. Inken Mays for proofreading my thesis.

I am very grateful to all my family members and friends for their unconditional love and support.

I once again thank everyone for their never ending support and encouragement which they have given me at various stages of the thesis work.

Jaspreet Singh Sachdeva

Stavanger, Norway
June 2015

TABLE OF CONTENTS

LIST OF FIGURES

LIST OF TABLES

1. INTRODUCTION

Water produced together with the hydrocarbons is an undesirable by-product. Besides formation water, the injected water for pressure maintenance or during water flooding also contributes to the water content of the total produced water at the surface. High water cut is a big problem in the matured oil and gas fields worldwide. Lifting, separation, processing and disposing off/re-injecting the unwanted water not only leads to an increase in the operational costs but also to major delays in the ongoing projects, which has a negative impact on the overall hydrocarbon production economics. The produced water after separation still contains small amounts of hydrocarbons, metals, sands and chemicals which can cause or accelerate corrosion if re-injected or be harmful to the environment if disposed off. Therefore, proper treatment is an obligatory step for the produced water before any further step can be taken to ensure that the safety regulations are conformed to. As per the recent statistical surveys, the oil companies are spending approximately $40 billion per year in dealing with unwanted water (Bailey et al., 2000). These costs include the expenses to lift and process the unwanted water on the surface, re-inject or dispose of the processed water, and the capital investment in the construction of surface facilities to handle the unwanted water (Bøye, Rygg, Jodal & Klungland, 2011).

Water production can be controlled by the use of either mechanical methods or chemical methods. The mechanical methods include use of packers, bridge plugs and cement to block water bearing channels and zones, and are effective near the wellbore. The chemical methods involve the injection of mixtures of certain chemicals as solutions into the formation which form gels at the reservoir conditions. These chemical systems can either be injected to near-well area to block the most water productive layers or for in-depth treatments to block high water permeability fractures/zones (Simjoo, Vafaie Sefti, Dadvand, Hasheminasab & Sajjadian, 2007). These gelling systems include silicate gels that are prepared by adding acidic activators to sodium or potassium silicate, and polymer gels prepared by crosslinking of polymers with chromium, zirconium or other organic crosslinkers. These mixtures are prepared on the surface in such a way that when they are pumped into the treatment wells, they will have sufficient time to reach the designated areas before they form a gel under reservoir conditions. This thesis work deals with both polymers and silicates.

The scope of this thesis is to evaluate the already commercially existing silicates and polymers for Disproportionate Permeability Reduction (DPR) / Relative Permeability Modification (RPM) effects which is a phenomenon whereby many water-soluble polymers and silicate gels reduce the permeability to water flow to a greater extent than to oil or gas. The selection of a proper gel technology depends highly on the mode of water entering into the wellbore and is vital for any successful DPR/RPM water-shutoff treatment. Two types of silicates, sodium silicate and potassium silicate, are available for evaluation with different

acid activator systems to get an estimate of their gel points, to evaluate their post-gelation behaviour, to investigate the effect of divalent ion concentration, temperature and activator concentration, and to derive a general equation for the gelation time calculations. Three polymers are evaluated with different crosslinkers to establish their gel-forming capabilities through bulk measurements followed by a core flooding experiment with the polymer found most suitable from the bulk measurement tests to investigate the single-phase DPR effect of polymer injection on porous media.

The thesis is divided into different sections. The second section includes the literature review about the water production problems and possible solutions from various available books and scientific papers followed by a review of the proper gel technology selection and the pitfalls and risks associated with their application in the field. The third section covers the description of silicates, polymers and crosslinkers that have been used in this work, followed by their advantages and disadvantages. It also covers the equipment and procedures that have been used for rheological measurements and bulk measurements. The fourth section deals with the experimental work performed on the silicates with the discussion of the results obtained. The experimental work performed on the polymers is discussed and deliberated in the fifth section and the sixth section deals with the discussion of the core flooding experiment performed. Lastly, in section 7, conclusions and recommendations for future work are presented.

2. LITERATURE REVIEW

A thorough review of the available books and scientific papers is presented in this section. First, the water production sources and possible solutions to handle excessive water production are presented. The next part deals with the concept of Disproportionate Permeability Reduction (DPR) and the question of where the DPR water-shutoff treatments can be applied. Lastly, a closer look to the gel technology selection is presented: how they should be used, benefits of a good-gel treatment, the risks associated with their application in the field, and the treatment elements for the successful execution of the gel-treatment in the field.

2.1. WATER PRODUCTION SOURCES

It is convenient to differentiate between produced water problems which occur during the primary and the secondary oil recovery (Usaitis, 2011, pp. 3-5). During the primary oil recovery, some of the typical sources of water are moving oil-water contact due to the replacement of produced oil by water from the underlying aquifer, coning in case of vertical wells and cusping in case of horizontal wells, and faults and fractures from water layer for vertical and horizontal wells. These problems are illustrated in figure 1.

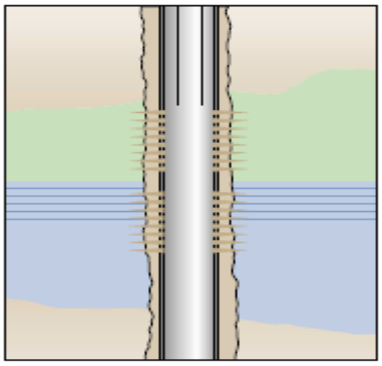

^ Moving oil-water contact.

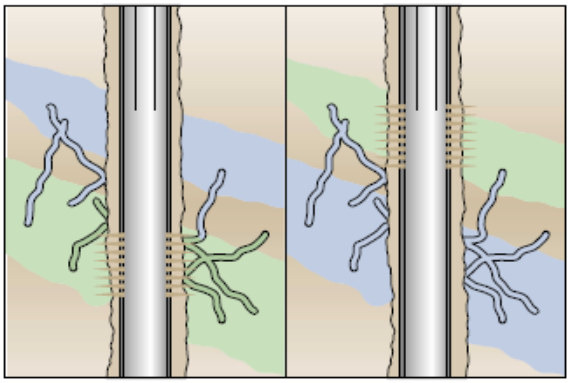

^ Fractures or faults from a water layer (vertical well).

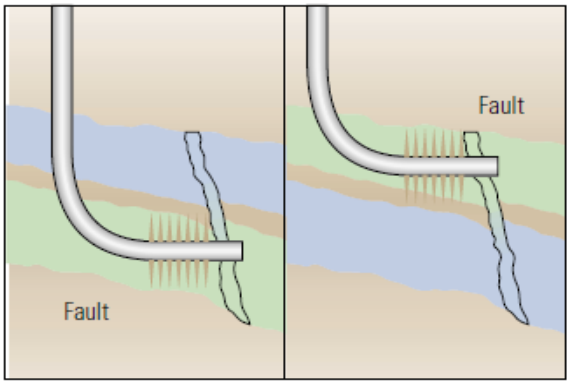

^ Fractures or faults from a water layer (horizontal well).

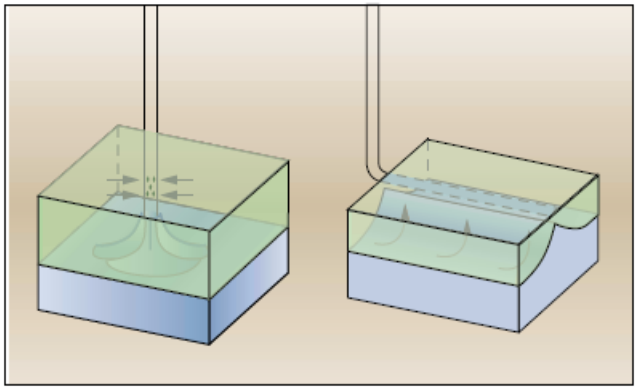

^ Coning or cusping.

Figure 1: Sources of water production during primary oil recovery (Bailey et al., 2000)

During the secondary oil recovery, some of the typical sources of water production are fractures or faults connecting an injector to a producer and gravity segregation taking place due to the larger density of the displacing fluid compared to the formation fluid during water flooding. These sources can be a cause of early water breakthrough from high permeability layers causing a higher water cut from the well. These problems are illustrated in figure 2.

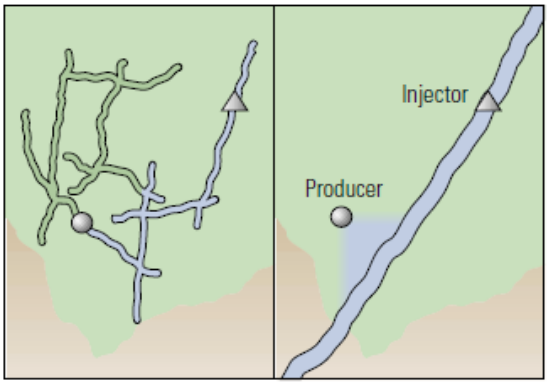

^ Fractures or faults between an injector and a producer.

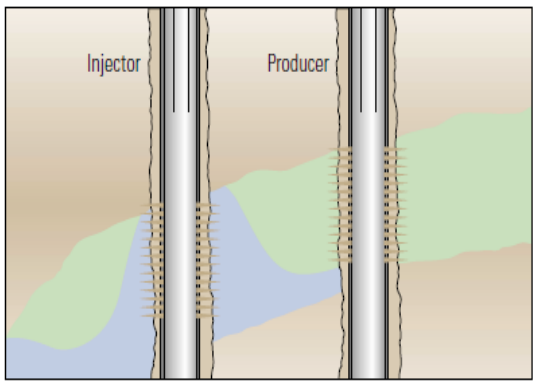

^ Gravity-segregated layer.

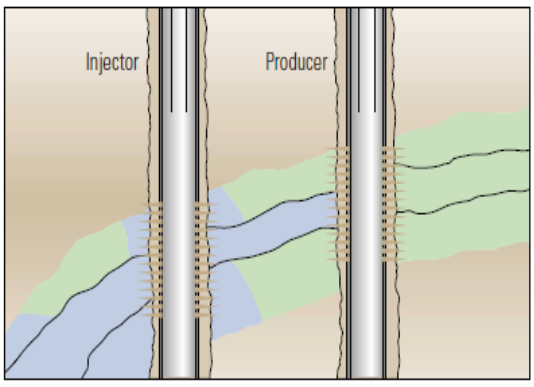

^ Watered-out layer with crossflow.

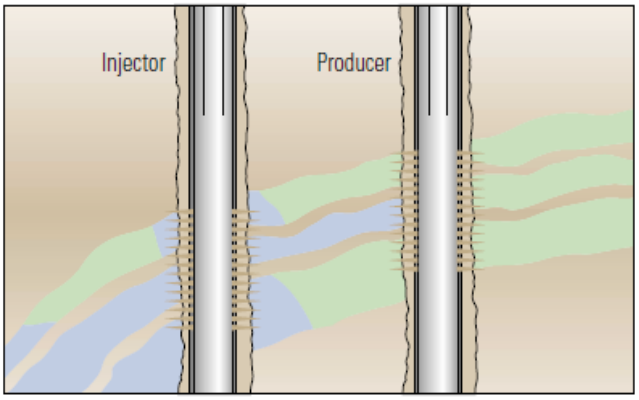

^ Watered-out layer without crossflow.

Figure 2: Sources of water production during secondary oil recovery (Bailey et al., 2000)

There can be some more reasons of unwanted water production which are depicted in figure 3. These additional failures occur close to the borehole due to a bad cementing job or mechanical failure of casing or packers.

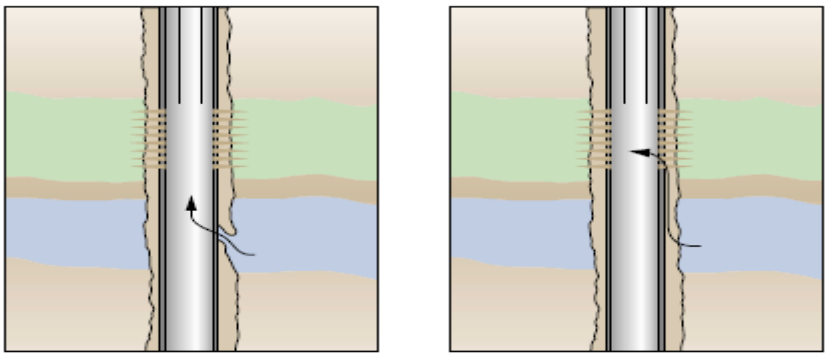

^ Casing, tubing or packer leaks.

^ Flow behind casing.

Figure 3: Sources of water production due to mechanical failures (Bailey et al., 2000)

2.2. WATER CONTROL SOLUTIONS

Several mechanical and chemical methods are available that can be applied to reduce the amount of unwanted water. These methods can be effectively applied as a means of both near-well and in-depth formation treatment techniques. For these techniques to be successfully implemented, the mechanisms causing excess water production must be thoroughly evaluated and proper treatment procedures must be designed (Hatzignatiou & Olsen, 1999; Bailey et al., 2000). If the different producing layers in a reservoir are not in communication with each other, then bridge plugs can be deployed to isolate the oil producing layers and water-shutoff treatment can be applied for the other layers from where water is being produced. This is an example of mechanical near-well treatment. However, if these layers are in communication with each other, then due to the cross-flow between these layers, the mechanical methods will not affect the fractional flow

(Skrettingland, Giske, Johnsen and Stavland, 2012). For such cases, the chemical methods are deployed. Chemical mixtures, designed in such a way that they form gel at designated places (such as high water permeability zones, thief zones, fractures etc.) at reservoir conditions, are injected into the formation. Subsequently, the injected water is forced to divert to the unswept zones in the reservoir yielding increased oil recovery.

After the source of excess water production has been identified, the proper treatment technique has to be designed. The treatment techniques can be assigned to three broad categories of water production:

1. Prevention of early water breakthrough
2. Reduction of excess water production
3. Isolation of water flow pathways/water-shutoff

2.2.1. PREVENTION OF EARLY WATER BREAKTHROUGH

From the start, solutions and techniques should be planned and designed in such a way that excess water production can be prevented in the first place. Such techniques include:

- Proper placement of production well
- Drilling horizontal wells into the reservoir zones to delay the onset of water coning
- Installation of intelligent well completions to effectively manage the oil and water production rates
- Injection of particular chemicals, like polymers, that can be injected with water during water flooding operations and increase the injected water viscosity to help prevent early water breakthrough

2.2.2. REDUCTION OF EXCESS WATER PRODUCTION

After the water breakthrough, the amount of water brought to surface with hydrocarbons keeps on increasing with time. This subsequently leads to increased production costs. It also leads to an increase in the environmental risks associated with the processing of the produced fluids on the surface. Several solutions and techniques are available that can be applied to reduce the excess water production. One of the most efficient techniques to reduce the water cut is to install a downhole oil-water separation system. This separation system can be installed in the wells with a high water cut to separate the oil and water phases. The separated water is then injected into another zone which has already been watered out or the zone from where there is no oil production (Bowers, Brownlee & Schrenkel, 1998). Techniques like Microbial Enhanced Oil Recovery (MEOR) also help to reduce the water cut and improve the volumetric sweep efficiency.

2.2.3. ISOLATION OF WATER FLOW PATHWAYS/WATER-SHUTOFF

This category mainly includes use of mechanical and chemical methods that can completely shut-off the water-bearing channels, zones and fractures in the reservoir and prevent water from entering the wellbore.

The mechanical methods include use of packers, bridge plugs and cement to block near-wellbore water bearing channels and zones. These methods can help in addressing issues like channelling behind casing, rising of bottom water, casing leaks, watered-out layers in a reservoir with no cross-flow between different layers etc. (Bedaiwi, Al-Anazi & Paiaman, 2009).

The chemical methods help in addressing the water issues at the formation depths away from the wellbore. The chemical systems are injected as solutions into the formation and gels are formed at the reservoir conditions. These gels are designed in such a way that they allow enough time to inject the solutions to be injected and placed at the designated areas inside the reservoir, and also that they are strong enough to withstand the applied pressure during the hydrocarbon production. They should also be capable of handling the rigidness for long periods of time, wide range of formation temperatures and different values of salinity and pH. The resulting profile modification diverts the injected water to the unswept reservoir zones and hence, improves the fluid distribution in heterogeneous reservoirs leading to an increase in the overall oil recovery. These chemical systems can either be injected to near-well area to block the most water productive layers or for in-depth treatments to block high water permeability fractures/zones (Simjoo et al., 2007).

There are various advantages of using chemical methods over mechanical methods. These include their flexibility for pumping without a workover rig, ease of cleaning, higher control of setting time, lack of milling time, easy removal from wellbore by water re-circulation, deeper placement of gels in the formation etc. (Perez, Fragachan, Ramirez & Ferraud, 2001).

2.3. LIST OF WATER PRODUCTION PROBLEMS AND TREATMENT CATEGORIES

Seright et al. (2001) proposed a strategy for the use of polymer-gel treatments to solve excess water-production problems. As per this strategy, the easiest water production problem remedies are to be applied first, meaning that the conventional methods for water-shutoff, such as cement or mechanical devices, should be used first, wherever applicable.

Table 1 provides a general ranking of water-production problems and treatment categories in order of increasing difficulty of treatment (Seright et al., 2001).

Treatment category	Problems
Category A: Conventional treatments as an effective choice	1. Casing leaks without flow restrictions (apertures greater than 1/16 in.) 2. Flow behind pipe without flow restrictions (apertures greater than 1/16 in.) 3. Unfractured wells with no crossflow between layers
Category B: Gelant treatments as an effective choice	1. Casing leaks with flow restrictions (apertures less than 1/16 in.) 2. Flow behind pipe with flow restrictions (apertures less than 1/16 in.) 3. 2D coning through a hydraulic fracture from an aquifer
Category C: Pre-formed or partially formed gels as an effective choice	1. Natural fracture system in communication with an aquifer 2. Faults or fractures crossing a deviated or horizontal well 3. Single fracture causing channelling between wells 4. Natural fracture system allowing channelling between wells
Category D: Difficult problems, gel treatments not used	1. 3D matrix rock coning 2. Cusping 3. Channelling through strata (no fractures) with crossflow

Table 1: Excess water production problems and treatment categories

This work deals with treatment category B wherein the gelant treatments are considered to be an effective choice. The designing of a good gelant system which can reduce the relative permeability to water and hence reduce the amount of unwanted water production has been the demand of the industry in recent times. The techniques to be used for remediation purposes depend highly on the method of entry of water into the wellbore. The treatment options include sealant treatments and relative permeability modifiers (also referred to as the disproportionate permeability modifiers) (Reddy et al., 2003).

Among the various already existing sealant systems and disproportionate permeability modifiers, silicate gel systems and polymer systems are known to be effective for water control and are environment-friendly. Silicate gel systems are prepared by adding acidic activators to liquid silica, and polymer systems are prepared by adding the polymer to water, followed by a crosslinker to form a three-dimensional cross-linked polymer network known as gel. These mixtures are prepared on the surface in such a way that when they are pumped into the treatment wells, they will have sufficient time to reach the designated areas before they form a gel under reservoir conditions.

2.4. DISPROPORTIONATE PERMEABILITY REDUCTION (DPR)

Disproportionate permeability reduction (DPR) is a phenomenon whereby many water-soluble polymers and aqueous polymer gels reduce the permeability to water flow to a greater extent than to oil or gas. DPR is also referred to as relative permeability modification (RPM). DPR is a term used only when the gel water-shutoff treatments are applied to production wells (White, Goddard & Phillips, 1973; Sparlin, 1976; Weaver, 1978; VanLandingham, 1979; Dunlap, Boles & Novotny, 1986; Sydansk & Seright, 2006). The ability of acrylamide polymers to impart DPR to water flow in porous media was recognised as early as 1964 by Sandiford and 1973 by White et al.

The bullheadable RPM/DPR water-shutoff treatments are considered to be very attractive for the petroleum industry because they normally do not require the use of mechanical zone isolation during treatment-fluid placement, which saves the requirement of expensive workover operations. In addition, the use of mechanical zone isolation is also not feasible when the well possesses a slotted liner or gravel-pack completion or when the well involves a sub-sea tieback flow line. Therefore, during the past few decades, the industry is trying to make the best use of RPM/DPR water-shutoff treatments (Seright, 2001; Sydansk & Seright, 2006).

As stated by Sydansk & Seright (2006), there will always be a reduction in the oil permeability in the volume of matrix reservoir rock where the treatment has been employed, and a reduction in the post-treatment oil production rate. Therefore, it is not possible to apply an ideal RPM/DPR water-shutoff treatment. A successful application of RPM/DPR water-shutoff treatment means a treatment which reduces the oil production by only 5%, but reduces the water production by 90%.

RPM/DPR water-shutoff treatment schemes can be successfully applied for water-shutoff/reduction treatments only when the following conditions are met (White et al., 1973; Sparlin, 1976; Weaver, 1978; VanLandingham, 1979; Dunlap et al., 1986; Sydansk & Seright, 2006):

- A conformance problem in a matrix rock reservoir involving differing geological strata
- No fluid crossflow within the reservoir between the water and the oil or gas producing geological strata
- The water-producing zone is producing at an undesirably high water cut, and the oil or gas-producing strata will produce for the economic life of the water-shutoff treatment at 100% oil or gas cut.
- DPR treatment inducing an increase in the drawdown pressure on the producing interval

As shown in figure 4, RPM/DPR water-shut off treatments will be successful in the reservoirs with no fluid crossflow between the water and dry-oil producing strata because no water-block problem forms in the oil-producing zone (Zaitoun, Kohler, Bossie-Codreanu & Denys, 1999; Mennella, Chiappa, Lockhart & Burrafato, 2001; Botermans, Van Batenburg & Bruining, 2001; Kalfayan & Dawson, 2004; Sydansk & Seright, 2006). To maintain this favourable result, the oil producing zone must continue to produce dry oil for the economic life of the treatment.

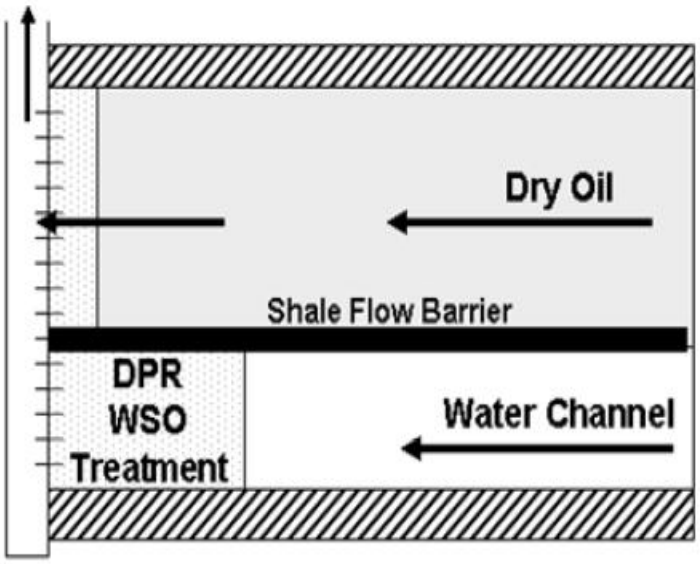

Figure 4: DPR water-shutoff treatment applied to a reservoir having a water and a dry-oil producing strata with no crossflow (Sydansk & Seright, 2006)

An example of how relative permeability curves may look after the RPM/DPR water-shutoff treatment with polymer gel is given in figure 5.

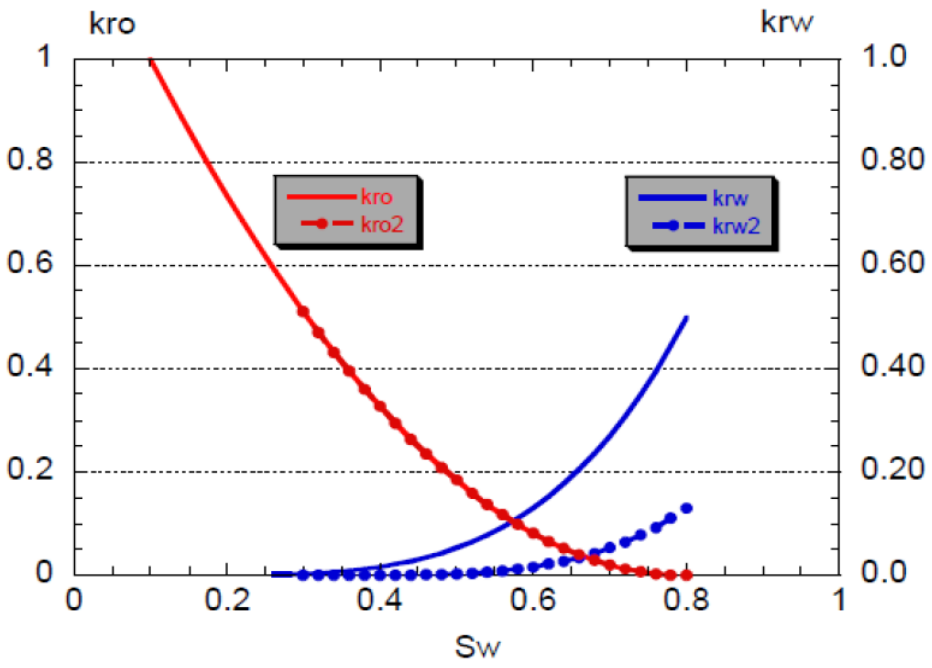

Figure 5: Relative permeabilities before and after DPR gel treatment (Stavland & Nilsson, 2001)

In this figure, k_{ro} and k_{rw} represent the relative permeabilities to oil and water respectively before the gel treatment, and k_{ro2} and k_{rw2} represent the relative permeabilities to oil and water respectively after the formation of gel. This figure depicts a successful RPM/DPR water-shutoff treatment with polymer gel. The effective permeability to water has reduced from 0.5 to 0.15 after gel treatment and there has been no effect on the effective permeability to oil after gel treatment.

2.5. GEL TECHNOLOGY SELECTION

A prerequisite for selecting the appropriate gel technology for conformance-improvement treatments is to eliminate all the gel technologies that are prohibited by the locally applicable safety and environmental regulations ("Conformance Improvement Gel Treatment Design", 2015).

The first step in the designing of a gel treatment is to correctly identify the nature of the conformance problem that needs to be treated. A conformance problem can typically be of two types: a matrix-rock problem or a high permeability fracture problem. For treating a matrix-type problem, it needs to be evaluated whether it is to be treated near to wellbore or deep in the reservoir. The strength of the gel required and the gelation time required at the reservoir temperature needs to be established. Sometimes a computer thermal simulation work may be needed to establish the thermal history for the gelant.

When treating a high permeability conformance problem, a gel treatment fluid that can be injected in a mature or partially mature state is selected and for the matrix-rock conformance problems, a gel treatment that can be injected in the gelant state is selected.

Then an initial selection of gel technologies is performed to rule out the technologies which do not fit the criteria described above. If economically justified, comparative laboratory studies may be performed on the selected ones to select the one which will be most effective in treating the conformance problem, otherwise the gel technology which seems to be the most effective and which meets the specialised needs of the operator who is applying the gel treatment is selected.

2.6. INJECTION RATE

Injection rate plays an important role during the gel placement. While treating a fracture conformance problem, it is desirable to inject the polymer gel as rapidly as possible, as it undergo gel dehydration during placement if the gel is to be placed deep into the fracture without exceeding the parting or fracture pressure. In case the strength of the gel formed is the main objective, then the gel should be injected as slowly as possible (Lane & Seright, 2000; "Conformance Improvement Gel Treatment Design", 2015).

Maximising the injection rate helps reduce the pumping time and costs. It also maximises the amount of gel that can be injected within the gelation-onset-time constraint. If while pumping the gel high or rapidly increasing injection pressures are encountered, the best options are to either stop the gel injection and clear the injection tubulars with water or reduce the chemical loading in the injected gel (Lane & Seright, 2000; "Conformance Improvement Gel Treatment Design", 2015).

2.7. OVERDISPLACEMENT

The choice and the volume, to be injected, of the overdisplacement fluid following gel injection is a crucial element of the treatment design and can have a major effect on the treatment performance ("Conformance Improvement Gel Treatment Design", 2015). The three basic varieties of overdisplacement fluids commonly used are:

1. Water or brine (usually injection water or produced water)
2. Polymer solution (often the polymer solution of the gel without the addition of the crosslinking agent)
3. Liquid hydrocarbon (reservoir crude oil)

Liquid hydrocarbon has been advocated as a means to establish favourable relative permeability to oil flow in the near-wellbore environment for water-shutoff gel treatments. Its pros and cons have been found to be reservoir specific, but it is relatively more advantageous when treating matrix-rock problems. Sometimes, the polymer solutions are

preferred over the other two as an overdisplacement fluid because of its high viscosity. The viscous polymer solution helps to mitigate the problem of fingering into the gelant system, in the wellbore and near-wellbore environment, which may be caused if the less viscous brine is used as an overdisplacement fluid.

2.8. SHUT-IN TIME

The time for which the well has to be shut-in after the placement of the gel depends on the time the gelant will take to reach its near-full gel strength under reservoir conditions. Post-treatment shut-in of wells is mandatory in almost all of the gel treatments applied to the production wells in matrix rock reservoirs ("Conformance Improvement Gel Treatment Design", 2015).

2.9. OPENING THE WELL AFTER THE SHUT-IN TIME

The manner in which the well is brought back to production after the shut-in time post-treatment can have a major impact on the success of the gel treatment. It is generally recommended to slowly return the treated production well to full production over a period of a couple of days ("Conformance Improvement Gel Treatment Design", 2015).

2.10. BENEFITS OF USING A GOOD GEL-TREATMENT

The following benefits can be achieved from a good gel-treatment on a production well (Sydansk & Southwell, 2000; Seright, Lane & Sydansk, 2001):

- Generate incremental oil production through conformance improvement, hence leading to increased recovery factor.
- Reduce the undesirable water production, leading to less environmental risks associated with processing of the unwanted water.
- Reduce the undesirable gas production, leading to less environmental risks associated with flaring off the gas.
- Extend the economic lives of marginal wells and oil fields.
- Reduce the overall operating expenditures, leading to better economics.
- Reduce certain environmental liabilities by reducing the amount of excessive unnecessary production of unwanted environmental unfriendly fluids.

2.11. PROPERTIES OF AN IDEAL GEL SYSTEM

An ideal conformance improvement gel technology should be (Sydansk & Southwell, 2000; Seright et al., 2001):

- Insensitive to oilfield and reservoir environments and chemical interferences (especially H_2S and CO_2)
- Insensitive to all reservoir minerals and fluids
- Stable in the long term
- Able to form rigid gels
- Applicable over a broad range of pH values
- Applicable over a broad range of reservoir temperatures
- Able to provide controllable and predictable gelation onset times.
- Involve a simple and straightforward gel-forming chemical system.

2.12. CANDIDATE SELECTION

Good well candidates for the application of gel conformance-improvement treatments have the following attributes ("Conformance Improvement Gel Treatment Design", 2015):

1. Injection wells:

- Substantial mobile oil saturation within the well pattern
- Unexpectedly low oil recovery within the well pattern
- Early injectant breakthrough

2. Production wells:

- High water/oil ratio (WOR) or gas/oil ratio (GOR)
- Excessive production of water or gas along with the hydrocarbons.
- Substantial mobile oil saturation within the well pattern
- Unexpectedly low oil recovery within the well pattern
- Early water or gas breakthrough
- Good geological position of the wells

2.13. QUALITY CONTROL

Quality control is of vital importance when it comes to the success of a conformance-improvement gel treatment and the degree of benefits derived from those treatments ("Conformance Improvement Gel Treatment Design", 2015). The quality control programme includes:

- Ensuring that the proper chemicals are being used in the actual gel formula of the treatment
- Ensuring complete and proper mixing of the gel chemicals before injection
- Ensuring that the gelant solution can be injected easily into the matrix reservoir rock without causing any plugging problems.
- Taking gelant samples at the wellhead during the pumping of the gelant.

2.14. PITFALLS AND RISKS

Common pitfalls and risks associated with a water-shutoff treatment with a polymer gel include ("Conformance Improvement Gel Treatment Design", 2015):

- Improper quality control
- Using too small amounts of gel-treatment volumes
- Improper diagnosis of the conformance problem
- Applying a gel treatment designed for matrix rock application to a high permeability anomaly conformance problem
- Incomplete understanding of how microgels function
- Incomplete dissolution/mixing of the chemicals before gelant's injection.
- Gel formed being thermally unstable at the reservoir conditions
- Poor well candidate or well pattern selection
- Poor designing and/or execution of the gel treatment
- Failure to selectively place the gel in only the high-permeability geological strata for a vertical conformance problem in a radial-flow matrix rock reservoir.

An improperly designed or executed gel conformance improvement treatment can lead to ("Conformance Improvement Gel Treatment Design", 2015):

- Reduction of oil and/or gas production rate(s)
- Reduction in the ultimate recovery of oil and/or gas from the treated well or well pattern
- Operational problems in the injection or production wells
- Excessive back production of the injected gel due to poor designing of the gel treatment

2.15. SUCCESSFUL EXECUTION OF GEL TREATMENTS

A successful execution of gel treatment requires that all the following five treatment elements are successfully implemented because otherwise there is a high risk of failure ("Conformance Improvement Gel Treatment Design", 2015):

1. Identification of conformance problem
2. Selection of proper and effective gel system
3. Proper design and size of the gel treatment
4. Proper application and placement of gelant solution
5. Proper functioning of gel after pumping it downhole

3. THEORETICAL BACKGROUND

This section is divided into three parts. The first part deals with the silicate systems: their chemistry, advantages and disadvantages, and definitions of some terms linked to the rheological measurements of the silicates. In the second part, the polymers and the crosslinkers considered in this work are described with the advantages and disadvantages of using polymer gels for water-shutoff purposes. Finally, in the last part, the equipment and procedures used for the rheological measurements and the bulk measurements are presented.

3.1. SILICATE SYSTEMS

3.1.1. CHEMISTRY OF SILICATES

The chemistry of commercially available water-soluble silicates is complex.

Sodium silicate is manufactured by heating silica and sodium carbonate to temperatures above 1300°C to form a water-soluble glass. According to Iler (1979), the following reactions are involved in the manufacturing of sodium silicate:

$$3SiO_2 + Na_2SO_4 + \frac{1}{2}C \rightarrow \frac{1}{2}CO_2 + SO_2 + 3SiO_2.Na_2O$$

$$3SiO_2 + Na_2CO_3 \rightarrow CO_2 + 3SiO_2.Na_2O$$

When this sodium silicate is dissolved in water, different silicate species tend to dominate at different pH values. The equilibrium equations, as given by Iler (1979) are given below:

$$SiO_2 + H_2O \rightarrow Si(OH)_4$$

$$Si(OH)_4 + OH^- \rightarrow HSiO_3^- + 2H_2O$$

$$2HSiO_3^- \rightarrow Si_2O_5^{2-} + H_2O$$

$$Si_2O_5^{2-} + H_2O \rightarrow HSi_2O_6^{3-} + H^+$$

$$HSiO_3^- + OH^- \rightarrow SiO_3^{2-} + H_2O$$

Potassium silicate, on the other hand, is synthesised by dissolving a reactive silica source (mainly silica sand) in the alkaline potassium hydroxide solution at elevated temperatures according to the equation ("Sodium and Potassium Silicates", 2004):

$$2KOH + nSiO_2 \rightarrow K_2O.nSiO_2 + H_2O$$

Generally silicates are identified by $SiO_2:M_2O$ *(M = Na, K)* ratio defined by n, which is also referred to as the molar ratio. The higher the value of n, the lower is the alkalinity and hence the lower is the pH value and vice versa. Also, for both silicate systems, the viscosity of solutions is affected by molar ratio, temperature and concentration. The only significant difference, however, is that potassium silicate solutions are somewhat more viscous than corresponding sodium silicate solutions at equal concentrations ("Sodium and Potassium Silicates", 2004).

3.1.2. GEL FORMATION

The polymerisation, and thus the gel formation, occurs when the pH is reduced below 11 by the addition of some kind of activator, mainly an acid which is one of the simplest methods to control the pH. The minimum gelation time is found just below the neutral pH (Stavland, Jonsbråten, Vikane, Skrettingland & Fischer, 2011).

The different steps of polymerisation from monomer to large particles and finally a gel were described by Iler (1979) and are illustrated in figure 6.

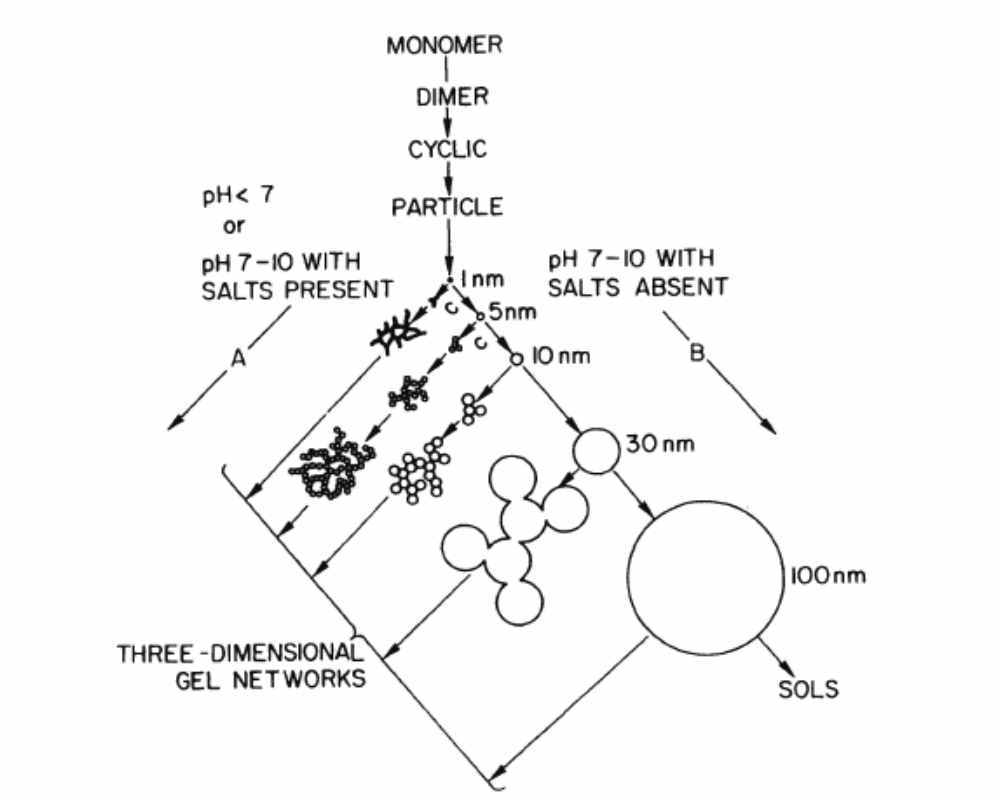

Figure 6: Systematic illustration of polymerization of silica (Iler, 1979)

The figure above shows the following steps in the development of gel (Iler, 1979):

1. Polymerization of monomer to form particles
2. Growth of particles
3. Linking of particles together into branched chains, then networks, finally extending throughout the liquid medium, thickening it to form a gel.

There are several factors that affect the rate and extent of polymerization for the silicate systems. These have been outlined in table 2.

S.No.	Factor	Effect on rate and/or extent of polymerization
1.	pH	Degree of polymerization is higher in the pH range 5-8
2.	Temperature	Higher temperature accelerates the polymerization process
3.	Molar ratio	Higher molar ratio results in greater degree of polymerization
4.	Salinity	Presence of salts accelerates the polymerization process
5.	Dilution rate	At a constant pH, dilution de-polymerizes silica and the polymerization process occurs slowly

Table 2: Effect of various factors on rate and extent of polymerization for the silicate systems

Jurinak and Summers (1991) found that the gelation time of silicate as a function of temperature and at a fixed pH and salinity follows the Arrhenius equation:

$$t_g = Ae^{E_a/RT} \quad \text{..... (1)}$$

where Ea is the activation energy, R is the gas constant, T is the absolute temperature and A is the pre-exponential factor. According to this equation, the polymerization rate increases as the temperature increases, hence the gelation time decreases.

Addition of salt to an alkaline solution results in charge screening, which decreases gelation time but the main factor that controls the rate and extent of polymerization is the pH of the solution. This relationship is different in different pH intervals and is presented in table 3.

pH interval	Effect on gelation time	Reason
11 - 14	Does not gel	Solution is stable
5.5 - 11	Decrease in gelation time	Reduction in negative charge
2 - 5.5	Increase in gelation time	Catalysed by OH^-
0 - 2	Decrease in gelation time	Catalysed by F^- from metal ions

Table 3: Stability of silicate species in solution when the pH is reduced (Usaitis, 2011, p. 21)

3.1.3. ADVANTAGES AND DISADVANTAGES OF SILICATE SYSTEMS

3.1.3.1. ADVANTAGES OF SILICATE SYSTEMS (Lakatos et al., 1999; Hatzignatiou, Askarinezhad, Giske & Stavland, 2015):

- Environment-friendly
- Low cost compared to polymers
- Properties dependent on SiO_2:Na_2O molar ratio
- Treatment fluid solution has water-like viscosity
- Less severe corrosion problems
- Easy gel breaking in case of technical failures
- Simple and cost-effective surface technology
- Excellent thermal stability
- Short to moderate pumping times

3.1.3.2. DISADVANTAGES OF SILICATE SYSTEMS (Lakatos et al., 1999)

- Formed gel is rigid and prone to fracture
- Gel shows syneresis and hence causes reduction in blocking efficiency
- Gelation mechanism is hard to control
- Precipitation of water-insoluble salts in contact with formation water

3.1.4. DEFINITION OF IMPORTANT TERMS

3.1.4.1. STORAGE MODULUS (G') (pronounced as "G-prime") - Unit: Pa

G' represents the elastic behaviour of a material. It is a measure of the deformation energy stored by the sample during the shear process. After the load is removed, this energy is completely available and acts as the driving force for the reformation process which will compensate partially or completely the previously obtained deformation of the structure (Meyers & Chawla, 1998; Mezger, 2011). The value of storage modulus G' is given by:

$$G' = \frac{\sigma_o}{\varepsilon_o} \cos \delta \qquad \text{..... (2)}$$

where

σ_o = value of stress in the material at the starting of the application of load on the material

ε_o = corresponding value of strain observed in the material at the starting of application of load on the material

δ = phase angle between stress and strain

3.1.4.2. LOSS MODULUS (G'') (pronounced as "G-double-prime") - Unit: Pa

G'' represents the viscous behaviour of a material. It is a measure of the deformation energy used by the sample during the shear process and therefore afterwards, it is lost for the sample. This energy is spent during the process of changing the material's structure, i.e. when the sample is flowing partially or altogether. Due to the relative motion between the molecules of the material, frictional heat occurs. This process is also called "viscous heating". Energy is consumed during this friction process. A part of this energy may heat up the sample, and another part may be lost in the form of heat to the surrounding environment. Energy losing materials are showing irreversible deformation behaviour since after a load cycle, they occur with a changed shape (Meyers & Chawla, 1998; Mezger, 2011). The value of loss modulus G'' is given by:

$$G'' = \frac{\sigma_o}{\varepsilon_o} \sin \delta$$

..... (3)

where the symbols σ_o, ε_o and δ denotes the same as described above.

3.1.4.3. PHASE ANGLE

The ratio of loss modulus to storage modulus (G''/G') is known as the loss factor or the damping factor. The loss factor is calculated as the quotient of the lost and the stored deformation energy. It therefore reveals the ratio of the viscous and the elastic portion of the visco-elastic deformation behaviour (Meyers & Chawla, 1998; Mezger, 2011). The phase angle is given by:

$$\delta = arctan \frac{G''}{G'}$$

..... (4)

For ideally elastic behaviour: $\delta = 0°$, for ideally viscous behaviour: $\delta = 90°$, and for visco-elastic behaviour: $0° < \delta < 90°$. Therefore:

$$0 \leq \tan \delta \leq \infty$$

Ideally elastic behaviour can be expressed as $\delta = 0°$ or $\tan \delta = 0$. Here, G' completely dominates G''. Ideally viscous behaviour can be expressed as $\delta = 90°$ or $\tan \delta = \infty$. Here, G'' completely dominates G'. If viscous and elastic behaviour are exactly balanced, i.e. G' = G'', then $\delta = 45°$ or $\tan \delta = 1$.

3.1.4.4. GEL POINT

Gel point is also known as the sol-gel transition point. It is the point at which the gel starts to form. This point is reached when the value of $\tan\delta$ becomes equal to 1 (Meyers & Chawla, 1998; Mezger, 2011).

Hence:

For the fluid or liquid state (sol state): $\tan\delta > 1\ (since\ G'' > G')$

For the gel-like state (solid state): $\tan\delta < 1\ (since\ G' > G'')$

At the gel point: $\tan\delta = 1\ (since\ G^{'} = G'')$

3.2. POLYMER GELS

The different polymers and crosslinkers used in this work followed by the concept of gel syneresis and gel codes are described in this section.

3.2.1. DESCRIPTION OF POLYMERS

Three different polymers used in this work are described below.

3.2.1.1. HPAM (ANIONIC HYDROLYSED POLYACRYLAMIDE) POLYMERS

This is the most widely employed water-soluble polymer for conformance polymer-gel treatments. HPAM tends to adsorb less on the rock surfaces compared to the unhydrolysed polyacrylamides. For use in crosslinked polymer-gel treatments, the optimum level of hydrolysis is in the range of 5 to 10 mol percent because gel strength is maximised and unproductive intra-molecular crosslinking is minimised (Sydansk & Romero-Zeron, 2011, p. 60).

3.2.1.2. AMPS (ACRYLAMIDO-METHYL-PROPANE SULFONATE) POLYMERS

They are a type of hydrolysed polyacrylamide polymers whose performance and stability properties are better for polymer flooding and polymer injection at high temperatures (≥200°F) and in high-salinity reservoirs (Sydansk & Romero-Zeron, 2011, p. 61).

3.2.1.3. HYDROPHOBICALLY ASSOCIATIVE POLYMERS

Associative polymers are different from the classical water-soluble polymers in the sense that the amount of hydrophobic monomers capable of creating physical associations with each other is low (Sydansk & Romero-Zeron, 2011, p. 61). Even though they have high molecular weights, still they rely a lot on hydrophobic interactions between different polymer chains for the viscosity effects, and they exhibit very high viscosities at low shear rates. In aqueous solution, the hydrophobic groups interact and form an intermolecular polymer network. If a screenshot of the structure of this polymer network is taken at any

given time, it shows a gel-like network (showing visco-elastic properties) but over time, flow does occur because the Brownian motion breaks the end-group associations for very small periods of time before one end-group forms another association with a similar group on the same chain or the adjacent chain (visualised in figure 7 below). Due to the formation of these complex polymer networks, the viscosities become significantly larger than the one of independent, individual polymer chains, which offers a lot of advantages when it comes to polymer injection into the porous media (Reichenbach-Klinke, Stavland, Langlotz, Wenzke & Brodt, 2013; Reichenbach-Klinke, Stavland, Zimmermann, Bittner & Brodt, 2015). Moreover, low concentration of this polymer is required to achieve a given mobility ratio, which also makes them an attractive option for polymer flooding. These polymers have never been tested for conformance control treatments, but the laboratory results show that with some particular crosslinkers, they can be used for selective water-shutoff applications. More detailed studies are required to affirm this theory. Figure 7 shows the interactions between hydrophobic groups in associative polymers.

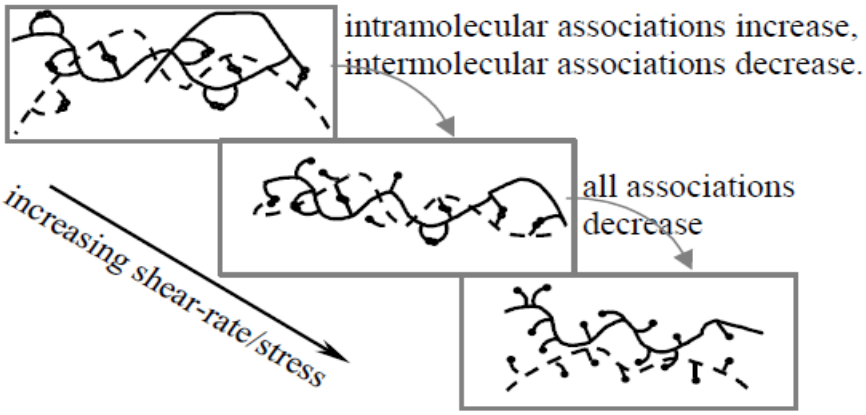

Figure 7: Interactions between hydrophobic groups in associative polymers (Barnes, 2000, p. 147)

3.2.2. PHYSICAL AND CHEMICAL PROPERTIES OF CROSSLINKERS

3.2.2.1. POLYETHYLENIMINE SOLUTION - LINEAR PEI ("Poly(ethyleneimine) solution", 2013)

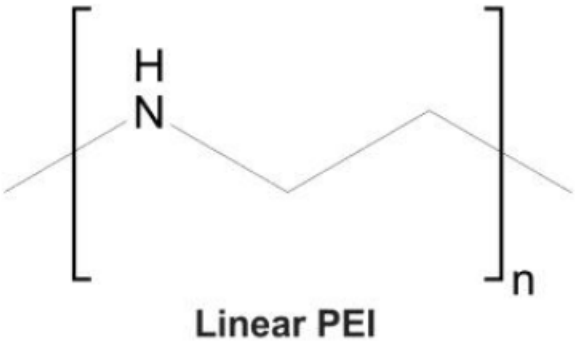

Figure 8: Chemical structure of linear polyethylenimine (PEI) (Kafil & Omidi, 2011)

a)	Appearance	Form: liquid
b)	Relative molecular mass	600,000-1,000,000
c)	Concentration	~50% in H_2O
d)	Density ("Polyethylenimine", 2008)	1.08 g/ml at 25°C
e)	Vapour pressure ("Polyethylenimine", 2008)	9mm Hg at 20°C
f)	Chemical stability	Stable under recommended storage conditions
g)	Incompatible materials	Strong oxidising agents
h)	Adverse effects	Toxic to aquatic life with long lasting effects

3.2.2.2. POLYETHYLENIMINE SOLUTION - BRANCHED PEI **("Polyethylenimine, ethylenediamine branched", 2014)**

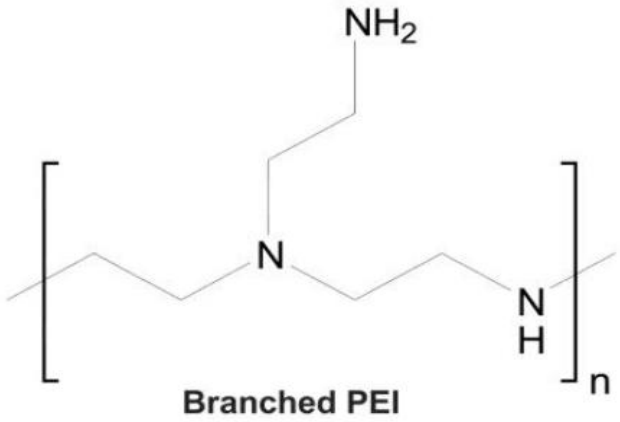

Figure 9: Chemical structure of branched polyethylenimine (PEI) (Kafil & Omidi, 2011)

a)	Appearance	Form: clear, liquid, light yellow in colour
b)	Molecular weight	(i) Weight average molecular weight (M_w) of ~800 by Light Scattering (LS) method (ii) Number average molecular weight (M_n) of ~600 by Gas Permeation Chromatography (GPC) method
c)	Density	1.05 g/cm^3 at 25°C
d)	Vapor pressure ("Polyethylenimine", 2008)	9mm Hg at 20°C
e)	Refractive index ("Polyethylenimine", 2008)	*n*20/D 1.5240
f)	pH	ca. 11 at 10 g/l
g)	Melting point/freezing point	Setting point: -19.99°C
h)	Water solubility	Soluble
i)	Chemical stability	Stable under recommended storage conditions

j)	Incompatible materials	Strong oxidising agents
k)	Adverse effects	Harmful to aquatic life with long lasting effects

3.2.2.3. CHITOSAN (FROM SHRIMP SHELLS) ("Chitosan", 2012)

Chitosan is a polysaccharide obtained by de-acetylating chitin, a homopolymer containing β-(1-4)-2-acetamido-2-deoxy-D-glucose that occurs in the shell of anthropods or crustaceous water animals (Reddy et al., 2003).

Synonyms: Poly(D-glucosamine)
Deacetylated chitin

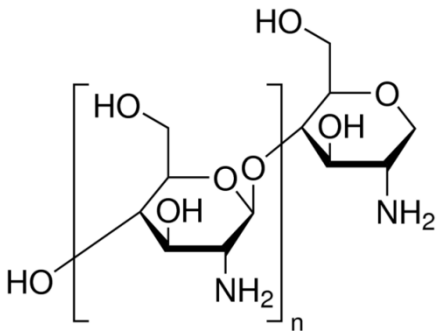

Figure 10: Chitosan (from shrimp shells)

a)	Appearance	Form: powder, yellow in colour
b)	Biological source	from shrimp shells
c)	Viscosity	>200 cP, 1.5 wt% in 1% acetic acid (20 °C)
d)	Incompatible materials	Strong oxidising agents
e)	Effects on the health	May be harmful if inhaled, swallowed or absorbed through skin

3.2.2.4. CHROMIUM (III) ACETATE HYDROXIDE ("Chromium (III) Acetate Hydroxide", 2014)

$$(CH_3CO_2)_7Cr_3(OH)_2$$

Figure 11: Linear Formula for Chromium (III) Acetate Hydroxide

a)	Appearance	Form: powder, green in colour
b)	Molecular weight	603.31 g/mol
c)	Percentage chromium	23.0-25.0 % (titration by $Na_2S_2O_3$)
d)	Melting point/freezing point	>400°C at ca. 1.013 hPa
e)	Flammability	not auto-flammable
f)	Relative density	1.56 g/cm^3 at 22.95°C
g)	Water solubility	675 g/l at 20°C
h)	Partition coefficient: n-octanol/water	log Pow: 0.2 at 22°C

i)	Chemical stability	Stable under recommended storage conditions
j)	Incompatible materials	Strong oxidising agents

3.2.3. ADVANTAGES AND DISADVANTAGES OF POLYMER GEL SYSTEMS

3.2.3.1. ADVANTAGES OF POLYMER GEL SYSTEMS

- Better control over the mechanics of gel formation
- Less severe corrosion problems
- Easy gel breaking in case of technical failures
- Simple and cost-effective surface technology
- Easier control of the injected fluids
- Short to moderate pumping times
- Easier control of the gelation times
- Provides sufficient gel strength for resisting drawdown pressure inside the wellbore and stopping water flow

3.2.3.2. DISADVANTAGES OF POLYMER GEL SYSTEMS

- Highly expensive compared to silicates
- Viscosities of the treatment fluid solutions are higher than the silicates
- Gel shows syneresis and hence causes reduction in blocking efficiency
- Formed gel is rigid and prone to fracture

3.2.4. GEL CODES

The gel formation process occurs in various steps. These steps are denoted by gel codes. Various gel code notations are available in the literature but in this work, the gel codes introduced by Stavland et al. (2011) have been used. This gel code notation is based on the visual inspection of the gelling fluid through a transparent test tube at short intervals of time. The gel codes are described in table 4.

Gel Code	Description
0	Clear and low viscous fluid
1	Cloudy and low viscous fluid
2	Cloudy and high viscous fluid
3	Rigid gel

Table 4: Description of gel codes used in this work (Stavland et al., 2011)

The fact to be noted here is that gel codes 0 and 3 are more precise than the gel codes 1 and 2 because there is no clear boundary defined between the various gel codes. It only depends on the perspective of the observant.

3.2.5. GEL SYNERESIS

Gel syneresis refers to the process by which the silicate and polymer gels tend to expel water by contracting. It affects the long term stability of the gel. It is believed that syneresis is an inevitable part of any gelation process (Vinot, Schechter & Lake, 1989; Usaitis, 2011, p. 31). The progress of gel syneresis in a porous medium is illustrated in figure 12.

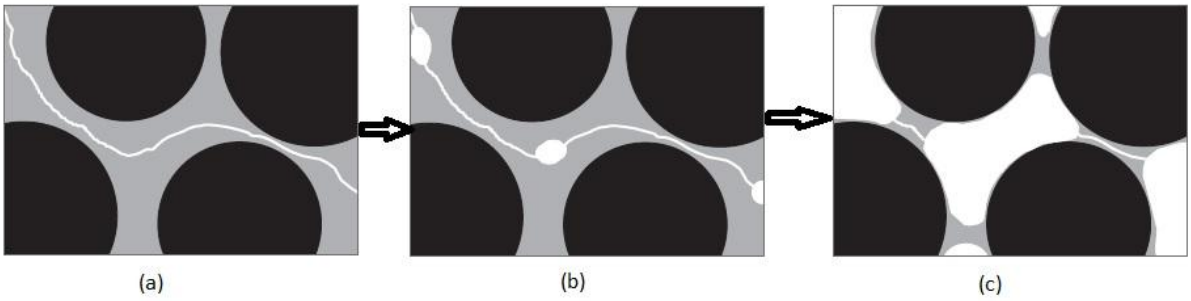

Figure 12: Progress of gel syneresis within a porous medium. (a) Before syneresis, (b) At a low degree of syneresis, (c) At a high degree of syneresis (Bryant, Rabaioli & Lockhart, 1996)

Although the permeability of a gel-treated porous medium does increase as syneresis proceeds, the degree of permeability reduction in core samples remains technologically useful even when 95% syneresis is observed in bulk samples. The activator/crosslinker mediates the silicate/polymer solution-to-gel transformation. In cases where too much of gelling agent is present, the crosslinking continues well past the point of gelation. This causes the silicate/polymer gel to contract in volume, expelling water. Studies have shown that the process of syneresis occurs due to the formation of new bonds (siloxane bonds) during gel development by condensation of two silanol groups (-Si-OH). Gel shrinkage occurs because the siloxane bond formed takes less space than the two individual silanol groups from which it is derived (Brinker & Scherer, 1990; Hamouda & Akhlaghi Amiri, 2014)

3.2.6. GEL STRENGTH

After the gel is formed, it should be able to withstand the high pressure gradients when used in water control applications. These pressure gradients are highest in the vicinity of the borehole and gets weaker away from the borehole and deeper into the formation. Therefore, a sensible placement of the gel at the proper location plays an important role as it needs to be strong enough to block the water flow from the formation at that location. In other words, the formed gel should be strong enough to withstand the injection pressure when the flow is resumed after shut-in time. In this work, the elastic strength of a gel has been measured by using dynamic oscillatory viscosity. The measure of the elastic strength of

a gel relates to the resistance to physical deformation that a gel will exhibit while extruding through a constriction in its flow path (Sydansk, 1990).

3.3. CORE FLOODING

The core flooding experiment was performed on a Berea sandstone core. The important terms used in the evaluation of this experiment are described in this section.

3.3.1. DEFINITION OF TERMS

3.3.1.1. POROSITY (denoted by 'ϕ')

The porosity of a rock is a measure of its ability to hold a fluid. It is the fraction of void spaces in the rock. It is given by the ratio of pore volume to the bulk volume (matrix + pore spaces) of the rock.

Mathematically,

$$\phi = {V_p}/{V_b}$$

..... (5)

where

V_p = pore volume of the rock

V_b = bulk volume of the rock

Porosity is always between 0 and 1.

3.3.1.2. PERMEABILITY (denoted by 'k')

The permeability of a rock is a measure of its ability to transmit fluids. It is of three types:

Absolute permeability (denoted by 'k_{abs}'): It is the permeability measurement when a single fluid or phase is present in the rock. It is typically measured in darcies or millidarcies.

Effective permeability (denoted by 'k_{eff}'): It is a measure of the rock's ability to preferentially transmit a particular fluid when two or more immiscible fluids are present in the rock. It is typically measured in darcies or millidarcies.

Relative permeability (denoted by 'k_r'): In multiphase flow in porous media, the relative permeability of a phase is the ratio of effective permeability of that phase to the absolute permeability. Mathematically,

$$k_r = {k_{eff}}/{k_{abs}}$$

..... (6)

The calculation of relative permeabilities of different phases flowing together in porous media allows comparison of their abilities to flow in the presence of each other, since the presence of more than one fluid in the rock generally inhibits flow.

3.3.1.3. RESISTANCE FACTOR (denoted by 'RF')

The resistance factor is defined as the ratio of the mobility of water to the mobility of a polymer solution.

$$RF = {\lambda_w}/{\lambda_p} = \left({k_w}/{\square_w}\right) \Big/ \left({k_p}/{\square_p}\right)$$

..... (7)

where

k_w = permeability to water

μ_w = viscosity of water

k_p = permeability to polymer solution

μ_p = viscosity of polymer solution

$\lambda_w = k_w/\mu_w$ is the mobility of the water and

$\lambda_p = k_p/\mu_p$ is the mobility of the polymer solution

The resistance factor is used in order to characterise the behaviour of pressure built up during flooding of different polymers (Littmann, 1988). It is a measure of polymer-induced mobility reduction.

3.3.1.4. RESIDUAL RESISTANCE FACTOR (denoted by 'RRF')

The residual resistance factor is defined as the ratio of the mobility of a phase before the treatment with polymer solution to that after the treatment with polymer solution. It can also be expressed as the ratio of permeability of a phase before and after polymer injection.

$$RRF = {k_{before}}/{k_{after}}$$

..... (8)

The residual resistance factor is a measure of the tendency of the polymer to adsorb and thus partially block the porous media (Littmann, 1988). Hence it is a measure of polymer-induced permeability reduction.

3.4. EQUIPMENT AND PROCEDURE

The Anton Paar Rheometer MCR 302 was used in this study to measure the rheological properties of all prepared samples. The concentric cylinder measuring system CC27, also known as the bob/cup assembly system was used for the silicate systems and the cone/plate system was used for the polymer-crosslinker systems.

Silicate gels display visco-elastic behaviour, therefore oscillatory tests were chosen for this work since they are used to examine all kinds of visco-elastic materials.

3.4.1. OSCILLATORY SHEAR MEASUREMENTS ("RHEOLOGY", 1998)

When a sample fluid mixture of silicate system and activator is subjected to an oscillatory stress, both elastic and viscous characteristics are observed. An illustration of bob and cup assembly in a MCR series of Anton Paar Rheometer is given in figure 13.

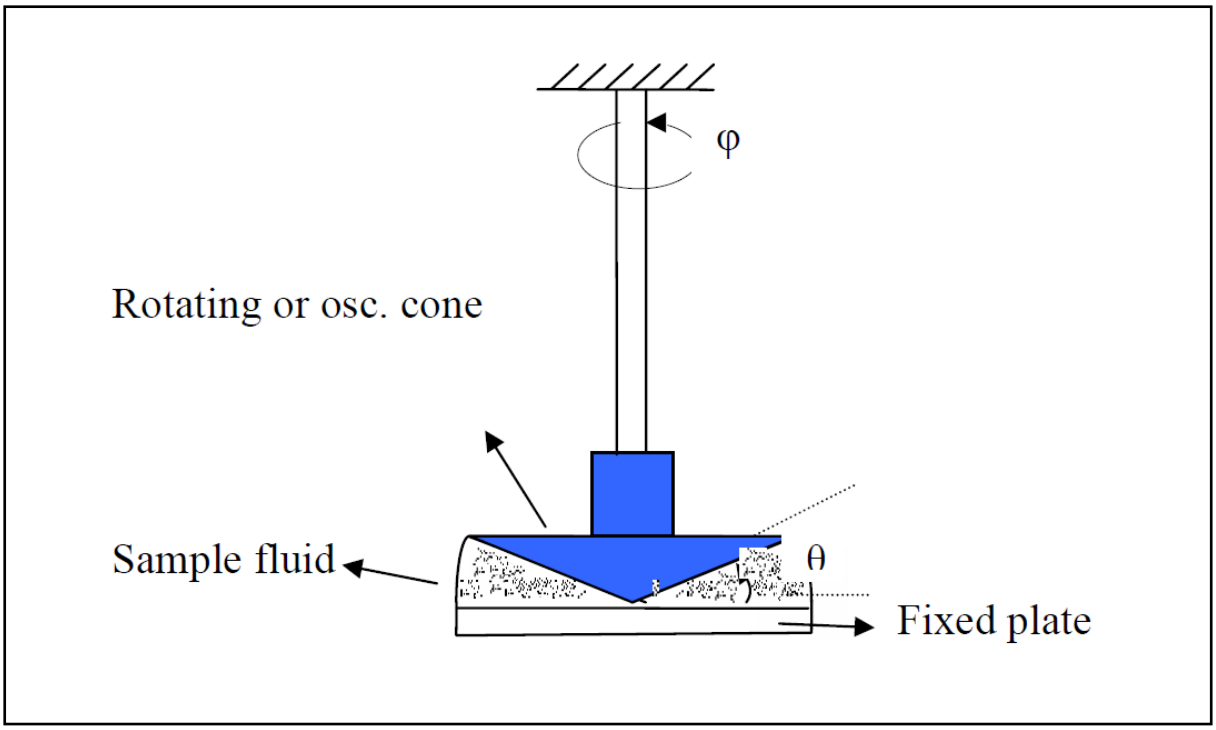

Figure 13: Illustration of bob and cup assembly in a MCR-series of Anton Paar Rheometer ("Rheology", 1998)

The bob and cup assembly of the rheometer is used to measure the damping characteristics. The cone-shaped bob is forced into oscillatory rotational stress with angular frequency ω. The sample is placed in the cup which has a mark inside it corresponding to 20 ml which is the required volume of the sample fluid mixture.

As described above, G' denotes the elastic response and G'' denotes the viscous behaviour response. Both responses are independent of the strain amplitude when the oscillatory shear measurements are performed in the linear visco-elastic regime.

When a sample is exposed to a sinusoidal strain (γ) in an oscillatory shear experiment, it will respond with a gradual approach to a steady sinusoidal stress (σ) at a constant angular frequency ω.

$$\gamma = \gamma_o \sin \omega t$$

..... (9)

$$\sigma = \gamma_o \left(G'(\omega) \sin wt + G''(\omega) \cos \omega t\right)$$

..... (10)

Hence the storage modulus G' and loss modulus G'' can be easily determined. It can even be used to determine the dynamic viscosity η' = G''/ω, the experiments for which are done at low shear rates.

The different types of systems of the rheometer that are used in this work are described below.

3.4.1.1. CONCENTRIC CYLINDER SYSTEMS (Instruction Manual MCR Series, 2011)

The sample volume of the fluid mixture required for concentric cylinder systems is indicated by a marker inside the measuring system cup. The cup is filled with the sample fluid up to this mark. After lowering the measuring head to measuring position, the measuring bob should be completely immersed in the sample. Then a few drops of n-decane are added on top of the sample to avoid the evaporation of the sample at high temperatures. The correct way to fill the measuring cup and immersing the measuring bob in the cup is illustrated in figure 14.

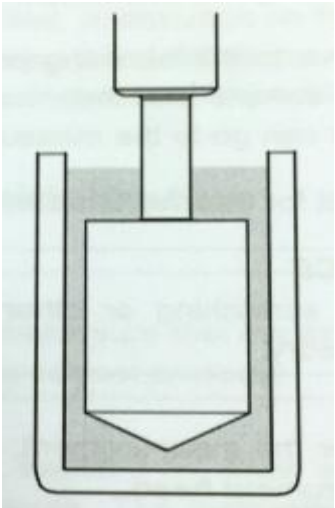

Figure 14: Concentric cylinder system filling (Instruction Manual MCR Series, 2011)

There are advantages and disadvantages of using the concentric cylinder systems.

3.4.1.1.1. Advantages of concentric cylinder systems

- no sample drying effects
- accurate temperature within entire cup
- no gap leakage at high shear rates

3.4.1.1.2.Disadvantages of concentric cylinder systems

- relatively high sample volume required (~20ml)
- difficult to clean
- entrapment of air bubbles in paste-like samples
- turbulences at high shear rates
- slow temperature equilibration

3.4.1.2. CONE-PLATE SYSTEMS (Instruction Manual MCR Series, 2011)

The sample should be just outside the rim of the measuring cone. Both too much and too little sample will lead to large errors in the measurement data. The correct filling with sample for a cone-plate system is shown in figure 15.

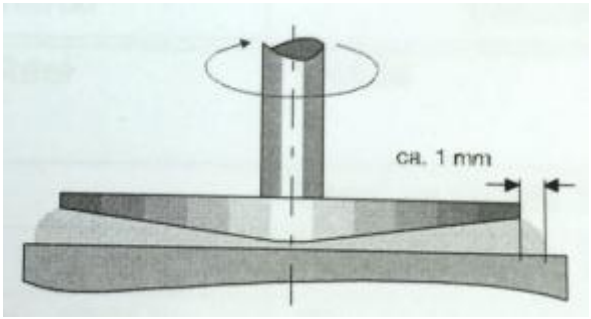

Figure 15: Cone-plate system filling (Instruction Manual MCR Series, 2011)

There are advantages and disadvantages of using the cone-plate systems.

3.4.1.2.1. Advantages of cone-plate systems

- constant shear rate within entire gap due to cone shape
- small sample volume
- easy to fill and to clean
- quick temperature equilibration

3.4.1.2.2. Disadvantages of cone-plate systems

- gap leakage of the substance at too high shear rates
- particles in sample can disrupt the measurement
- sample drying effects

3.4.2. MEASURING TEST MODES

Two types of oscillation test modes were used:

3.4.2.1. DYNAMIC-MECHANICAL ANALYSIS (DMA) MODE

This test mode was run at isothermal conditions to determine the gel point. During the DMA test, the sample is subjected to a controlled shear strain $\gamma(t) = \gamma_o . \sin \omega t$ with a constant angular frequency ω = 10 rad/s and a constant oscillatory strain γ_o = 1% (Mezger, 2011). These two parameters define how fast and how much the bob turns during the test (Pham & Hatzignatiou, 2015).

3.4.2.2. AMPLITUDE SWEEP (AS) MODE

During this test, the sample is subjected to an increasing oscillatory strain (0.01 % to 100000 %) in a logarithmic ramp profile, while the angular frequency and temperature are kept constant (ω = 10 rad/s and temperatures = 40°C, 60°C and 80°C). This test mode is applied to determine the limit of Linear Visco-Elastic (LVE) range, which defines the limiting shear strain γ_L of a formed gel. This limiting shear strain γ_L represents the largest deformation or shear strain amplitude, below which the measured storage and loss moduli, G' and G'', retain a constant plateau value, indicating that the sample structure is preserved. When the oscillatory strain crosses the limiting shear strain, i.e. $\gamma > \gamma_L$ the formed gel breaks and the structure is completely destroyed (Mezger, 2011). The value of shear stress τ corresponding to this strain γ gives the maximum gel strength that it can withstand against applied external forces (Pham & Hatzignatiou, 2015).

3.4.3. BOTTLE TESTING

Bottle testing provides a very straightforward and cost-effective means to obtain a semi-quantitative measure of gel strength, gelation time and gelation rate (Sydansk, 1990). It is also a convenient method to evaluate the long-term stability of gels at a given test temperature. Bottle testing method has been used for bulk measurements of the different polymer-crosslinker combinations considered in this work. For a newly designed conformance-improvement gel treatment, bottle testing is an effective quality control and quality assurance tool to evaluate the gel. In addition, this testing provides a degree of assurance that there are no chemical interferences involving the field make-up water that will interfere with the gel and that the mixture of chemicals being used to form gel are the part of a correct formula. This test involves placing a specified amount of gelant sample in a small test tube and keeping them in the oven at desired temperatures which correspond to reservoir temperatures. The gelant samples are visually inspected at frequent intervals to observe the gelation times and once a gel is formed, they are again kept under observation at the same temperature for any specific post-gelation behaviour which mainly involves gel syneresis/shrinkage.

4. EXPERIMENTAL WORK - RHEOLOGICAL MEASUREMENTS

This section covers the rheological measurements performed on the silicates mixed with activators to estimate their sol-gel transition time. It further deals with the silicate gel kinetics to establish a unified sol-gel transition time correlation for the silicate systems.

Two silicate systems, the sodium silicate system and the potassium silicate system, have been tested for evaluating their rheological properties and to determine which one is a better system for the water-shutoff treatments.

All the experiments were performed at three temperature readings of 40°C, 60°C and 80°C to get a better understanding of their rheological properties at different temperature settings.

4.1. SODIUM SILICATE SYSTEM

Experiments were performed by mixing sodium silicate solution with four different activator systems which are defined below:

1. Citric acid activator with varying calcium ion concentration
2. HCl activator with varying calcium ion concentration
3. Citric acid and Ethylenediaminetetraacetic acid (EDTA) activators with varying calcium ion concentration
4. Citric acid and Ethylenediaminetetraacetic acid (EDTA) activators with zero calcium ion concentration and varying EDTA activator concentration

The different combinations of chemicals used for the first activator system, i.e. citric acid activator with varying calcium ion concentration to test the sodium silicate system are given in table 5. Table 6 gives the gelation time for the different samples at the three temperature readings of 40°C, 60°C and 80°C.

CITRIC ACID ACTIVATOR WITH VARYING CALCIUM ION CONCENTRATION						
Sample Number	Sodium Silicate System (SS)	10 wt% Citric Acid	0.1M $CaCl_2$	Percent $CaCl_2$	Distilled Water	Total weight of sample
	g	g	g	%	g	g
SS1	9.22	2.00	0.00	0.00	8.78	20
SS2	9.22	2.00	1.00	0.05	7.78	20
SS3	9.22	2.00	2.00	0.10	6.78	20
SS4	9.22	2.00	3.00	0.15	5.78	20

Table 5: Concentrations of different components used to determine the effect of constant 10 wt% citric acid activator and varying calcium concentration on the sodium silicate system

CITRIC ACID ACTIVATOR WITH VARYING CALCIUM ION CONCENTRATION			
Sample Number	Gel point at 80°C	Gel point at 60°C	Gel point at 40°C
	hours	hours	hours
SS1	0.450	2.154	5.643
SS2	0.280	0.871	2.945
SS3	0.240	0.392	1.303
SS4	0.131	0.263	0.712

Table 6: Gelation time at different temperatures for the samples prepared to determine the effect of constant 10 wt% citric acid activator and varying calcium concentration on the sodium silicate system

From table 6, it is evident that the gelation time is seen to be decreasing with increase in the salinity. In addition, the gel points for a particular sample are seen to be decreasing with increase in the temperature as expected.

The case with the second activator system, i.e. HCl activator with varying calcium ion concentration has been described in section 4.4.

The different combinations of chemicals used for the third activator system, i.e. citric acid and EDTA activators with varying calcium ion concentration to test the sodium silicate system are given in table 7. Table 8 gives the gelation time for the different samples at the three temperature readings of 40°C, 60°C and 80°C.

CITRIC ACID AND EDTA ACTIVATORS WITH VARYING CALCIUM ION CONCENTRATION							
Sample Number	Sodium Silicate System (SS)	10 wt% Citric Acid	0.1M $CaCl_2$	Percent $CaCl_2$	0.1M EDTA	Distilled Water	Total weight of sample
	g	g	g	%	g	g	g
SS5	9.22	2	0	0.000	1.5	7.28	20
SS6	9.22	2	1.5	0.075	1.5	5.78	20
SS7	9.22	2	2.5	0.125	1.5	4.78	20

Table 7: : Concentrations of different components used to determine the effect of constant 10 wt% citric acid activator, constant 0.1M EDTA activator and varying calcium concentration on the sodium silicate system

CITRIC ACID AND EDTA ACTIVATORS WITH VARYING CALCIUM ION CONCENTRATION			
Sample Number	Gel point at 80°C	Gel point at 60°C	Gel point at 40°C
	hours	hours	hours
SS5	0.356	1.607	4.210
SS6	0.274	0.799	2.342
SS7	0.172	0.399	0.936

Table 8: Gelation time at different temperatures for the samples prepared to determine the effect of constant 10 wt% citric acid activator, constant 0.1M EDTA activator and varying calcium concentration on the sodium silicate system

The same point is observed from table 8 as well. The gelation time is found to be decreasing as the salinity of the solution is increasing. In addition, the gel points for a particular sample are seen to be decreasing with increase in the temperature as expected.

The different combinations of chemicals used for the last activator system, i.e. citric acid and EDTA activators with zero calcium ion concentration and varying EDTA activator concentration to test the sodium silicate system are given in table 9. Table 10 gives the gelation time for the different samples at the three temperature readings of 40°C, 60°C and 80°C.

CITRIC ACID AND EDTA ACTIVATORS WITH ZERO CALCIUM ION CONCENTRATION AND VARYING EDTA ACTIVATOR CONCENTRATION							
Sample Number	Sodium Silicate System (SS)	10 wt% Citric Acid	0.1M $CaCl_2$	0.1M EDTA	Percent EDTA	Distilled Water	Total weight of sample
	g	g	g	g	%	g	g
SS8	9.22	2.00	0.00	0.00	0	8.78	20
SS9	9.22	2.00	0.00	1.50	0.075	7.28	20
SS10	9.22	2.00	0.00	2.50	0.125	6.28	20

Table 9: Concentrations of different components used to determine the effect of constant 10 wt% citric acid activator, constant 0.1M EDTA activator, zero calcium concentration and varying 0.1M EDTA concentration on the sodium silicate system

CITRIC ACID AND EDTA ACTIVATORS WITH ZERO CALCIUM ION CONCENTRATION AND VARYING EDTA ACTIVATOR CONCENTRATION			
Sample Number	Gel point at 80°C	Gel point at 60°C	Gel point at 40°C
	hours	hours	hours
SS8	0.450	2.154	7.319
SS9	0.356	1.607	4.210
SS10	0.284	0.945	2.176

Table 10: Gelation time at different temperatures for the samples prepared to determine the effect of constant 10 wt% citric acid activator, constant 0.1M EDTA activator, zero calcium concentration and varying 0.1M EDTA concentration on the sodium silicate system

It is evident from table 10 that the gelation time is decreasing as the concentration of 0.1M EDTA in the solution is increasing at a particular temperature. The reason for all the three above-mentioned cases is described in the section 4.3. Appendix A gives an example of what the plots look like when the DMA measuring mode is applied on a sample to measure the gel point.

4.2. POTASSIUM SILICATE SYSTEM

Experiments were performed by mixing potassium silicate solution with three different activator systems which are defined below:

1. Citric acid activator with varying calcium ion concentration
2. Citric acid and Ethylenediaminetetraacetic acid (EDTA) activators with varying calcium ion concentration
3. Citric acid and Ethylenediaminetetraacetic acid (EDTA) activators with zero calcium ion concentration and varying EDTA activator concentration

The different combinations of chemicals used for the first activator system, i.e. citric acid activator with varying calcium ion concentration to test the potassium silicate system are given in table 11. Table 12 gives the gelation time for the different samples at the three temperature readings of 40°C, 60°C and 80°C.

CITRIC ACID ACTIVATOR WITH VARYING CALCIUM ION CONCENTRATION						
Sample Number	Potassium Silicate System (KS)	10 wt% Citric Acid	0.1M $CaCl_2$	Percent $CaCl_2$	Distilled Water	Total weight of sample
	g	g	g	%	g	g
KS1	9.22	2.00	0.00	0.00	8.78	20
KS2	9.22	2.00	1.00	0.05	7.78	20
KS3	9.22	2.00	2.00	0.10	6.78	20
KS4	9.22	2.00	3.00	0.15	5.78	20

Table 11: Concentrations of different components used to determine the effect of constant 10 wt% citric acid activator and varying calcium concentration on the potassium silicate system

CITRIC ACID ACTIVATOR WITH VARYING CALCIUM ION CONCENTRATION			
Sample Number	Gel point at 80°C	Gel point at 60°C	Gel point at 40°C
	hours	hours	hours
KS1	0.342	2.202	9.278
KS2	0.235	1.262	5.244
KS3	0.208	0.641	2.552
KS4	0.112	0.477	1.255

Table 12: Gelation time at different temperatures for the samples prepared to determine the effect of constant 10 wt% citric acid activator and varying calcium concentration on the potassium silicate system

From table 12, it is evident that the gelation times for the samples with potassium silicate are also showing the same behaviour as the samples with sodium silicate. The gel points are seen to be decreasing with increase in the salinity. In addition, the gel points for a particular sample are seen to be decreasing with increase in the temperature as expected.

The different combinations of chemicals used for the second activator system, i.e. citric acid and EDTA activators with varying calcium ion concentration to test the sodium silicate system are given in table 13. Table 14 gives the gelation time for the different samples at the three temperature readings of 40°C, 60°C and 80°C.

CITRIC ACID AND EDTA ACTIVATORS WITH VARYING CALCIUM ION CONCENTRATION							
Sample Number	Potassium Silicate System (KS)	10 wt% Citric Acid	0.1M $CaCl_2$	Percent $CaCl_2$	0.1M EDTA	Distilled Water	Total weight of sample
	g	g	g	%	g	g	g
KS5	9.22	2	0	0.000	1.5	7.28	20
KS6	9.22	2	1.5	0.075	1.5	5.78	20
KS7	9.22	2	2.5	0.125	1.5	4.78	20

Table 13: Concentrations of different components used to determine the effect of constant 10 wt% citric acid activator, constant 0.1M EDTA activator and varying calcium concentration on the potassium silicate system

CITRIC ACID AND EDTA ACTIVATORS WITH VARYING CALCIUM ION CONCENTRATION			
Sample Number	Gel point at 80°C	Gel point at 60°C	Gel point at 40°C
	hours	hours	hours
KS5	0.270	1.896	5.861
KS6	0.246	0.954	4.020
KS7	0.146	0.602	1.705

Table 14: Gelation time at different temperatures for the samples prepared to determine the effect of constant 10 wt% citric acid activator, constant 0.1M EDTA activator and varying calcium concentration on the potassium silicate system

From table 14, a similar observation can be made as for the case with the first activator system. The gelation time is found to be decreasing as the salinity of the solution is increasing. In addition, the gel points for a particular sample are seen to be decreasing with increase in the temperature as expected.

The different combinations of chemicals used for the last activator system, i.e. citric acid and EDTA activators with zero calcium ion concentration and varying EDTA activator concentration to test the sodium silicate system are given in table 15. Table 16 gives the gelation time for the different samples at the three temperature readings of 40°C, 60°C and 80°C.

CITRIC ACID AND EDTA ACTIVATORS WITH ZERO CALCIUM ION CONCENTRATION AND VARYING EDTA ACTIVATOR CONCENTRATION							
Sample Number	Potassium Silicate System (K45)	10 wt% citric acid	0.1M $CaCl_2$	0.1M EDTA	Percent EDTA	Distilled Water	Total weight of sample
	g	g	g	g	%	g	g
KS8	9.22	2.00	0.00	0.00	0.000	8.78	20
KS9	9.22	2.00	0.00	1.50	0.075	7.28	20
KS10	9.22	2.00	0.00	2.50	0.125	6.28	20

Table 15: Concentrations of different components used to determine the effect of constant 10 wt% citric acid activator, constant 0.1M EDTA activator, zero calcium concentration and varying 0.1M EDTA concentration on the potassium silicate system

CITRIC ACID AND EDTA ACTIVATORS WITH ZERO CALCIUM ION CONCENTRATION AND VARYING EDTA ACTIVATOR CONCENTRATION			
Sample Number	Gel point at 80°C	Gel point at 60°C	Gel point at 40°C
	hours	hours	hours
KS8	0.342	2.202	10.737
KS9	0.270	1.234	5.861
KS10	0.236	0.810	3.317

Table 16: Gelation time at different temperatures for the samples prepared to determine the effect of constant 10 wt% citric acid activator, constant 0.1M EDTA activator, zero calcium concentration and varying 0.1M EDTA concentration on the potassium silicate system

It is evident from table 16 that the gelation time is decreasing as the concentration of 0.1M EDTA in the solution is increasing at a particular temperature. The reason for all the three above-mentioned cases is described in section 4.3.

4.3. EFFECT OF DIFFERENT ACTIVATOR SYSTEMS ON SODIUM SILICATE AND POTASSIUM SILICATE AT THREE DIFFERENT TEMPERATURE SETTINGS

The different activator systems have been described below to compare the effect of these systems on both silicates at the three temperature settings.

a) Effect of 10 wt% citric acid activator with varying calcium ion concentration

Figure 16 shows the effect of 10 wt% citric acid activator on the two silicates at the three temperature settings and varying calcium (Ca^{2+}) concentrations.

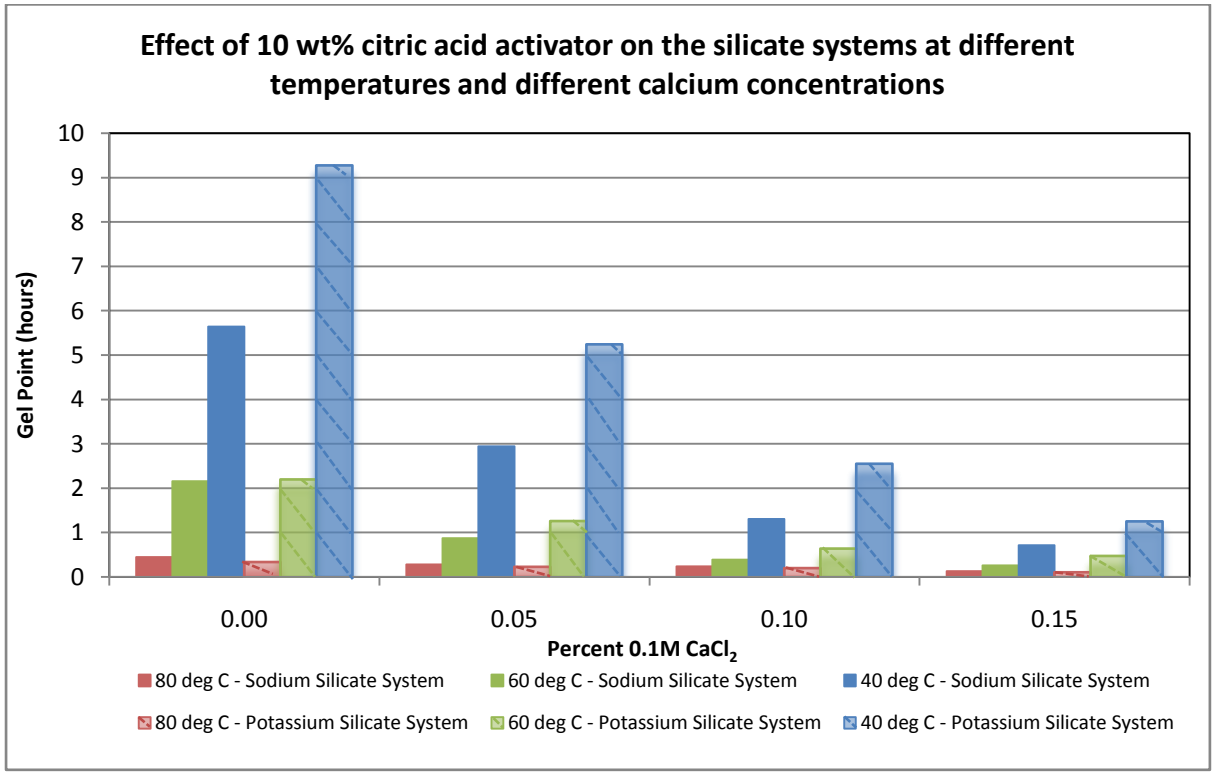

Figure 16: Effect of 10 wt% citric acid activator on the silicate systems at different temperatures and different calcium concentrations

In this plot, gelation time has been plotted as a function of percentage of 0.1M $CaCl_2$ in the sample volume. As expected, as the percentage of $CaCl_2$ is increasing in the sample volume, the gelation time for both silicate systems is decreasing at the same temperatures.

This is due to the fact that when the salt is added to an alkaline solution, it results in charge screening, which decreases gelation time. Divalent metal ions such as Ca^{2+} are more effective in screening the silica particles, and consequently accelerate the gelling kinetics more than monovalent cations (Jurinak & Summers, 1991; Hamouda & Akhlaghi Amiri, 2014). They also form metal silicate precipitations via ion exchange, which are relatively insoluble over a wide range of pH values (Jurinak & Summers, 1991; Hamouda & Akhlaghi Amiri, 2014).

In the case of calcium chloride, the reaction is as follows (Krumrine & Boyce, 1985):

$$2(\equiv SiO^{-}Na^{+}) + CaCl_2 \rightarrow 2 \equiv SiO^{-}Ca^{2+} + 2NaCl$$

b) Effect of 10 wt% citric acid and 0.1M EDTA activators with varying calcium ion concentration

Figure 17 shows the effect of 10 wt% citric acid and 0.1M EDTA activators on the two silicates at the three temperature settings and varying calcium (Ca^{2+}) concentrations.

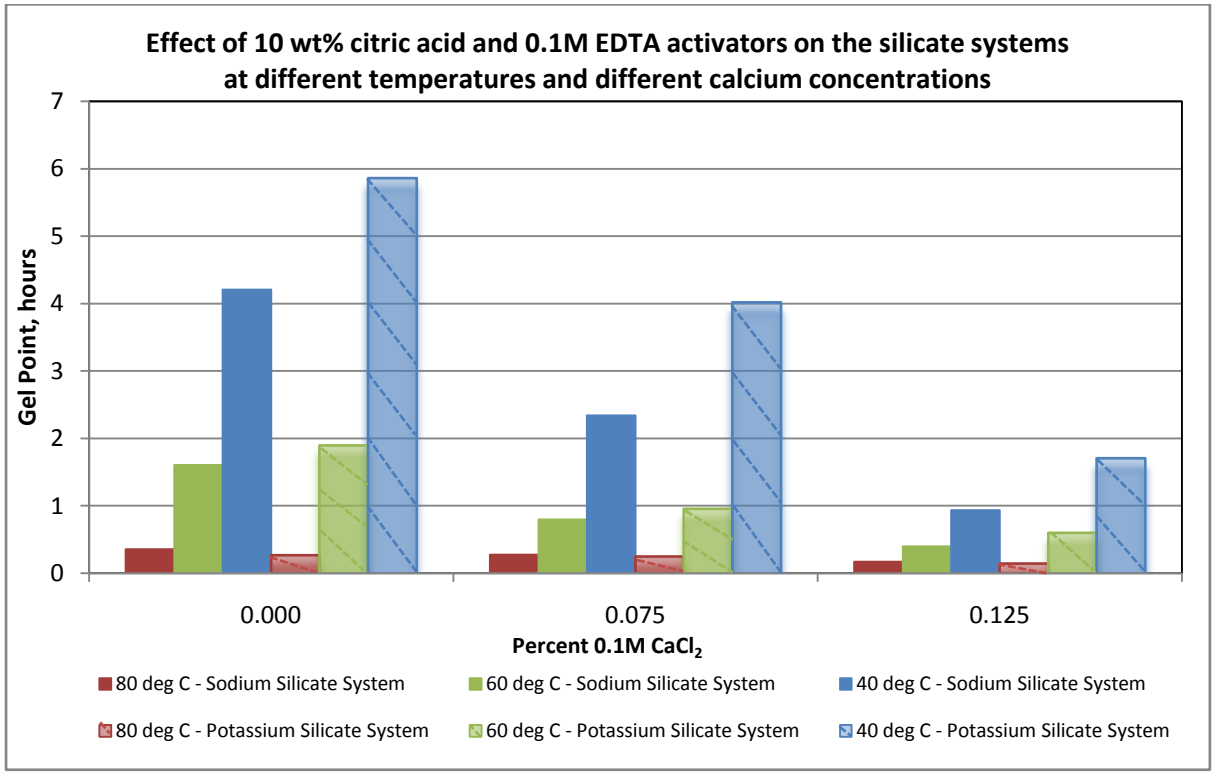

Figure 17: Effect of 10 wt% citric acid and 0.1M EDTA activators on the silicate systems at different temperatures and different calcium concentrations

In this plot, gelation time has been plotted as a function of percentage of 0.1M $CaCl_2$ in the sample volume. Similar to the last case (with only 10 wt% citric acid as the activator), the gelation time for both silicate systems is decreasing at the same temperatures as the percentage of $CaCl_2$ is increasing in the sample volume.

The difference to be seen in this case is the difference due to the effect of adding 0.1M EDTA to the sample volume when the amount of 10 wt% citric acid is kept constant. From the plots and the tables, it is clear that the gelation time is decreasing if both plots are evaluated at the same temperature for both activator systems. It proves that EDTA is acting like an activator here and is responsible for a decrease in the gelation time for both silicate systems as compared to the system which does not contain EDTA.

The addition of a salt which is a neutral solution, to an alkaline silicate system also acts as an acid for that system and tries to bring down the pH of the solution. Therefore, in this case, all the three components added to the silicate system - 10 wt% citric acid, 0.1M EDTA and 0.1M $CaCl_2$ are affecting the gelation time, meaning that both pH effects and salinity effects

are acting together to decrease the pH of the system, hence the gelation is faster compared to the cases described in cases (a) and (c).

c) Effect of different concentrations of 0.1M EDTA with zero calcium ion concentration and constant 10 wt% citric acid concentration

Figure 18 shows the effect of varying concentrations of 0.1M EDTA activator on the two silicates at the three temperature settings with zero calcium (Ca^{2+}) concentration and a constant 10 wt% citric acid concentration.

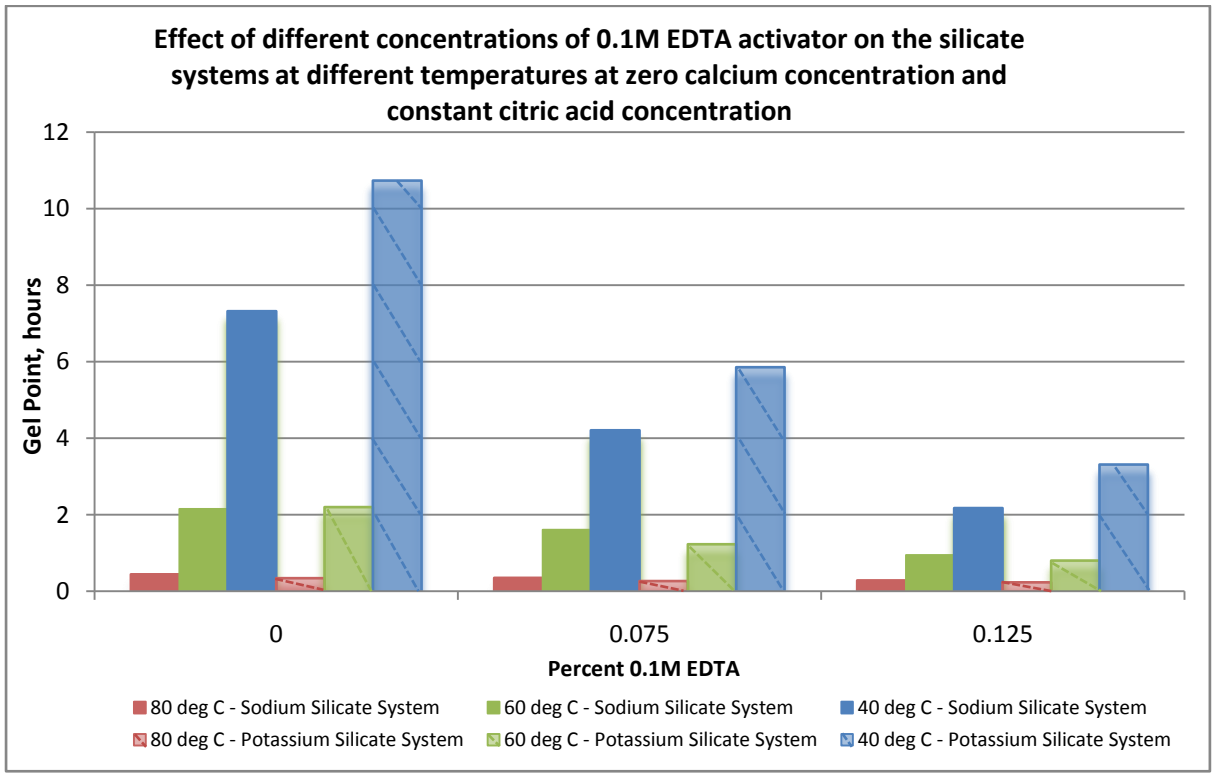

Figure 18: Effect of different concentrations of 0.1M EDTA activator on the silicate systems at different temperatures at zero calcium concentration and constant citric acid concentration

In this plot, gelation time has been plotted as a function of percentage of 0.1M EDTA in the sample volume which contains no salt. Hence, for this case, only the pH is changed and the salinity is kept constant. As can be seen from the plot, the gelation time for both silicate systems is decreasing at the same temperatures as the percentage of 0.1M EDTA is increasing in the sample volume.

The point to be noted here is that if we compare cases (b) and (c), we see an increase in the gelation time for both silicate systems at the same temperatures in case (c). This is due to the fact that firstly, there is no salt being added to the solutions here and therefore the salinity is not affecting the gelation time in this case. Secondly, the EDTA concentration is varying here. If the case with a percentage of 0.075% of 0.1M EDTA is considered for the cases (b) and (c), we see that the gelation time without the salt is higher than the gelation time with the salt. Therefore, it can be said that the same concentration of EDTA is having

the same effect on the pH of both solutions at all the temperatures. However, due to the absence of salt, which acted as an additional source to decrease the pH of the solution and hence decreased the gelation time in case (b), the overall gelation time is much larger in case (c).

4.4. ADDITIONAL CASE FOR THE SODIUM SILICATE SYSTEM WITH 10% 2M HCl ACTIVATOR

One more case was considered for the sodium silicate system where 10% 2M HCl was used as an activator. The sample volumes are given in table 17.

HCl ACTIVATOR WITH VARYING CALCIUM ION CONCENTRATION						
Sample Number	**Sodium Silicate System (SS)**	**10% 2M HCl**	**0.1M $CaCl_2$**	**Percent $CaCl_2$**	**Distilled Water**	**Total weight of sample**
	g	**g**	**g**	**%**	**g**	**g**
SS11	9.22	0.8	1.00	0.05	8.98	20
SS11-1	9.22	1.5	1.00	0.05	8.28	20
SS12	9.22	0.8	2.00	0.10	7.98	20
SS13	9.22	0.8	3.00	0.15	6.98	20

Table 17: Concentrations of different components used to determine the effect of 10% 2M HCl activator and varying calcium concentration on the sodium silicate system

The experiments were done at only one temperature, 60°C, to establish an idea about the gelation time to plan the sample volumes at other temperatures but no experiment was successful as per the remarks given in table 18.

HCl ACTIVATOR WITH VARYING CALCIUM ION CONCENTRATION		
Sample Number	**Gel point at 60°C hours**	**Remarks**
SS11	Greater than 12 hours	Experiment stopped, no traces of gel being formed. Hard traces of acid observed on the bob and cup assembly.
SS11-1	Greater than 10 hours	Experiment stopped to avoid any hard traces, no traces of gel being formed.
SS12	Greater than 10 hours	Experiment stopped to avoid any hard traces, no traces of gel being formed.
SS13	-	Local gels observed, no rigid gel formed.

Table 18: Gelation time at 60°C for different samples prepared to determine the effect of 10% 2M HCl activator and varying calcium concentration on the sodium silicate system

The experiment was conducted four times in total with different samples for SS13, wherein 9.22g of silicate (diluted by adding 6.98 g of distilled water) is mixed with a mixture of 0.8g of 10% 2M HCl and 3.00g of 0.1M $CaCl_2$ but in all cases, the initial phase angle remained considerably below 90 degrees from the beginning of the experiment. The experiments were continued for these different samples, with the same trend that was formed in the beginning, to see the effect of the gel formed later on, but even after 15-20 minutes of gelation time, when the test was stopped and the bob and cup assembly was removed, the sample was found to be in a liquid state and there was no indication of gel being formed. Some local gels were observed to form when all the chemicals were being mixed on the magnetic stirrer before starting the test. The viscosity curves also did not show any increase in the viscosity values after the sol-gel transition time.

The experiment was performed for sample number SS11 wherein 9.22g of silicate (diluted by adding 8.98 g of distilled water) is mixed with a mixture of 0.8g of 10% 2M HCl and 1g of 0.1M $CaCl_2$. The experiment was stopped after ~12 hours because hard traces were observed on the wall of the cup and on the top surface of the bob, probably due to the prolonged exposure of the bob and cup assembly to a very strong acid. There were no traces of a gel being formed when the experiment was stopped.

The experiment was repeated for sample number SS12 also but it was also stopped after ~10 hours. The reason for not continuing the experiment with this sample was to avoid the formation of any more hard traces on the bob and cup assembly. There were no traces of gel observed when the experiment was stopped.

To further test the feasibility of forming a gel with HCl activator, one additional case SS11-1 was designed and the experiment was repeated with the sodium silicate system. In this case, 9.22g of silicate solution (diluted by adding 8.28 g of distilled water) was mixed with a mixture of 1.5g of 10% 2M HCl and 1.00g of 0.1M $CaCl_2$. In this case, the test was again continued for ~10 hours but there was no indication of gel. Therefore, the experiment was stopped for the same reason as above.

The experiments with HCl activator have shown that even though HCl is a strong acid and is capable of reducing the pH of the alkaline silicate solution to a great extent, it is still not a good activator for the sodium silicate system. Likely reasons can be:

1. HCl, being a very strong acid, reduces the pH of the solution a lot more than what is desired to form a gel.
2. Microgels may have formed in the solution, hindering the effect of the HCl activator or not allowing the bob to oscillate properly and provide the required constant oscillatory strain or constant angular frequency to the solution within the measuring cup.

4.5. COMPARISON BETWEEN SODIUM AND POTASSIUM SILICATE SYSTEMS FOR GEL POINTS AT DIFFERENT TEMPERATURES FOR DIFFERENT SCENARIOS

A comparison was made for gelation times at different temperatures for both systems to establish the system which gels faster at a particular temperature at different concentrations of salt.

Figure 19 shows a plot of sol-gel transition time in hours as a function of percentage of 0.1M $CaCl_2$ in the sample volume at 80°C for the three systems for both silicate systems.

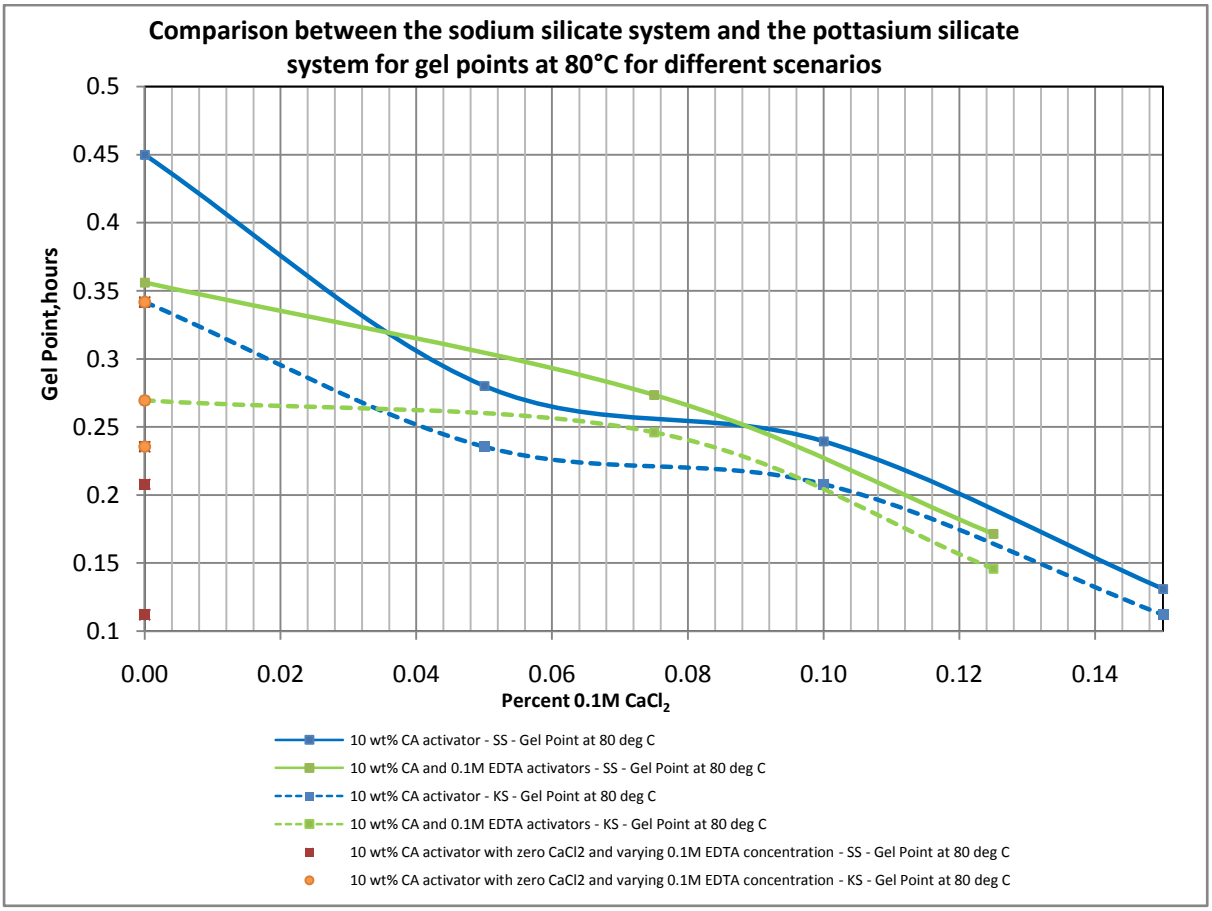

Figure 19: Comparison between the sodium silicate system and the potassium silicate system for gel points at 80°C for different scenarios

In figure 19, the gel points are plotted against the percentage of 0.1M $CaCl_2$. The plot clearly shows that the potassium silicate system gels faster than the sodium silicate system for different calcium concentrations but when there is no salt in the system, then the sodium silicate system gels faster than the potassium silicate system.

Figure 20 shows a plot of sol-gel transition time in hours as a function of percentage of 0.1M $CaCl_2$ in the sample volume at 60°C for the three systems for both silicate systems.

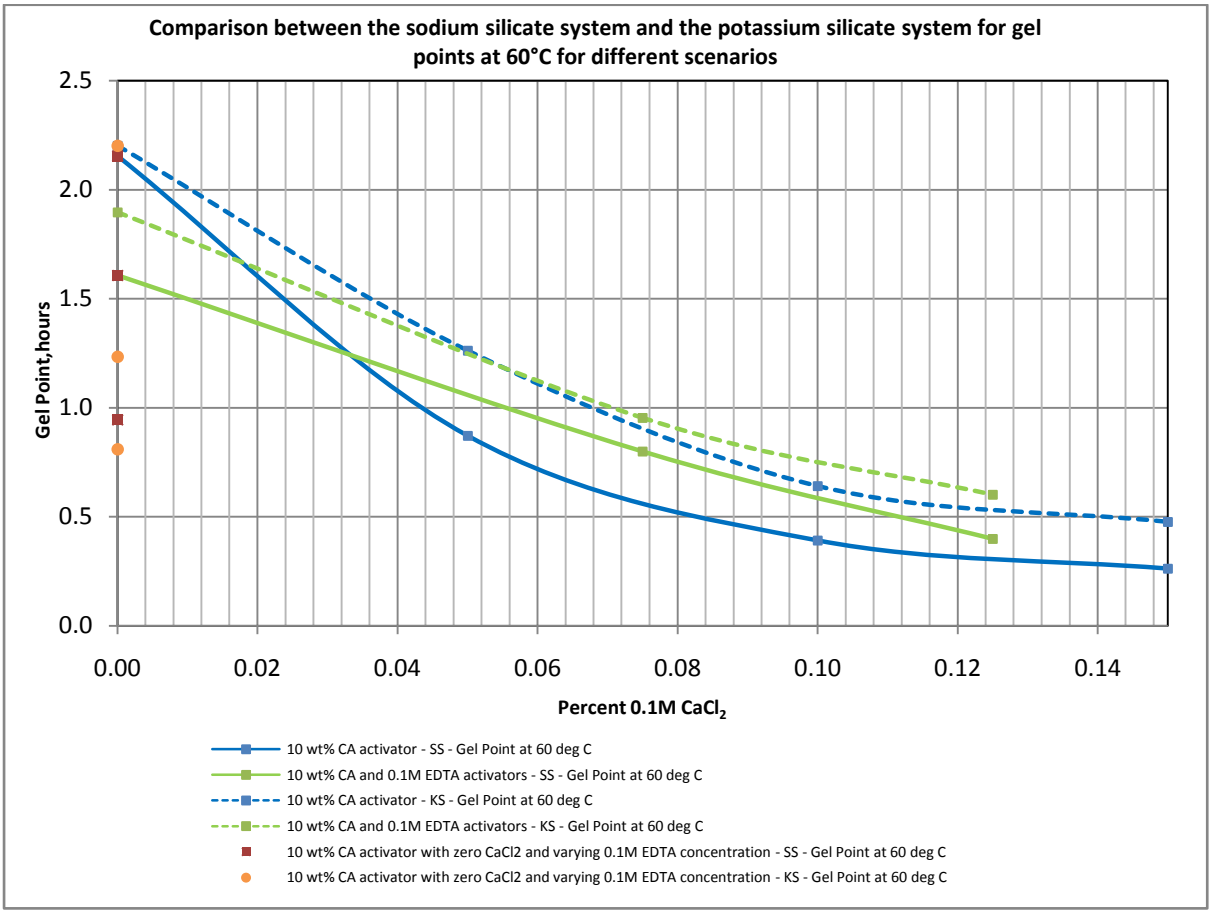

Figure 20: Comparison between the sodium silicate system and the potassium silicate system for gel points at 60°C for different scenarios

The plot shows that when the temperature is decreased to 60°C, the effect is still the same, i.e. the gelation time is still decreasing for both systems as the concentration of calcium is increasing in the sample volumes but in this case, the potassium silicate system gels faster compared to the sodium silicate system.

Figure 21 shows a plot of sol-gel transition time in hours as a function of percentage of 0.1M $CaCl_2$ in the sample volume at 40°C for the three systems for both silicate systems.

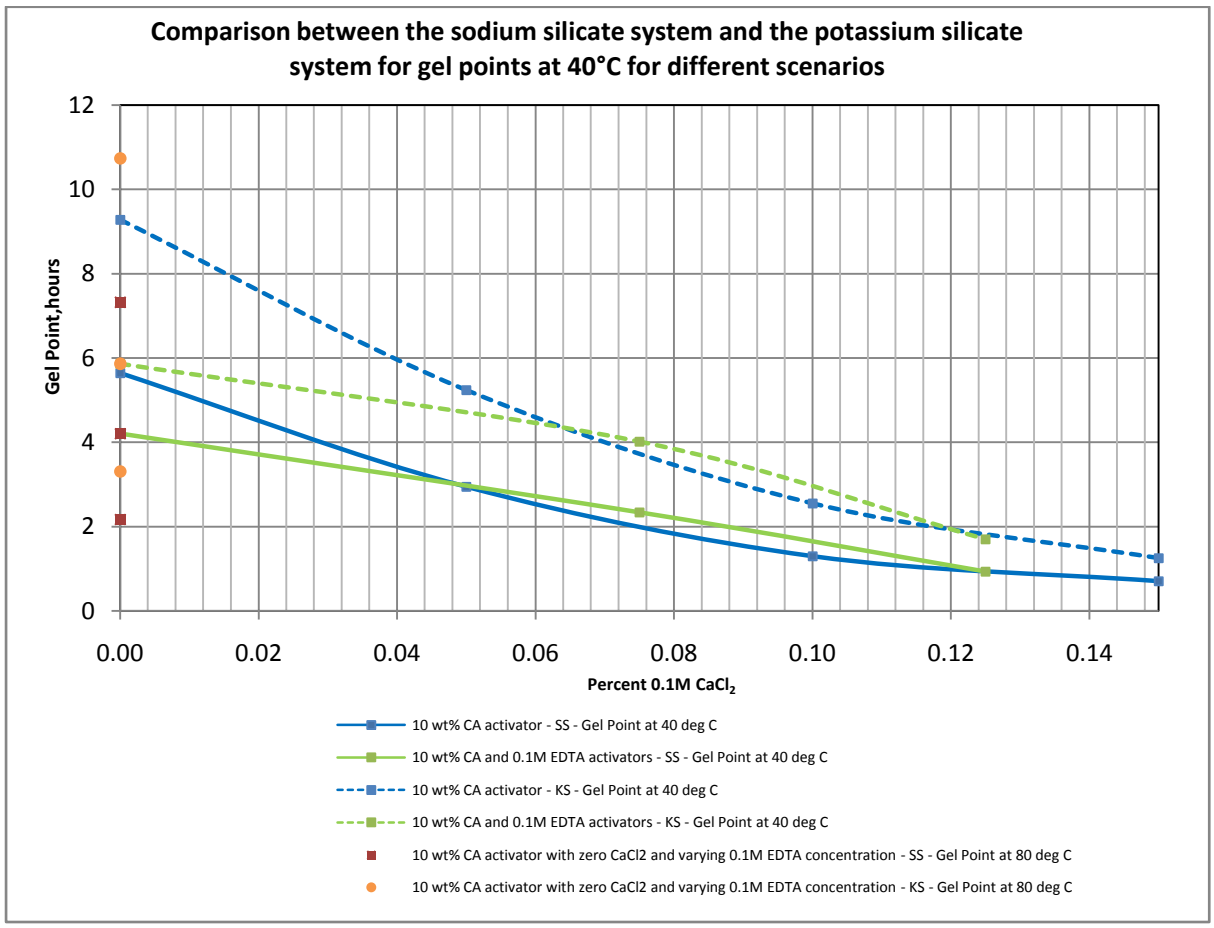

Figure 21: Comparison between the sodium silicate system and the potassium silicate system for gel points at 40°C for different scenarios

The same observation can be made here as well. The increase in the salinity of the sample leads to a faster gelation of the sample. It is also observed that the sodium silicate system gels faster than the potassium silicate system at this temperature.

The main conclusion that can be drawn from the figures 19, 20 and 21 is that the sodium silicate system forms a gel faster at temperatures 40°C and 60°C but at higher temperatures, like 80°C, the potassium silicate system gels faster than the sodium silicate system. This is possibly due to the fast thermodynamical reactions taking place between the activators and the potassium silicate system at higher temperatures.

All the gel points in the individual cases at one particular temperature when plotted against the concentration of 0.1M $CaCl_2$ or 0.1M EDTA are following an exponential function with a trendline having an R squared value of greater than 0.920 which shows a pretty good match with the experimental data. All these cases have been given in Appendix B.

4.6. SILICATE GEL KINETICS

Stavland et al. (2011) presented the following general equation for bulk gelation time for a silicate gel system, which was assumed for a system with sodium silicate solution mixed with 2M HCl activator and $CaCl_2$ (to study the effects of salinity):

$$t_g = A * e^{\alpha[Si]} * e^{\beta[HCl]} * e^{\gamma\sqrt{[Ca^{2+}]}} * e^{E_a/RT}$$

..... (11)

where

t_g = gelation time (days)

[Si] = silicate concentration (wt%)

[HCl] = 2M HCl concentration (wt%)

$[Ca^{2+}]$ = concentration of calcium ion (PPM)

E_a = activation energy (kJ/mol)

T = absolute temperature (K)

R = universal gas constant = 8.314 kJ/mol.K

A, α, β, γ = empirical constants, obtained by matching the measured data to the general equation

For the general equation: A = 2.1 x 10^{-8} days, α = -0.6, β = -0.7, γ = -0.1 and E_a = 77 kJ/mol

Based on this equation, a unified sol-gel transition time correlation has been developed for the results obtained for the silicates considered in this work. The equation is of the following form:

$$t_g = A * f_1([EDTA]) * f_2([Ca^{2+}]) * e^{E_a/RT}$$

..... (12)

where

t_g = sol-gel transition time (hours)

[EDTA] = 0.1M EDTA concentration (wt%)

$[Ca^{2+}]$ = calcium ion concentration (wt%)

The point to be noted here is that the unified sol-gel transition time is a function of only EDTA concentration, divalent ion (Ca^{2+}) concentration and temperature, and not the silicate concentration and the citric acid concentration in the sample volume. This is due to the fact

that the silicate concentration and the citric acid concentration have been kept constant for all the experiments performed. In all the experiments performed, the activator was added under agitation to the silicate system to avoid the production of local gel aggregates.

The equation is developed from three individual functions, where the sol-gel transition time is a function of only one when the others are kept constant. Stavland et al. (2011) stated that the temperature dependency is given by Arrhenius equation for most of the chemical reactions.

Hence, dividing the above equation into three different parts gives the following relations:

1. Sol-gel transition time as a function of EDTA concentration only

$$t_g = A_1 * f_1([EDTA]) \quad \text{..... (13)}$$

2. Sol-gel transition time as a function of $CaCl^2$ concentration only

$$t_g = A_2 * f_2([Ca^{2+}]) \quad \text{..... (14)}$$

3. Sol-gel transition time as a function temperature only

$$t_g = A_3 * e^{E_a/RT} \quad \text{..... (15)}$$

All the constants and equations are determined experimentally for each system.

4.6.1. SODIUM SILICATE SYSTEM

i. Effect of 0.1M EDTA concentration on sol-gel transition time

Case (c) described above gives the effect of the different concentrations of 0.1M EDTA when the sodium silicate concentration and the citric acid concentration are kept constant and there are no calcium ions in the solution.

The sol-gel transition time experimental data is plotted against the percentage of 0.1M EDTA in the sample volume. The best-fit trendline is an exponential function denoted by the following equation:

$$t_g = A_1 * e^{\alpha[EDTA]} \quad \text{..... (16)}$$

where the values of the constants A_1 and α at different temperatures, and the fitting coefficients R^2 for the best-fit trendline are given in table 19.

Temperature (°C)	A_1	α	R^2
80	0.454	-0.18	0.988
60	2.271	-0.31	0.923
40	7.663	-0.47	0.972

Table 19: Values of A_1 and α, and the fitting coefficients for the trendline depicting the effect of 0.1M EDTA concentration on sol-gel transition time at different temperatures for the sodium silicate system

Here [EDTA] denotes the concentration of 0.1M EDTA in weight % and the value of R^2 gives a measure of how well the regression line approximates the experimentally obtained data.

ii. Effect of 0.1M $CaCl_2$ concentration on sol-gel transition time

Case (a) described above gives the effect of different concentrations of calcium ions in the sample volume when the sodium silicate concentration and the citric acid concentration are kept constant and there is no EDTA activator in the solution.

The sol-gel transition time experimental data is plotted against the percentage of 0.1M $CaCl_2$ in the sample volume. The best-fit trendline is an exponential function denoted by the following equation:

$$t_g = A_2 * e^{\beta[Ca^{2+}]} \quad \text{..... (17)}$$

where the values of the constants A_2 and β at different temperatures, and the fitting coefficients R^2 for the best-fit trendline are given in table 20.

Temperature (°C)	A_2	β	R^2
80	0.447	-7.70	0.957
60	1.926	-14.2	0.973
40	5.685	-14.0	0.997

Table 20: Values of A_2 and β, and the fitting coefficients for the trendline depicting the effect of 0.1M $CaCl_2$ concentration on sol-gel transition time at different temperatures for the sodium silicate system

Here $[Ca^{2+}]$ denotes the concentration of 0.1M $CaCl_2$ in weight %.

iii. Temperature effects

There have been a large number of studies conducted so far to establish the effect of temperature on the sol-gel transition time (Stavland et al., 2011; Bøye et al., 2011) and, without exception, all studies have shown that temperature accelerates the gelation process.

In this work, all the experiments have been performed at three temperatures to study the effect of temperature on the gelation times of the sodium silicate system. Tables 6, 8 and 10 given above have clearly shown that the gelation times are reduced significantly when the temperatures are increased, which confirms the results of previous studies. The plot of sol-gel transition time and inverse of absolute temperature for different samples with the sodium silicate system is given in figure 22.

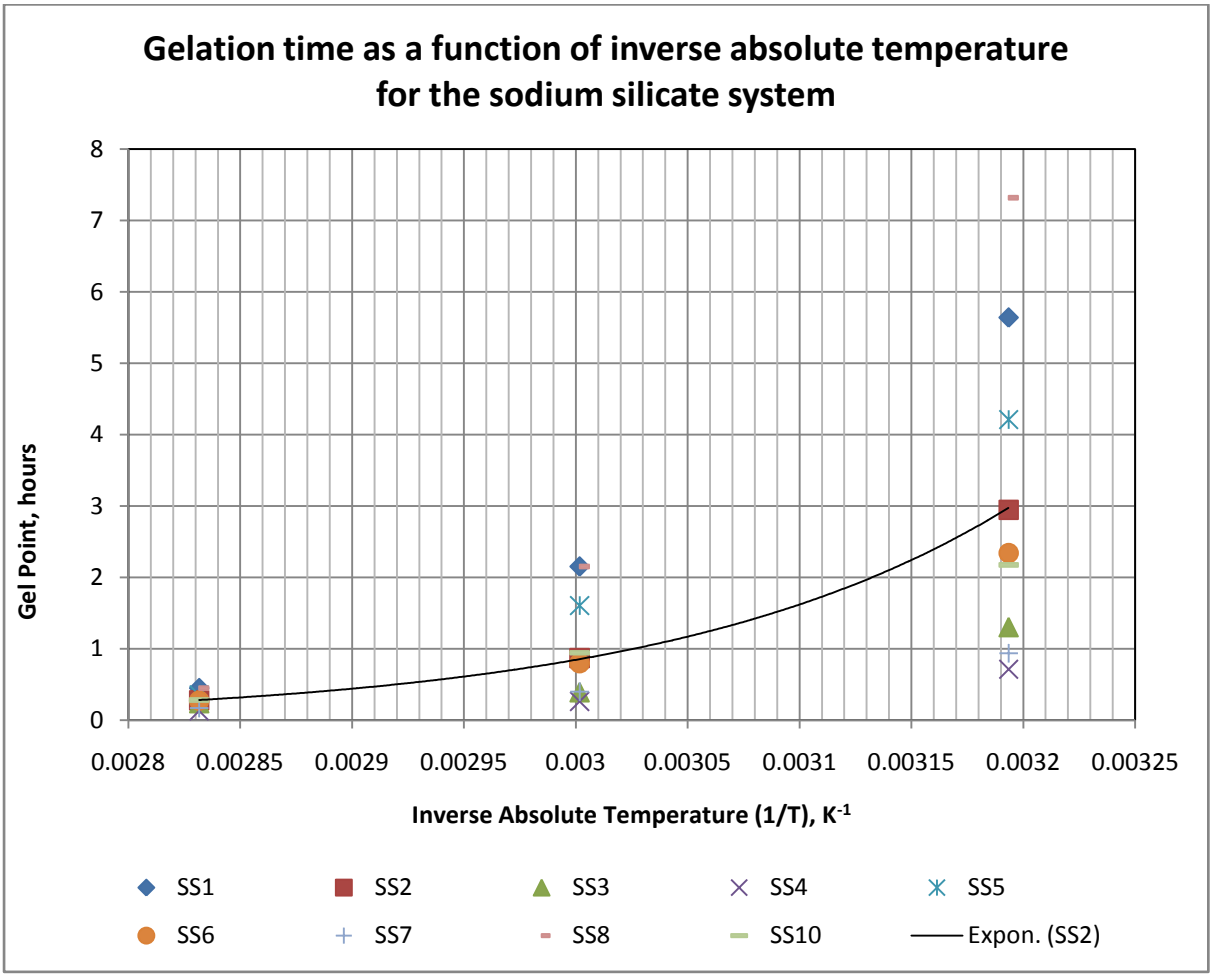

Figure 22: Gelation time as a function of inverse absolute temperature for the sodium silicate system

The temperature dependency is best described by the Arrhenius equation (Stavland et al., 2011). By comparing the gelation time with the inverse absolute temperature, figure 22 shows an exponential relationship for temperatures down to 40°C for the sodium silicate system. The calculated activation energies varied from 38 to 64 kJ/mole. The average activation energy of 54 kJ/mole has been taken into account here. As stated by Stavland et al. (2011), temperature dependency is more complicated than predicted by the Arrhenius equation. The temperature dependency for the gelation times for the sodium silicate system is given below:

$$t_g = A_3 * e^{E_a/RT} = 3 * 10^{-9} e^{6501/T_K}$$

..... (18)

where

$A_3 = 3*10^{-9}$, and

activation energy $E_a = 6501 * 8.314 * 10^{-3} = 54.0493$ kJ/mol.

The correlation fitting coefficient is $R^2 = 0.999$.

Here T_K denotes the absolute temperature (temperature in kelvin).

The correlation and fitting coefficient are shown in the plots in Appendix C.

4.6.1.1. UNIFIED SOL-GEL TRANSITION TIME CORRELATION FOR THE SODIUM SILICATE SYSTEM

The unified sol-gel transition time correlation is the combination of the three equations above. The correlation for the sodium silicate system at different temperatures is given by:

$$t_g = A * e^{\alpha[EDTA]} * e^{\beta[Ca^{2+}]} * e^{E_a/RT} \quad \text{..... (19)}$$

The value of A is found based on various attempts to match the unified sol-gel transition time correlation with the obtained experiment results at different temperatures (Pham & Hatzignatiou, 2015). The values of the constants A, α and β for the sodium silicate system at different temperatures are given in table 21.

Temperature (°C)	A	α	β
80	$4.12792*10^{-9}$	-0.18	-7.70
60	$5.92115*10^{-9}$	-0.31	-14.2
40	$4.97861*10^{-9}$	-0.47	-14.0

Table 21: Values of A, α and β in the unified sol-gel transition time correlations at different temperatures for the sodium silicate system

and the values of E_a and R for the sodium silicate system at all the temperatures are:

$E_a = 54.0493$ kJ/mol, and

R = 8.314 kJ/mol.K

4.6.2. POTASSIUM SILICATE SYSTEM

i. Effect of 0.1M EDTA concentration on sol-gel transition time

Case (c) described above gives the effect of the different concentrations of 0.1M EDTA when the potassium silicate concentration and the citric acid concentration are kept constant and there are no calcium ions in the solution.

The sol-gel transition time experimental data is plotted against the percentage of 0.1M EDTA in the sample volume. The best-fit trendline is an exponential function denoted by the following equation:

$$t_g = A_1 * e^{\alpha[EDTA]} \quad \text{..... (20)}$$

where the values of the constants A_1 and α at different temperatures, and the fitting coefficients R^2 for the best-fit trendline are given in table 22.

Temperature (°C)	A_1	α	R^2
80	0.340	-2.98	0.998
60	2.214	-7.97	0.999
40	11.02	-9.29	0.990

Table 22: Values of A_1 and α, and the fitting coefficients for the trendline depicting the effect of 0.1M EDTA concentration on sol-gel transition time at different temperatures for the potassium silicate system

Here [EDTA] denotes the concentration of 0.1M EDTA in weight %.

ii. Effect of 0.1M $CaCl_2$ concentration on sol-gel transition time

Case (a) described above gives the effect of different concentrations of calcium ions in the sample volume when the potassium silicate concentration and the citric acid concentration are kept constant and there is no EDTA activator in the solution.

The sol-gel transition time experimental data is plotted against the percentage of 0.1M $CaCl_2$ in the sample volume. The best-fit trendline is an exponential function denoted by the following equation:

$$t_g = A_2 * e^{\beta[Ca^{2+}]} \quad \text{..... (21)}$$

where the values of the constants A_2 and β at different temperatures, and the fitting coefficients R^2 for the best-fit trendline are given in table 23.

Temperature (°C)	A_2	β	R^2
80	0.350	-6.93	0.933
60	2.115	-10.5	0.979
40	9.683	-13.4	0.997

Table 23: Values of A_2 and β, and the fitting coefficients for the trendline depicting the effect of 0.1M $CaCl_2$ concentration on sol-gel transition time at different temperatures for the potassium silicate system

Here $[Ca^{2+}]$ denotes the concentration of 0.1M $CaCl_2$ in weight %.

iii. Temperature effects

Just like in the previously described experiments for the sodium silicate system, the experiments for the potassium silicate system have also been performed at three temperatures to study the effect of temperature on the gelation times. Tables 12, 14 and 16 given above have clearly shown that the gelation times are reduced significantly when the temperatures are increased. The plot of sol-gel transition time and inverse of absolute temperature for different samples with potassium silicate is given in figure 23.

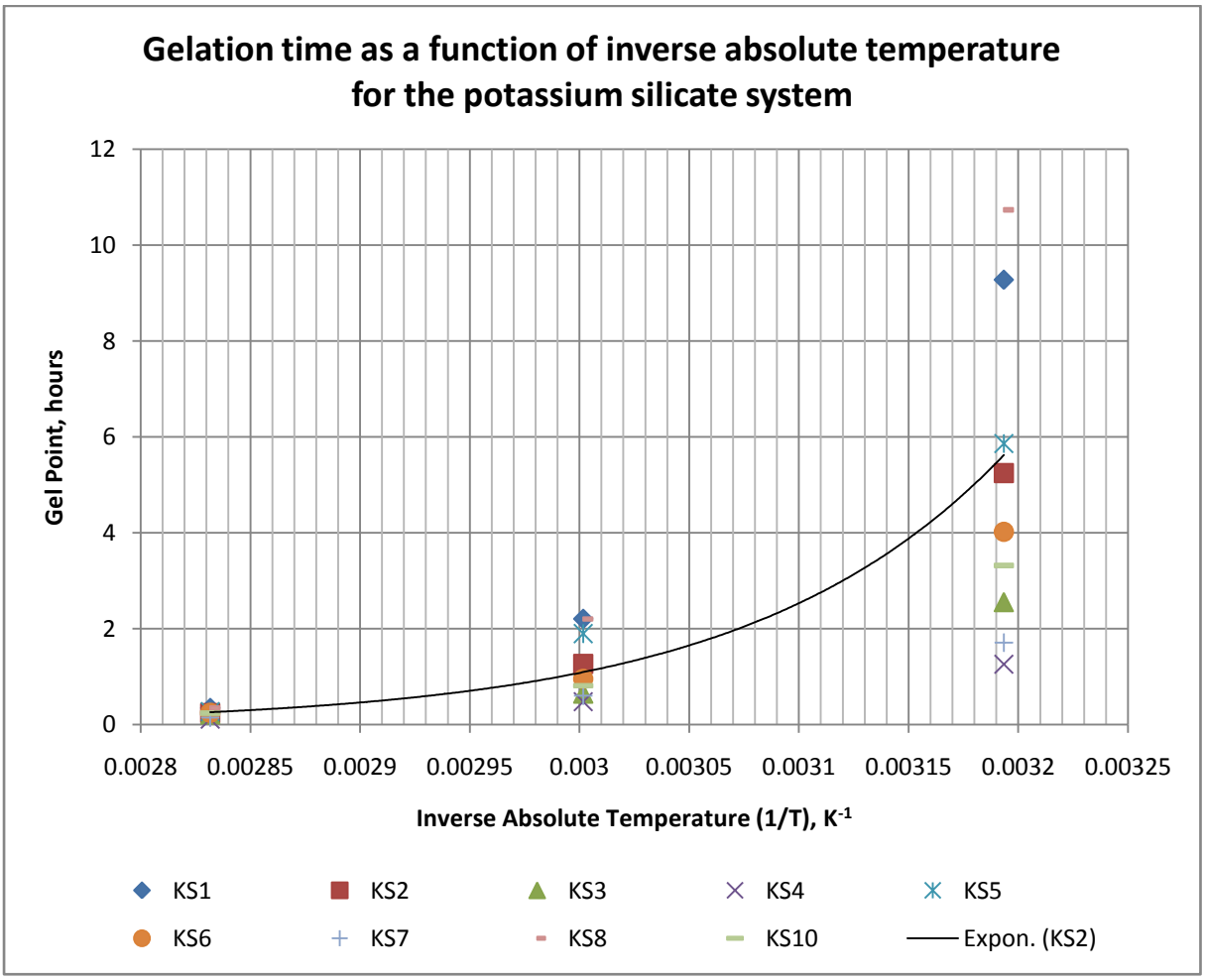

Figure 23: Gelation time as a function of inverse absolute temperature for the potassium silicate system

By comparing the gelation time with the inverse absolute temperature, figure 23 shows an exponential relationship for temperatures down to 40°C for the potassium silicate system. The calculated activation energies varied from 55 to 80 kJ/mole. The average activation energy of 71 kJ/mole has been taken into account here. The temperature dependency for the gelation times for the potassium silicate system is given below:

$$t_g = A_3 * e^{E_a/RT} = 8 * 10^{-12} e^{8556/T_K} \quad \text{..... (22)}$$

where

$A_3 = 8*10^{-12}$, and

activation energy $E_a = 8556 * 8.314 * 10^{-3} = 71.1346$ kJ/mol.

The correlation fitting coefficient is $R^2 = 0.993$.

Here T_K denotes the absolute temperature (temperature in kelvin).

The correlation and fitting coefficient are shown in the plots in Appendix C.

4.6.2.1. UNIFIED SOL-GEL TRANSITION TIME CORRELATION FOR THE POTASSIUM SILICATE SYSTEM

The unified sol-gel transition time correlation is the combination of the three equations above. The correlation for the potassium silicate system at different temperatures is given by:

$$t_g = A * e^{\alpha[EDTA]} * e^{\beta[Ca^{2+}]} * e^{E_a/RT} \quad \text{..... (23)}$$

The value of A is found based on various attempts to match the unified sol-gel transition time correlation with the obtained experiment results at different temperatures (Pham & Hatzignatiou, 2015). The values of the constants A, α and β for the potassium silicate system at different temperatures are given in table 24.

Temperature (°C)	A	α	β
80	$1.04041*10^{-11}$	-2.98	-6.93
60	$1.52038*10^{-11}$	-7.97	-10.5
40	$1.40874*10^{-11}$	-9.29	-13.4

Table 24: Values of A, α and β in the unified sol-gel transition time correlations at different temperatures for the potassium silicate system

and the values of E_a and R for the potassium silicate system at all the temperatures are:

$E_a = 71.1346$ kJ/mol, and

R = 8.314 kJ/mol.K

4.7. GEL STRENGTH TESTS

Amplitude Sweep (AS) mode was applied to assess the formed gel's strength that it can withstand against applied external forces. Two different procedures were followed:

1. Running the gel strength tests after almost identical period of time (10 to 12 minutes) after sol-gel transition time for all the samples
2. Running the gel strength test for one sample at temperatures 40°C, 60°C and 80°C after the gel has reached a particular value of apparent viscosity after the sol-gel transition time.

The strength of the gel obtained by following the two procedures are plotted against percentage of 0.1M $CaCl_2$ in the sample volume. Table 25 gives the strength of the gel estimated by the above-mentioned two procedures at the three temperatures for the potassium silicate system when mixed with constant 10% citric acid activator concentration and varying 0.1M $CaCl_2$ concentration.

POTASSIUM SILICATE SAMPLES PREPARED WITH 10% CITRIC ACID ACTIVATOR AND 0.1M $CaCl_2$ CONCENTRATION				
METHOD APPLIED	**Sample Number**	**Strength of gel at 80°C**	**Strength of gel at 60°C**	**Strength of gel at 40°C**
		Pa	**Pa**	**Pa**
Identical Times after sol-gel transition times	KS1	104.02	79.45	1.23
	KS2	186.90	134.10	3.77
	KS3	237.38	214.14	10.60
	KS4	**323.01**	**517.33**	**11.44**
Identical apparent viscosity after sol-gel transition times	**KS4**	**270.01**	**385.65**	**43.47**

Table 25: Strength of gels calculated by the two procedures for the potassium silicate samples prepared with constant 10% citric acid activator concentration and varying 0.1M $CaCl_2$ concentration

Both procedures were followed for the calculation of strength of gel for the sample KS4. Table 26 below gives the viscosity values of the samples of KS4 at different temperatures after sol-gel transition times when the strength test was started for the second procedure described above.

SAMPLE NUMBER KS4		80°C	60°C	40°C
Strength of gel	**Pa**	270.01	385.65	43.47
Apparent viscosity	**Pa.s**	32.97	22.64	21.53

Table 26: Apparent viscosity and maximum gel strength for the sample KS4 at the three temperature readings

As can be seen from the values of viscosity, the tests were done by keeping a control over the apparent viscosity values of the samples after the sol-gel transition times.

Figure 24 shows the strength of the gels calculated by the two different procedures at the three temperatures as a function of percentage of 0.1M $CaCl_2$ in a potassium silicate

solution containing 10% citric acid activator. Please note that in the plot, the word 'microgel' is being used instead of 'gel', the reason for which is described later in this section.

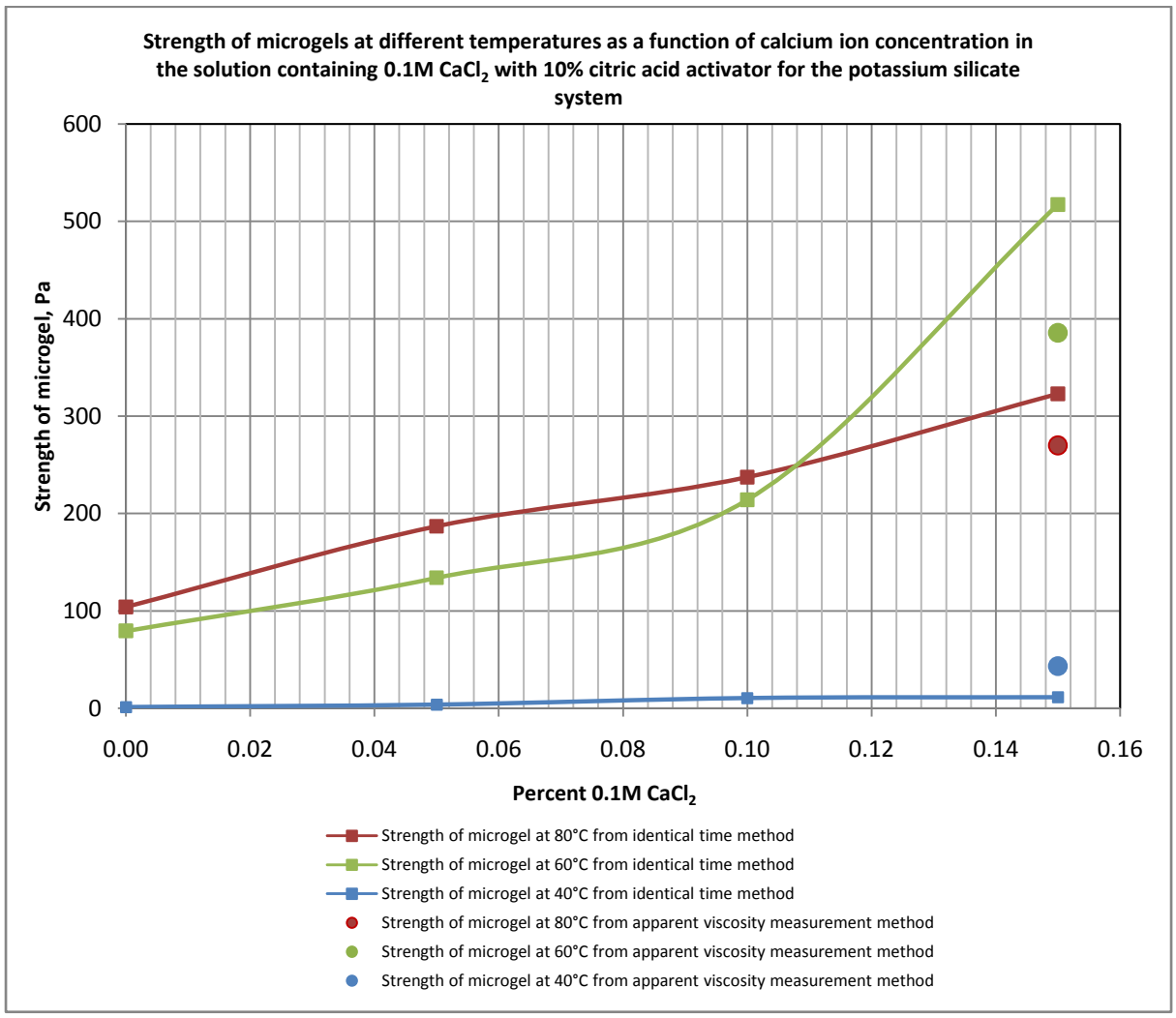

Figure 24: Plot showing strength of microgels estimated by two different procedures at different temperatures as a function of calcium ion concentration for the potassium silicate system

In this plot, curves with square markers denote the strength of microgels estimated by applying the method of running the strength tests for identical times after sol-gel transition times. The circle markers denote the points for the sample tested where the other method of running the strength tests for identical apparent viscosities after sol-gel transition times was applied.

As is clearly evident from the plot and as expected, the gel strengths for the samples at minimum temperature (40°C) were found to be the lowest by both procedures, but at higher temperatures (60°C and 80°C), an unexpected behaviour was observed. For low concentrations of calcium ions in the solution, the gel strengths at 60°C were lower than the gel strengths at 80°C, but when the concentration of calcium ions crossed a particular value, the gel strength of the sample at 60°C spiked and crossed the gel strength at 80°C. This point is noticed for both procedures followed as can be seen from the plot. A similar behaviour was observed when the strength tests were done for the samples with constant

10% citric acid activator and varying 0.1M EDTA concentrations in the sample volumes. There is no obvious explanation for this behaviour, but it could possibly be caused by the lower viscosity values at the start of the strength tests (in the range of 20 to 35 cP). Therefore, a strong gel may not have been formed yet at these viscosity values and there were only microgels present in the solution, which resulted in this behaviour. Thus, these values of gel strengths cannot be considered as true values of their maximum gel strength as they are likely to be still in a state in between solution and strong gel. This may be described as a state where microgels have formed, which is why the expression 'strength of microgel' is being used in the plot. For the sample at 40°C, it took 45 minutes after sol-gel transition time to reach the mentioned apparent viscosity value and hence it is showing more gel strength compared to the one estimated by the first procedure where the strength test was started after 10 minutes of sol-gel transition time. For the samples at 60°C and 80°C, it took 7 minutes and 2 minutes respectively after sol-gel transition times to reach the mentioned apparent viscosity values. That is why it is believed that the sample had still not formed a strong gel. If the experiment had continued for longer, a stronger gel would have formed and then the gel strengths at 80°C would have been expected to cross the gel strengths at 60°C.

Two recommendations are being presented here for the further studies to get a firm stand on this kind of behaviour:

1. The samples have to be kept for more time (ranging from a few minutes at higher temperatures to maybe a few hours at lower temperatures) after the sol-gel transition times to reach high apparent viscosity values (more than 500 Pa.s) where it is expected that strong gels will be formed.
2. More tests with high concentrations of calcium ions or EDTA are recommended to observe the trend of the maximum gel strengths beyond the tested concentrations to get a better picture of how the samples are behaving after sol-gel transition times for high concentrations of divalent ions or EDTA.

5. EXPERIMENTAL WORK - BULK MEASUREMENTS

This section covers the results for the bulk measurements performed for different polymers when mixed with different crosslinkers, followed by the advantages of associative polymers over the conventional polyacrylamides.

5.1. PREPARATION OF DIFFERENT SOLUTIONS

5.1.1. BRINE

Filtered 1M NaCl brine was used for the experimental purpose. 0.45 µm filter paper was used for the filtering purpose.

5.1.2. ACRYLAMIDO-METHYL-PROPANE SULFONATE (AMPS) POLYMER SOLUTION

To prepare a 5000 PPM of AMPS polymer solution, 1.5 grams of polymer was added to 300 grams of 1M NaCl brine solution. The polymer was added to the brine solution under agitation at high RPM (~700 RPM) and the mixture was kept stirring at this rate for 1 hour. The RPM was reduced to 300 for the next two hours and then the mixture was kept on the magnetic stirrer overnight.

5.1.3. ANIONIC HYDROLYSED POLYACRYLAMIDE (HPAM) POLYMER SOLUTION

A similar procedure was followed for the preparation of 5000 PPM of HPAM polymer solution as was followed for AMPS polymer solution.

5.1.4. ASSOCIATIVE (AS) POLYMER SOLUTION

A 10000 PPM polymer solution of associative polymer was prepared by adding 3 grams of this polymer to 300 grams of 1M NaCl solution under agitation. The mixture was kept stirring at 300 RPM for 30 minutes and then at 200 RPM overnight.

5.1.5. CHROMIUM (III) CROSSLINKER

A 10% Cr (III) solution of 100000 PPM was prepared by mixing the required amount of chromium (III) acetate hydroxide powder to distilled water. The mixture was kept on a magnetic stirrer for ~4 hours for proper mixing.

5.1.6. ZIRCONIUM (III) CROSSLINKER

A 10% Zr (III) solution of 100000 PPM concentration was available for crosslinking purposes.

5.1.7. CHITOSAN CROSSLINKER

The chitosan crosslinker used in all the experiments is the chitosan manufactured from shrimp shells. A 1.5% chitosan crosslinker solution was prepared by adding 7.5 grams of commercial solid chitosan sample to 500 grams of 1% acetic acid (Reddy et al., 2003). The solution was kept stirring at a high RPM of 700 for the first one hour and then at 300 for the next ~12 hours. The solid samples available for chitosan were insoluble in distilled water. The viscosities of the solutions formed by mixing chitosan crosslinker with polymer solutions depended on the degree of de-acetylation of the crosslinker.

5.1.8. PEI (POLYETHYLENIMINE) CROSSLINKER

A 1% PEI crosslinker solution was prepared by adding 2 grams of PEI crosslinker to 200 grams of distilled water. The solution was kept on a magnetic stirrer for 2 hours for proper mixing. Two different 1% PEI solutions were prepared. The main difference between the two mother solutions has been given in the description of their physical and chemical properties.

5.2. BULK MEASUREMENTS

The gel bottle testing method was applied for the bulk measurements. The gelant samples were stored in the test tubes sealed with a screw cap and were kept in temperature-controlled ovens at 40°C, 60°C and 80°C. The test tubes were visually inspected periodically at these temperatures for pre-gelation behaviour, gel formation, post gelation behaviour and/or gel syneresis.

Three different kinds of polymers were tested with different crosslinkers as described above. This section deals with the results of the bulk measurements for these polymers.

Please note that the gelation times noted down in this section are as per visual inspection of the test tubes periodically. They have been defined as per the gel codes defined by Stavland et al. (2011). The gelation time for any sample noted down is the time when the gel code reached 2.75 for that particular sample. Another point to be noted here is that for some samples, the status after a month or two is mentioned as (2) or (2.5). This means that the particular sample is at gel code 2 or 2.5 after keeping the sample in the oven for one month or two (as mentioned in the title of that column in the tables) at a particular temperature.

5.2.1. ASSOCIATIVE POLYMERS

Four different kinds of crosslinkers were used to test the associative polymers for their gel-forming capabilities. These crosslinkers include: Zirconium Zr (III), Chromium Cr (III), Chitosan (1.5 wt%) and PEI (1 wt%).

5.2.1.1. ASSOCIATIVE POLYMER WITH Zr (III) CROSSLINKER

The gelant sample mixtures of 10000 PPM associative polymer and Zr (III) crosslinker have shown positive results at the temperatures of 80°C. Table 27 gives the gelation time in hours, viscosity in cP and pH of the samples prepared with associative polymer and Zr (III) crosslinker.

ASSOCIATIVE POLYMER

CROSSLINKER - Zr (III)

Crosslinker concentration (PPM)	Polymer concentration (PPM)	Viscosity (cP)	pH	Gelation time (hr) - 80°C	Status of the sample at 80°C after ~2 months	Gelation time (hr) - 60°C	Status of the sample at 60°C after ~2 months	Observations/ Comments
	10000	556	-					Mother solution
100	2000	20.3	5.31	-	(0.5)	-	-	
250	2000	20.1	5.43	80.5	(2)	-	-	
500	4000	96.9	-	48	(1.5), shrinkage to 80% of original volume	91	Rigid gel, no shrinkage	Soft elastic gel
	2000	25.1	5.61	114	Rigid gel, shrinkage to 80% of original volume	-	(2.7)	
	1500	13.1	-	443	(0), complete precipitation	-	(0.7)	
	1000	8.1	-	-	(2), shrinkage to 7% of original volume	-	(0.5)	
750	2000	23.2	5.59	213.3	Rigid gel, shrinkage to 80% of original volume	-	(2.6)	
	1500	16.5	-	470.3	(2), shrinkage to 80% of original volume	-	(2.2)	
1000	2000	20.1	5.53	305.5	Rigid gel, shrinkage to 80% of original volume	-	(2.5)	

		1500	13	5.2	-	(2.5)	-	(2.2)	30% shrinkage observed in both samples
		1500	13	4.2	-	(0), complete precipitation	-	-	
	1250	2000	23.7	5.7	329.25	Rigid gel, shrinkage to 99% of original volume	-	-	
	1500	2000	20.6	5.64	354	(2.8)*	-	(2)	
		1000	8.15	-	-	(2), shrinkage to 20% of original volume	-	(0)	
	1750	2000	23.3	5.73	-	(1.5)*	-	-	
	2000	2000	22.2	5.83	-	(2.5)	-	-	
	4000	2000	25.4	5.75	-	(2.5)	-	-	
	10000	2000	19.5	5.62	-	(2)	-	-	Very elastic flowing gel

* denotes status of the sample after 380 hours

Table 27: Gelation times, viscosities and pH values for the samples of associative polymer with zirconium (III) crosslinker at 80°C and 60°C

The sample mixtures with 2000 PPM of polymer concentration offer a favourable viscosity value in the sense that when this concentration of polymer is used for RPM/DPR water-shutoff treatments, it can be easily injected into the porous media without blocking the flow pathways up to the surface of the well. The sample mixtures with high concentrations of polymer, such as 4000 PPM, are very viscous and thus need to have a very high injection pressure to inject them into the formation. They can even block the pathways which can subsequently lead to a significant decrease in the recovery of oil.

The mixtures with 2000 PPM of polymer concentration have also shown the formation of a good rigid gel (with a gel code of over 2.75 and most of the samples even going to the maximum gel code of 3). It is clear from table 27 that the gel forms faster at higher temperatures.

One very important observation that has been made from the sample mixtures of associative polymer with Zr (III) crosslinker is that gel syneresis plays a very important role in determining the condition of the gel after a certain period of time. This fact has to be kept in mind while applying any polymer gel for water-shutoff purposes. A lot of samples have shown significant shrinkage, as much as 95% of the original volume of the sample, when kept in the oven at a particular temperature for a long time.

Figure 25 gives the gelation times for various samples prepared by mixing 2000 PPM of associative polymer with Zr (III) crosslinker and kept in the oven at 80°C.

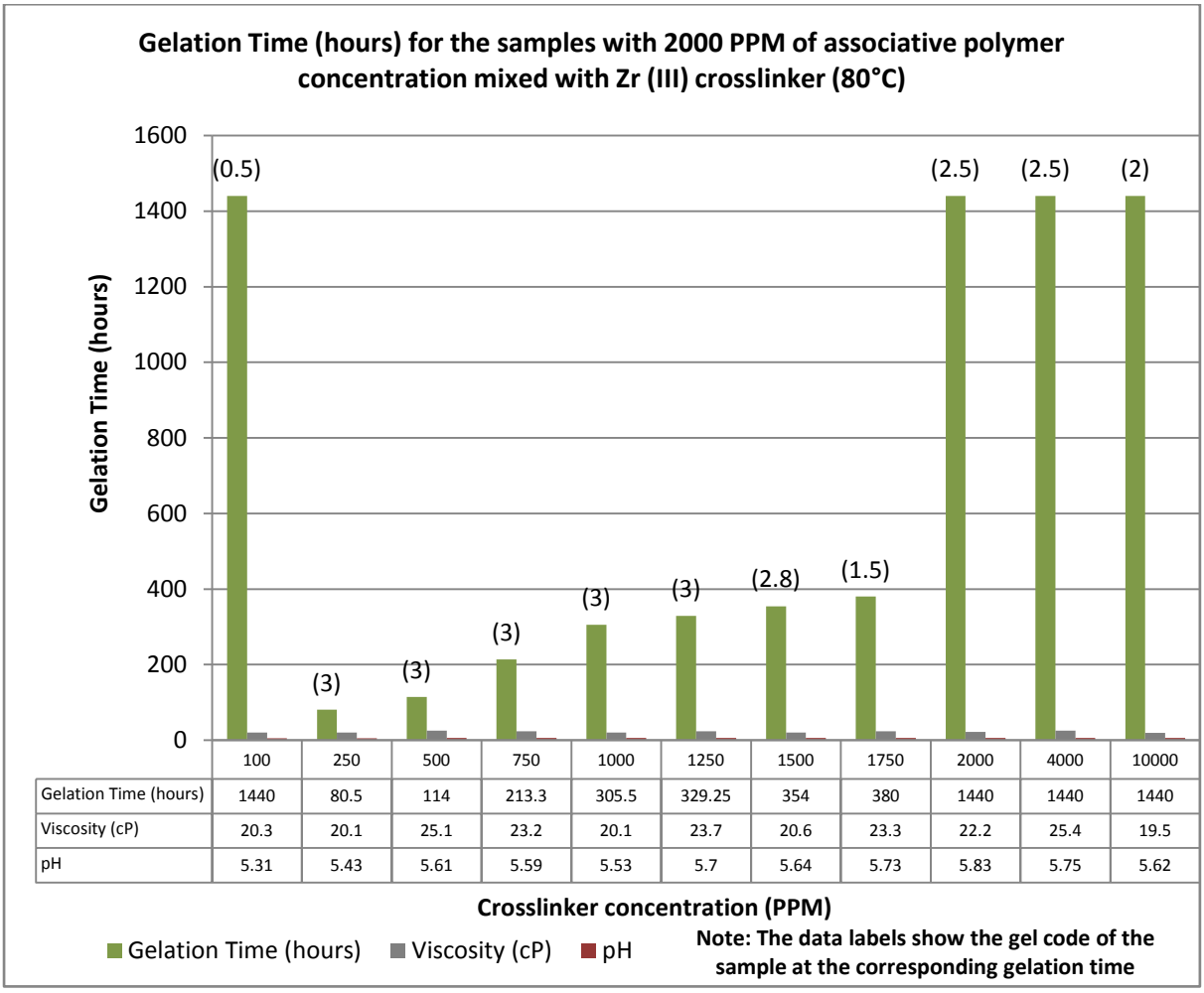

	100	250	500	750	1000	1250	1500	1750	2000	4000	10000
Gelation Time (hours)	1440	80.5	114	213.3	305.5	329.25	354	380	1440	1440	1440
Viscosity (cP)	20.3	20.1	25.1	23.2	20.1	23.7	20.6	23.3	22.2	25.4	19.5
pH	5.31	5.43	5.61	5.59	5.53	5.7	5.64	5.73	5.83	5.75	5.62

Figure 25: Gelation time for the samples with 2000 PPM of associative polymer as a function of Zr (III) crosslinker concentration (80°C)

The data labels in the plot show the gel code of the sample at the corresponding gelation time for the corresponding concentration of crosslinker mixed with 2000 PPM of polymer. Please note that the samples of 2000 PPM of polymer crosslinked to 1500 PPM and 1750 PPM of zirconium (III) show the status after 380 hours of testing. The sample with 1500 PPM of crosslinker is at a gel code of 2.8 after 380 hours (it crossed a gel code of 2.75 after 354 hours and that is why it is taken as a gelled sample) and the sample with 1750 PPM crosslinker is at a gel code of 1.5 after 380 hours. If the tests had continued for more time, these samples might have reached the gel code of 3.

As is visible from the plot, the sample that has a very low concentration of crosslinker (100 PPM) do not form a gel with 2000 PPM of associative polymer. This is due to the fact that not enough crosslinker is available for the polymer to form a closed network and a 'gel-like' structure. When Zr (III) crosslinker concentration is increased in the samples, it starts forming a gel with 2000 PPM of associative polymer. 250 PPM of crosslinker concentration has been found to be adequate to start forming the gel with 2000 PPM of associative polymer. As the crosslinker concentration is further increased, the gelation time is following an increasing trend until no more gel is formed with 2000 PPM of polymer concentration

when Zr (III) crosslinker concentration becomes equal to or more than 1750 PPM. This is due to very high concentrations of crosslinker available that do not allow the polymer to mix properly with the crosslinker to form the gel. Especially for the samples with 2000 PPM of polymer concentration, the different samples have not shown a lot of shrinkage when kept at 80°C for a long time, which can be taken as an advantage over the other polymer concentrations while designing a polymer gel treatment for water-shutoff purposes.

A correlation has been derived between the crosslinker concentration (250 PPM to 1500 PPM concentrations only because these have shown to form a gel with 2000 PPM of polymer concentration at 80°C) and the gelation time for 2000 PPM of polymer concentration at 80°C. This correlation is the best-fit to the experimental data and is given below:

$$t_g = 2 * 10^{-8}[CL]^4 - 0.111[CL]^2 + 24.34[CL] - 1077 \quad \text{..... (24)}$$

where

t_g = gelation time (hours)

[CL] = crosslinker concentration (PPM)

The correlation fitting coefficient is R^2 = 0.998 which shows an almost perfect match with the experimentally measured data.

Figure 26 gives the gel code for various samples prepared by mixing 2000 PPM of associative polymer with Zr (III) crosslinker and keeping in the oven at 60°C for ~2 months.

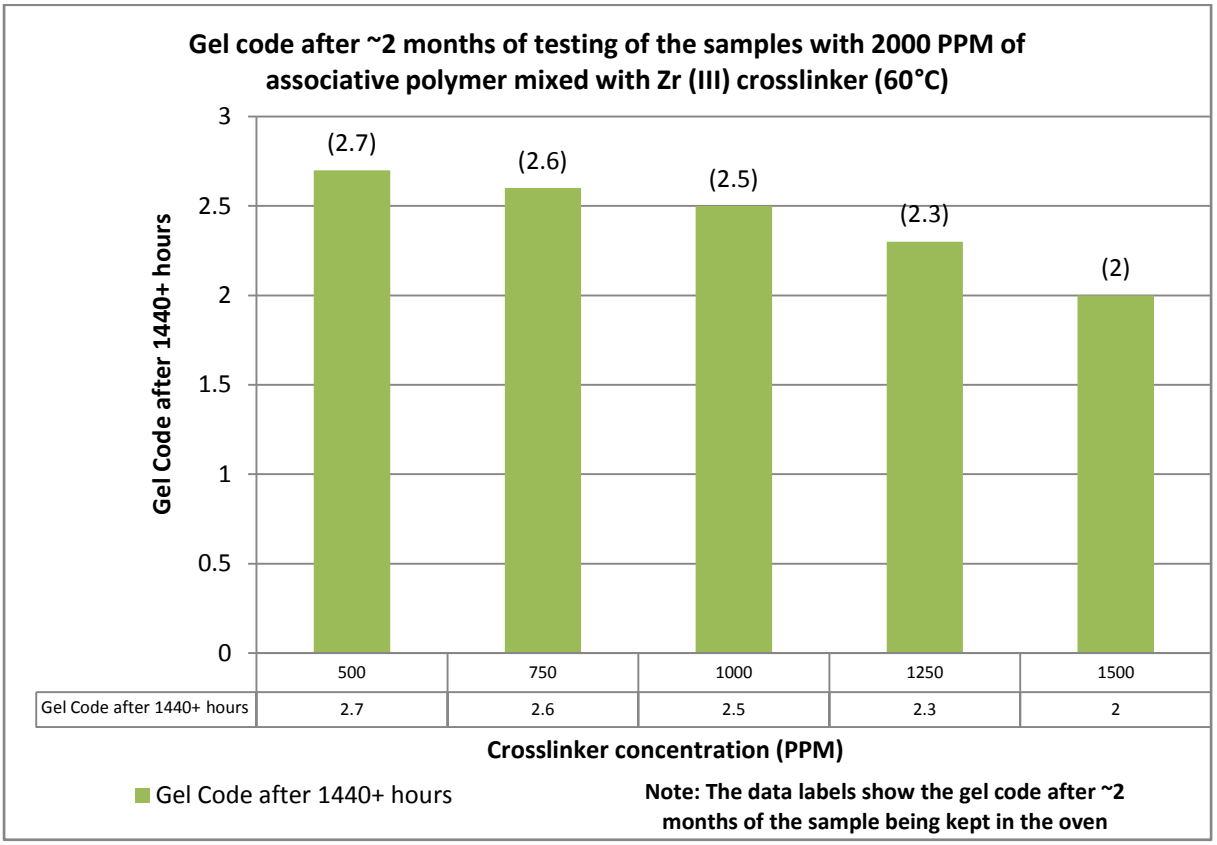

Figure 26: Gel code after ~2 months of testing of the samples with 2000 PPM of associative polymer as a function of Zr (III) crosslinker concentration (60°C)

It is clear from the plot that even though the gelation times are very long at 60°C compared to the samples at 80°C, it is still following the same trend that is seen for the samples at 80°C. The sample with 500 PPM of crosslinker is showing a gel code of 2.7 and the samples with increasing concentrations of crosslinker are following a decreasing trend in the gel code, meaning it will take more time than the sample with 500 PPM of Zr (III) crosslinker to form a rigid gel.

5.2.1.2. ASSOCIATIVE POLYMER WITH Cr (III) CROSSLINKER

Table 28 gives the gelation time in hours and viscosity in cP for the samples prepared with associative polymer and Cr (III) crosslinker.

ASSOCIATIVE POLYMER	CROSSLINKER - Cr (III)									
	Crosslinker concentration (PPM)	Polymer concentration (PPM)	Viscosity (cP)	Gelation time (hr) - 80°C	Status of the sample at 80°C after ~2 months	Gelation time (hr) - 60°C	Status of the sample at 60°C after ~2 months	Gelation time (hr) - 40°C	Status of the sample at 40°C after ~2 months	Observations /Comments
		10000	556							Mother solution
	500	4000	109	72	Soft elastic gel	96	Soft elastic gel	-	(2)	
		2000	25.3	-	(0)	-	(2)	-	-	
		1500	15.3	-	(0)	-	(0.5)	-	-	
		1000	7.57	-	(0)	-	(0)	-	(0)	
	1000	2000	26	-	(0.5), immersed gel particles	-	(2.1)	-	(1)	
		1500	17	-	(0), complete precipitation	-	(0)	-	(0)	
	1500	4000	104	166	(0.5), non-stabilised gel	~1200	stable gel	-	(1.5)	
		2000	24.5	-	(1), shrinkage to 10% of original volume	-	(2)	-	-	
		1500	15.9	-	(1), shrinkage to 10% of original volume	-	(0.3)	-	-	
		1000	7.49	-	(1.5), shrinkage to 2% of original volume	-	(0)	-	-	
	4000	2000	24.3	-	(1), shrinkage to 50% of original volume	-	-	-	-	
	10000	2000	24.1	-	(0.5)	-	-	-	-	

Table 28: Gelation times and viscosities for the samples of associative polymer with chromium (III) crosslinker at 80°C, 60°C and 40°C

As can be seen in table 28, the only samples that formed a hard gel with Cr (III) crosslinker were the ones with very high polymer concentration (4000 PPM) for which the viscosity values were very high. For most of the samples at other polymer concentrations, the sample remained almost in the solution form even after two months of testing period. There were a few samples with 2000 PPM of polymer concentration which showed a weak gel (with a gel code 2) at 60°C but due to high gelation times without the formation of a strong gel, they are still not considered to be suitable to be used in the real field scenarios. The plot for the gelation time in hours as a function of Cr(III) crosslinker concentration mixed with 2000 PPM of associative polymer at 80°C is given in the figure 27.

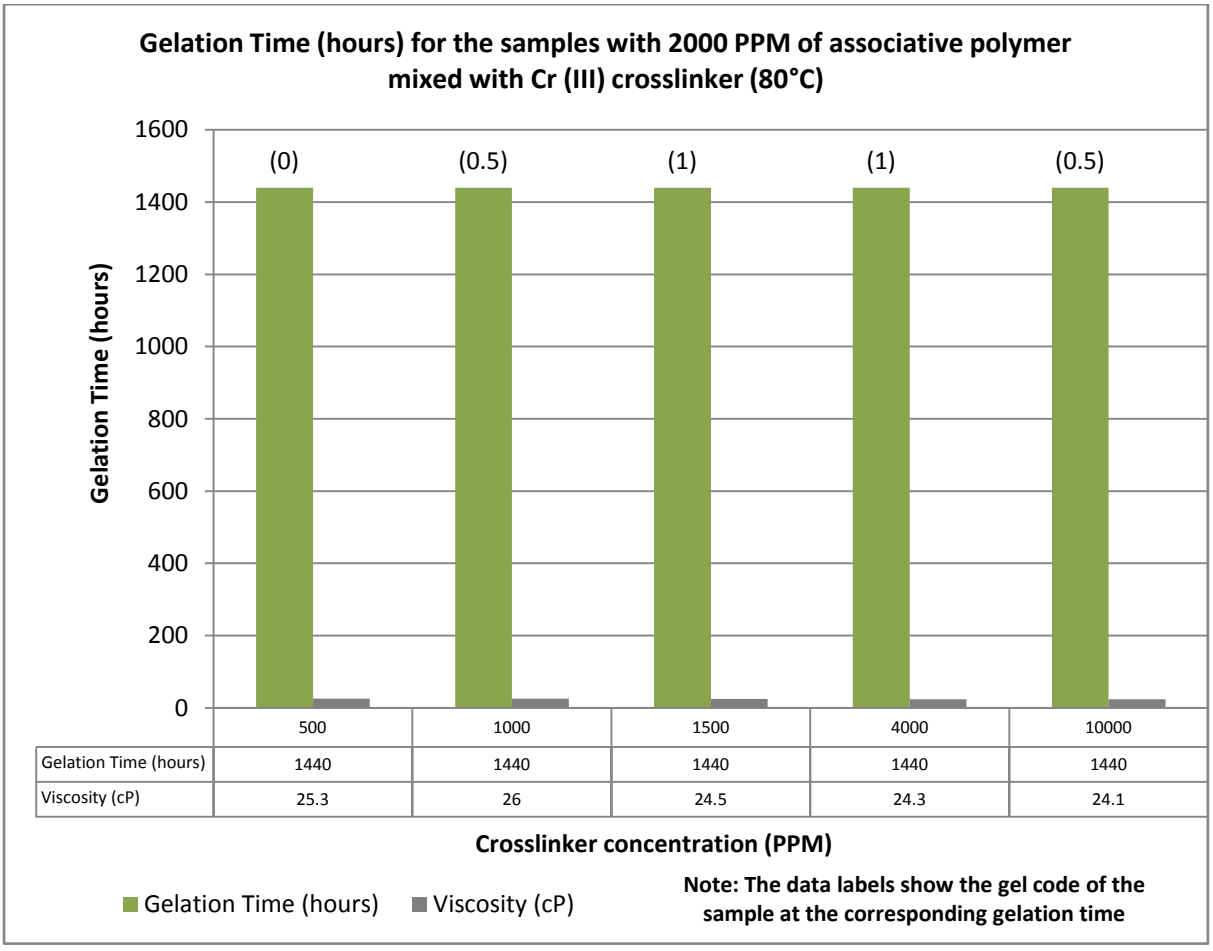

Figure 27: Gelation time for the samples with 2000 PPM of associative polymer as a function of Cr (III) crosslinker concentration (80°C)

The data labels in the plot show the gel code of the sample at the corresponding gelation time for the corresponding concentration of crosslinker mixed with 2000 PPM of Cr (III) crosslinker. For none of the samples, the gel code is above 1 even after two months of testing, which clearly states that Cr (III) crosslinker is not suitable for polymer gel treatments while using associative polymers.

5.2.1.3. ASSOCIATIVE POLYMER WITH CHITOSAN (1.5 WT%) CROSSLINKER

Table 29 gives the gelation time in hours, viscosity in cP and pH for the samples prepared by mixing different concentrations of associative polymer with different concentrations of chitosan (1.5 wt%) crosslinker.

ASSOCIATIVE POLYMER	CROSSLINKER - CHITOSAN (1.5 WT%)						
	Crosslinker concentration (PPM)	**Polymer concentration (PPM)**	**Viscosity (cP)**	**pH**	**Gelation time (hr) - 80°C**	**Status of the sample at 80°C after ~1.5 months**	**Observations/Comments**
		10000	556				Mother solution
	500	4000	47.8	4.24	-	(0)	Weak gel observed on addition of polymer to crosslinker at room temperature
		4000	99.7	6.89	-	(0), complete precipitation	
		1500	3.77	4.3	-	(2.5), shrinkage to 3% of original volume	
	750	2000	3.77	4.26	-	(2), shrinkage to 3% of original volume	
	1000	2000	2.57	4.28	-	(2), shrinkage to 15% of original volume	
		2000	16.9	6.46	-	(0.5)	
		2000	25.1	7.9	-	(0), complete precipitation	
		1500	1.96	4.28	-	(2), shrinkage to 15% of original volume	
		1500	2.34	6		(0)	
	1500	4000	7.76	4.2	-	(2), shrinkage to 10% of original volume	

		4000	26.3	5.99	-	(0.5)	
		3000	2.96	4.26	-	(1.5), shrinkage to 20% of original volume	
		3000	4.24	5.4	-	(0), complete precipitation	
		3000	50	7.69	-	(0), complete precipitation	
	10000	2000	80.7	4.33	-	(2.5), shrinkage to 10% of original volume	
		2000	72.5	6.23	-	(2.5), shrinkage to 10% of original volume	Microgels observed on addition of NaOH to increase the pH of the original solution
	4000	2000	5.22	4.26	-	(3), shrinkage to 20% of original volume	Formation of immersed gel particles since the starting made it difficult to precisely note the time when the gel was formed
		2000	5.72	6.14	-	(1.5), shrinkage to 20% of original volume	
		2000	123	8.31	-	(0), complete precipitation	Microgels observed on addition of NaOH to increase the pH of the original solution

Table 29: Gelation times, viscosities and pH for the samples of associative polymer with chitosan (1.5 wt%) crosslinker at 80°C

It can be seen from table 29 that at high concentrations of associative polymer (≥ 3000 PPM) with any concentration of chitosan, no sample has shown any positive result. However, for the samples with low PPM of polymer, even though the gelation times are high, they still have shown the formation of a weak gel (with a gel code ≥ 2). Gel syneresis is a big problem with the chitosan crosslinker. Almost all samples have shown the shrinkage problem and the volumes of the weak gel formed have been reduced by as much as 97% of original volume. Some samples have even completely precipitated. This shows that chitosan may be considered as a good alternative for a crosslinker if the wells can be shut-in for long periods of time after the treatment flooding, but the gel syneresis has to be kept in mind while designing the treatment.

5.2.1.4. ASSOCIATIVE POLYMER WITH PEI (1 WT%) CROSSLINKER

Two different kinds of PEI have been used in this work and their physical and chemical characteristics have already been defined earlier. Table 30 gives the gelation time in hours, viscosity in cP and pH of the samples prepared by mixing different concentrations of associative polymer with different concentrations of Branched PEI (1 wt%) crosslinker.

ASSOCIATIVE POLYMER	CROSSLINKER - BRANCHED PEI (1 WT%)						
	Crosslinker concentration (PPM)	**Polymer concentration (PPM)**	**Viscosity (cP)**	**pH**	**Gelation time (hr) - 80°C**	**Status of the sample at 80°C after ~1 month**	**Observations /Comments**
		10000	556	-			Mother solution
	500	1500	12.7	10.4	-	(0)	
		1500	12.9	6.13	-	(0)	
	1500	2000	20.4	10.59	-	(0)	
		2000	19.5	6.43	-	(0)	

Table 30: Gelation times, viscosities and pH for the samples of associative polymer with Branched PEI (1 wt%) crosslinker at 80°C

A part of the samples prepared were kept in the oven at 80°C at their original pH value. For the rest of the sample, the pH was reduced by adding a few drops of acid to bring it down to the favourable range (between 5.5 and 7.5) where the chances of a gel being formed are higher. These samples were also kept in the oven at 80°C to establish their gel forming capabilities. As is clearly visible from the table, no sample showed any kind of gel formation at 80°C. At the end of the testing period of one month, all the samples were still in solution form and there were no traces of any gel formation. Thus, it can be concluded that Branched PEI (1 wt%) is not a good crosslinker for low concentrations of associative polymers.

The second type of PEI used was Linear PEI. It was also diluted to 1% by weight. Table 31 gives the gelation time in hours, viscosity in cP and pH for the samples prepared by mixing different concentrations of associative polymer with different concentrations of Linear PEI (1 wt%) crosslinker.

ASSOCIATIVE POLYMER	CROSSLINKER - LINEAR PEI (1 WT%)						
	Crosslinker concentration (PPM)	**Polymer concentration (PPM)**	**Viscosity (cP)**	**pH**	**Gelation time (hr) - 80°C**	**Status of the sample at 80°C after ~1 month**	**Observations/Comments**
		10000	556				Mother solution
	500	1500	12.9	10.14	-	(0)	
		1500	7.32	6.73	-	(0)	
	750	2000	20.4	10.17	-	(0)	
		2000	9.32	4.65	-	(0)	
	1000	2000	20	10.45	-	(0)	
		2000	7.1	6.43	-	(0)	
		1500	12.1	10.53	-	(0)	
		1500	4.15	6.81	-	(0)	
	1500	2000	19.5	10.51	-	(0)	
		2000	1.44	4.23	-	A lot of microgels, shrinkage to 10% of original volume	Microgels observed on the addition of acid drops to lower the pH
		1500	12.2	10.47	-	(0)	
		1500	1.63	7.03	-	(2.5), shrinkage to 7% of original volume	Microgels observed on the addition of acid drops to lower the pH
	6000	2000	19.8	10.81	-	(1)	
		2000	1.19	6.31	-	(0)	Microgels observed on the addition of acid drops to lower the pH

Table 31: Gelation times, viscosities and pH for the samples of associative polymer with Linear PEI (1 wt%) crosslinker at 80°C

The same method was applied to the samples prepared with Linear PEI (1 wt%) also. The samples with the original pH value and the reduced pH value were kept in the oven at 80°C to determine their gel-forming capabilities but as can be seen from table 31, no sample showed any sort of gel-formation except for one sample with 1500 PPM of polymer and 1500 PPM of crosslinker at the reduced pH value of 7.03, which showed large shrinkage.

Hence, it is concluded that Linear PEI (1 wt%) is also not a good crosslinker for associative polymers.

5.2.2. ACRYLAMIDO-METHYL-PROPANE SULFONATE (AMPS) POLYMERS

Two different kinds of crosslinkers were used to test the AMPS polymers for their gel-forming capabilities. These crosslinkers are Zirconium Zr (III) and PEI (1 wt%).

5.2.2.1. AMPS POLYMER WITH Zr (III) CROSSLINKER

The AMPS polymer was mixed with various concentrations of Zr (III) crosslinker to check the feasibility of gel formation. Table 32 gives the gelation time in hours, viscosity in cP and pH of the samples prepared with AMPS polymer and Zr (III) crosslinker.

	CROSSLINKER - Zr (III)						
AMPS	**Crosslinker concentration (PPM)**	**Polymer concentration (PPM)**	**Viscosity (cP)**	**pH**	**Gelation time (hr) - 80°C**	**Status of the sample at 80°C after ~1 month**	**Observations/Comments**
		5000					Mother solution
	250	500	2.63	5.4	-	(0), complete precipitation	A lot of microgels observed in less than 24 hours
	500	2000	-	-	-	-	Instantaneous gelation was observed while mixing polymer with crosslinker at room temperature
		1000	-	-	-	-	Instantaneous gelation was observed while mixing polymer with crosslinker at room temperature
	750	2000	-	-	-	-	Instantaneous gelation was observed while mixing polymer with crosslinker at room temperature
	1000	2000	-	-	-	-	Instantaneous gelation was observed while mixing polymer with crosslinker at room temperature

Table 32: Gelation times, viscosities and pH for the samples of AMPS polymer with zirconium (III) crosslinker at 80°C

A very interesting observation is made from the bulk measurement experiments performed between AMPS polymer and Zr (III) crosslinker as can be observed from table 32. For a very low concentration of crosslinker, complete precipitation occurred within a very short span of time. When the concentration of crosslinker was increased, instantaneous gelation occurred at room temperature while mixing the polymer with the crosslinker and this gelation was observed for crosslinker concentrations as high as 1000 PPM. Hence, Zr (III) crosslinker can be used with this type of polymer if instantaneous gelation is required in any case but it cannot be used for water-shutoff treatments in the fields.

5.2.2.2. AMPS POLYMER WITH PEI (1 WT%) CROSSLINKER

Two different kinds of PEI have been tested with AMPS polymer as well. Table 33 gives the gelation time in hours, viscosity in cP and pH of the samples prepared by mixing different concentrations of AMPS polymer with different concentrations of Branched PEI (1 wt%) crosslinker.

AMPS	CROSSLINKER - BRANCHED PEI (1 WT%)						
	Crosslinker concentration (PPM)	**Polymer concentration (PPM)**	**Viscosity (cP)**	**pH**	**Gelation time (hr) - 80°C**	**Status of the sample at 80°C after ~1 month**	**Observations/ Comments**
		5000					Mother solution
	500	1500	11.8	10.42	-	(0)	
		1500	11.6	5.87	-	(0)	
	1500	2000	18.9	10.56	-	(0)	
		2000	18	6.3	-	(0)	

Table 33: Gelation times, viscosities and pH for the samples of AMPS polymer with Branched PEI (1 wt%) crosslinker at 80°C

Samples were kept in the oven at 80°C at both their original pH value and reduced pH value (favourable pH value between 5.5 and 7.5, where the chances of a gel being formed are higher). As is clearly visible from the table, no sample has shown any kind of gel formation at 80°C. At the end of the testing period of one month, all the samples were still in solution form and there were no traces of any gel formation which concludes that Branched PEI (1 wt%) is not a good crosslinker for medium concentrations of AMPS polymers.

Table 34 gives the gelation time in hours, viscosity in cP and pH of the samples prepared by mixing different concentrations of AMPS polymer with different concentrations of Linear PEI (1 wt%) crosslinker.

AMPS	CROSSLINKER - LINEAR PEI (1 WT%)						
	Crosslinker concentration (PPM)	**Polymer concentration (PPM)**	**Viscosity (cP)**	**pH**	**Gelation time (hr) - 80°C**	**Status of the sample at 80°C after ~1 month**	**Observations/ Comments**
		5000					Mother solution
	500	1500	12	10.22	-	(0)	
		1500	12.4	7.16	-	(0)	

Table 34: Gelation times, viscosities and pH for the samples of AMPS polymer with Linear PEI (1 wt%) crosslinker at 80°C

Only one sample was tested with Linear PEI (1 wt%) with 1500 PPM of AMPS polymer and 500 PPM of crosslinker at both original pH and reduced pH but neither of the samples showed any sign of gel formation. More tests with different concentrations of polymer and crosslinker are required for ascertaining the fact if Linear PEI (1 wt%) is a good crosslinker for AMPS polymer or not.

5.2.3. ANIONIC HYDROLYSED POLYACRYLAMIDE (HPAM) POLYMERS

Three different kinds of crosslinkers were used to test the HPAM polymers for their gel-forming capabilities. These crosslinkers are Zirconium Zr (III), Chromium (III) and Branched PEI (1 wt%).

5.2.3.1. HPAM POLYMER WITH Zr (III) CROSSLINKER

A few samples were tested for HPAM polymer with Zr (III) crosslinker. It was found that instantaneous gelation occurred at room temperature when Zr (III) crosslinker is added to 2000 PPM of HPAM polymer for mixing.

5.2.3.2. HPAM POLYMER WITH Cr (III) CROSSLINKER

Table 35 gives the gelation time in hours and viscosity in cP prepared by mixing different concentrations of HPAM polymer with different concentrations of Cr (III) crosslinker.

HPAM	CROSSLINKER - Cr (III)									
	Crosslinker concentration (PPM)	**Polymer concentration (PPM)**	**Viscosity (cP)**	**Gelation time (hr) - 80°C**	**Status of the sample at 80°C after ~1 month**	**Gelation time (hr) - 60°C**	**Status of the sample at 60°C after ~1 month**	**Gelation time (hr) - 40°C**	**Status of the sample at 40°C after ~1 month**	**Observations/ Comments**
		5000	114							Mother solution
	500	4000	110	16	(1.2)	24	(1.9)	120	Rigid gel	Very soft gel at 80°C and 60°C, stable at 40°C
		2500	29.2							Diluted mother solution
		2000	18.9	11	(0.5)	165.9	(1.2), shrinkage to 85-90% of original volume	~1200	(2.7), shrinkage to 50% of original volume	
		1500	11.7	-	(0.5)	-	(0)	-	(1), shrinkage to 5% of original volume	
		1000	6.43	-	(1), immersed gel particles	-	(0.5), immersed gel particles	-	(2.5), shrinkage to 7% of original volume	
	750	1500	10.9	-	(1), immersed gel particles	-	(2), shrinkage to 15% of original volume	-	(1), shrinkage to 10% of original volume	
	1000	2000	18.6	24	Rigid gel, shrinkage to 30% of original volume	40	(1), shrinkage to 60% of original volume	72	Rigid gel, shrinkage to 85% of original volume	
		1500	11.2	15	(1), shrinkage to 30% of original	21	(0), complete precipitation	(1)	(3), shrinkage to 20% of original	

					volume				volume	
	1500	4000	74.6	1.3	Rigid gel, shrinkage to 25% of original volume	2	Rigid gel, shrinkage to 20% of original volume	48	Rigid gel, shrinkage to 94% of original volume	
		1000	5.86	-	(0), complete precipitation	-	(0), complete precipitation	91.7	Rigid gel	
	4000	2000	11	-	(0), complete precipitation	-	-	-	-	
	10000	2000	10.2	-	(0), complete precipitation	-	-	-	-	

Table 35: Gelation times and viscosities for the samples of HPAM polymer with chromium (III) crosslinker at 80°C, 60°C and 40°C

Table 35 gives an overview of the gelation time at various temperatures when different concentrations of HPAM polymer are mixed with different concentrations of Cr (III) crosslinker. The samples with a very high concentration of crosslinker completely precipitate and hence are not found to be a good combination for gel formation. The samples with 1000 PPM of Cr (III) crosslinker form a strong gel at all three temperature settings but then shrink quickly afterwards. As can be seen from the table, this is not only the case with 1000 PPM of Cr (III) crosslinker but with other concentrations as well. Gel syneresis has been found to be a big problem when it comes to formation of gel using HPAM polymer. Samples have been observed to shrink by as much as 95% of original volume.

The plot for the gelation time in hours as a function of Cr(III) crosslinker concentration mixed with 2000 PPM of HPAM polymer at 80°C is given in the figure 28.

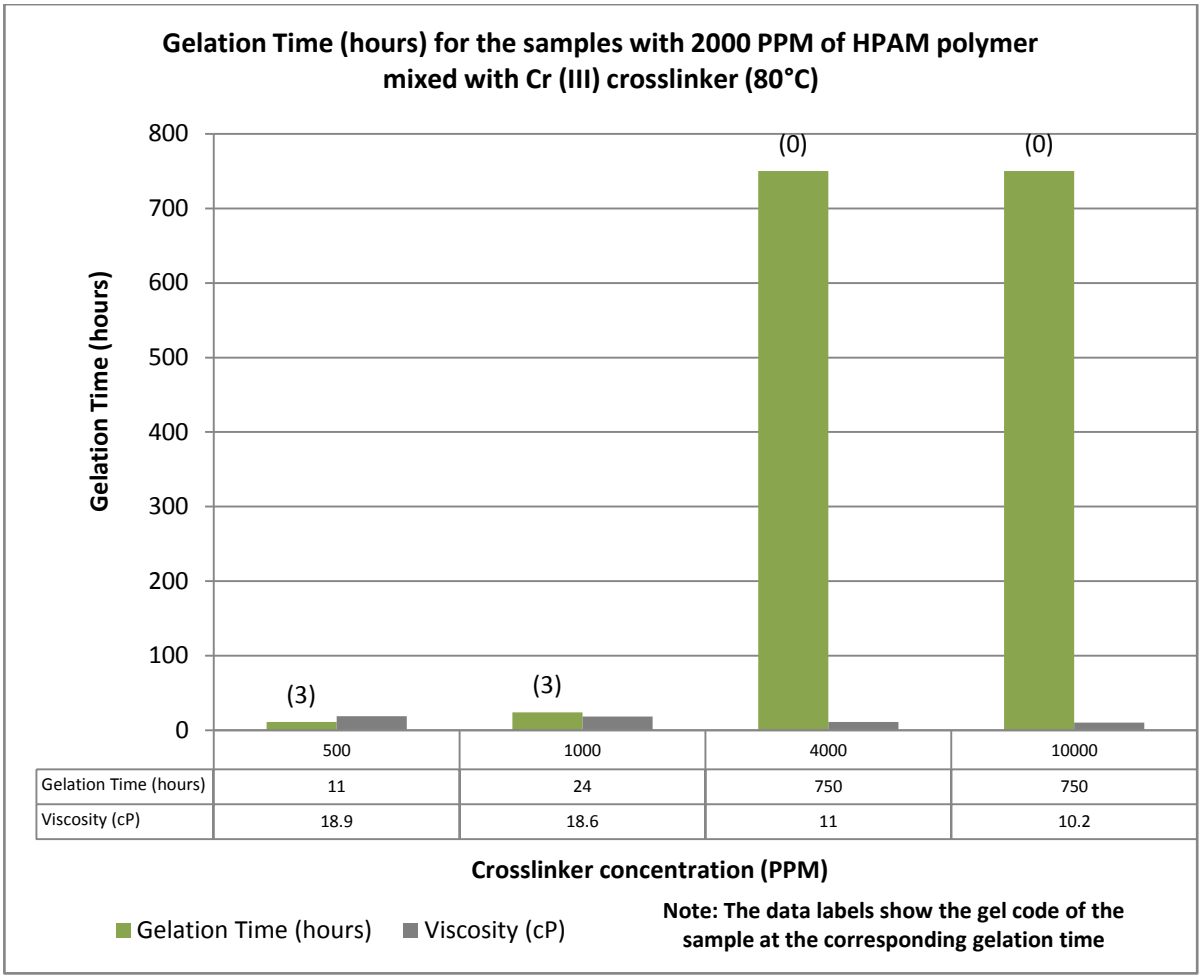

Figure 28: Gelation time for the samples with 2000 PPM of HPAM polymer as a function of Cr (III) crosslinker concentration (80°C)

This plot shows that HPAM polymer forms a strong gel very quickly at low concentrations of Cr (III) crosslinker while at very high concentrations of crosslinker, no effect related to the gel formation can be seen. The samples were found to be still in the solution state which is

due to the fact that enough extra crosslinker is present in the solution which does not allow the polymer to form a closed network with the crosslinker.

Hence, it can be concluded that Cr (III) crosslinker can be used for gel formation with HPAM polymers in the cases where low concentrations of crosslinker are required and/or available but gel syneresis has to be taken into account while designing the gel treatments with HPAM polymers.

5.2.3.3. HPAM POLYMER WITH BRANCHED PEI (1 WT%) CROSSLINKER

Table 36 gives the gelation time in hours, viscosity in cP and pH of the samples prepared by mixing different concentrations of HPAM polymer with different concentrations of Branched PEI (1 wt%) crosslinker.

HPAM	CROSSLINKER - BRANCHED PEI (1%)						
	Crosslinker concentration (PPM)	**Polymer concentration (PPM)**	**Viscosity (cP)**	**pH**	**Gelation time (hr) - 80°C**	**Status of the sample at 80°C after ~1 month**	**Observations/ Comments**
		5000	114	-			Mother solution
	500	1500	12.4	10.14	-	(0)	
		1500	12.2	6.45	-	(0)	
	1500	2000	20.1	10.4	-	(0)	
		2000	18.1	6.07	-	(0)	

Table 36: Gelation times, viscosities and pH for the samples of HPAM polymer with Branched PEI (1 wt%) crosslinker at 80°C

Samples were kept in the oven at 80°C at both their original pH value and reduced pH value (favourable pH value between 5.5 and 7.5, where the chances of a gel being formed are higher). As is clearly visible from the table, no sample has shown any kind of gel formation at 80°C. At the end of the testing period of one month, all the samples were still in solution form and there were no traces of any gel formation, which leads to the conclusion that Branched PEI (1 wt%) is not a good crosslinker for medium concentrations of HPAM polymers.

5.3. COMPARISON BETWEEN ASSOCIATIVE POLYMER AND HPAM POLYMER

A small comparative study has been conducted to see the effects of mixing three different concentrations of both polymers (4000 PPM, 1500 PPM and 1000 PPM) with different

concentrations of crosslinkers (Zr (III) and Cr (III)). Figure 29 shows the gelation time for the samples with 4000 PPM of polymer mixed with different crosslinkers at 80°C.

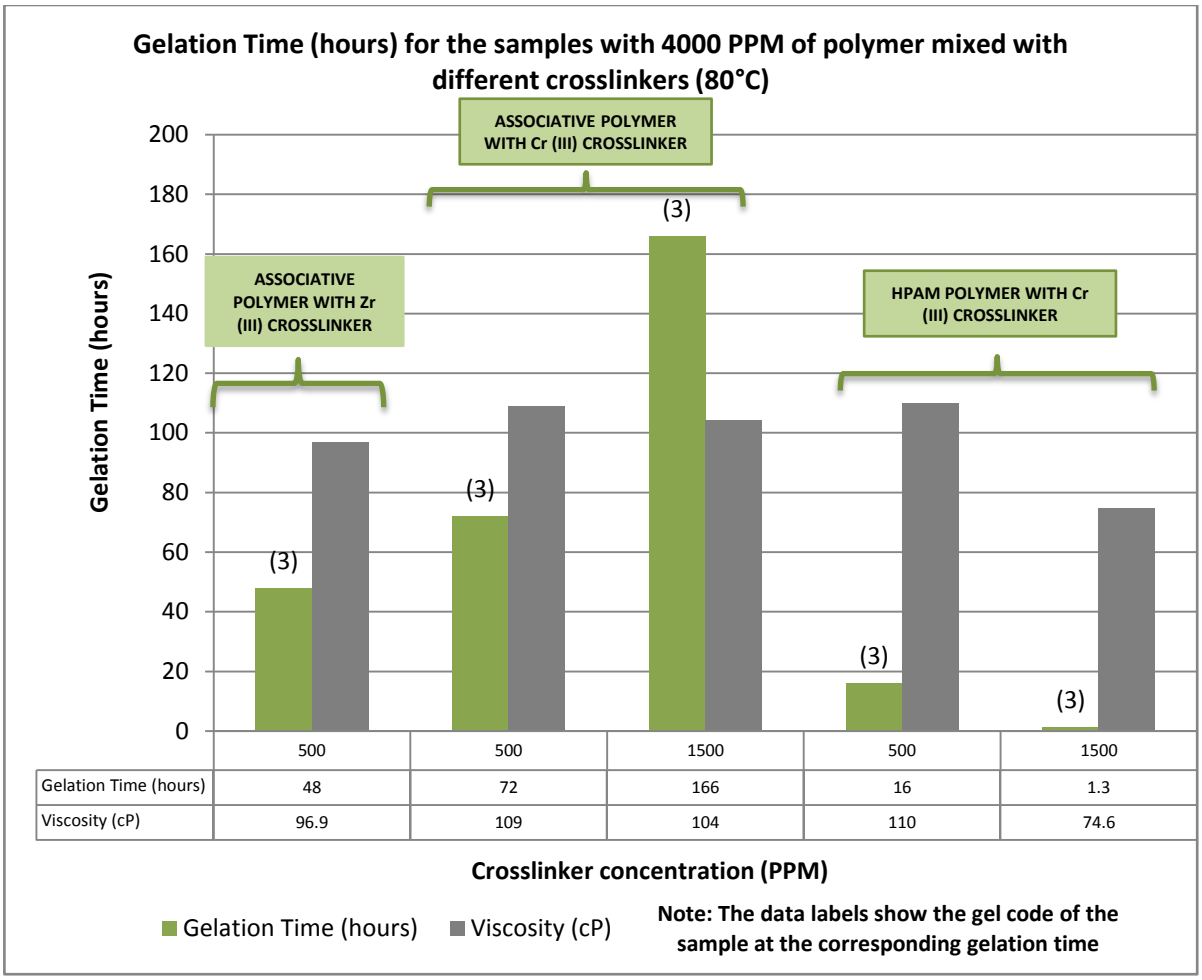

Figure 29: Gelation time for the samples with 4000 PPM of polymer mixed with different crosslinkers as a function of the corresponding crosslinker concentration (80°C)

From this plot, it can be observed that all the samples tested with both polymer systems mixed with Cr (III) crosslinker have formed a strong and rigid gel. For a concentration of 4000 PPM of associative polymer, as the concentration of Cr (III) crosslinker is increased, the gelation time increases. However, for the same concentration of HPAM polymer, the gelation time decreases when the concentration of Cr (III) crosslinker is increased.

Figure 30 shows the gelation time for the samples with 1500 PPM of polymer mixed with different crosslinkers at 80°C.

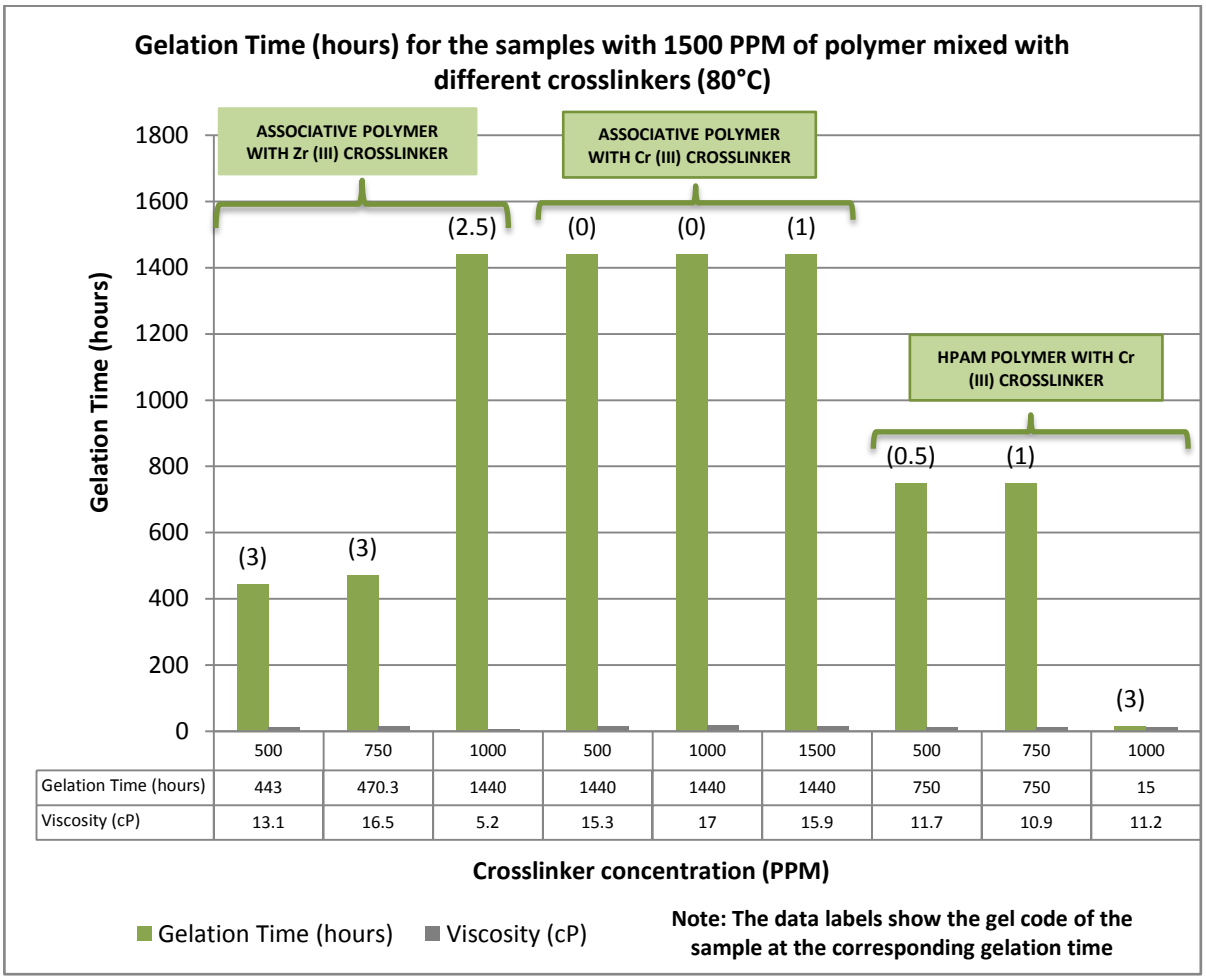

Figure 30: Gelation time for the samples with 1500 PPM of polymer mixed with different crosslinkers as a function of the corresponding crosslinker concentration (80°C)

This plot shows that a gel is formed at low concentrations of Zr (III) crosslinker with 1500 PPM of associative polymer but as the crosslinker concentration is increased above 1000 PPM, it takes a very long time to form a strong gel. It also shows that at this concentration of polymer, Cr (III) crosslinker does not form a gel but HPAM polymers do form a gel when the concentrations of Cr (III) crosslinker are high (≥ 1000 PPM).

Figure 31 shows the gelation time for the samples with 1000 PPM of polymer mixed with different crosslinkers at 80°C.

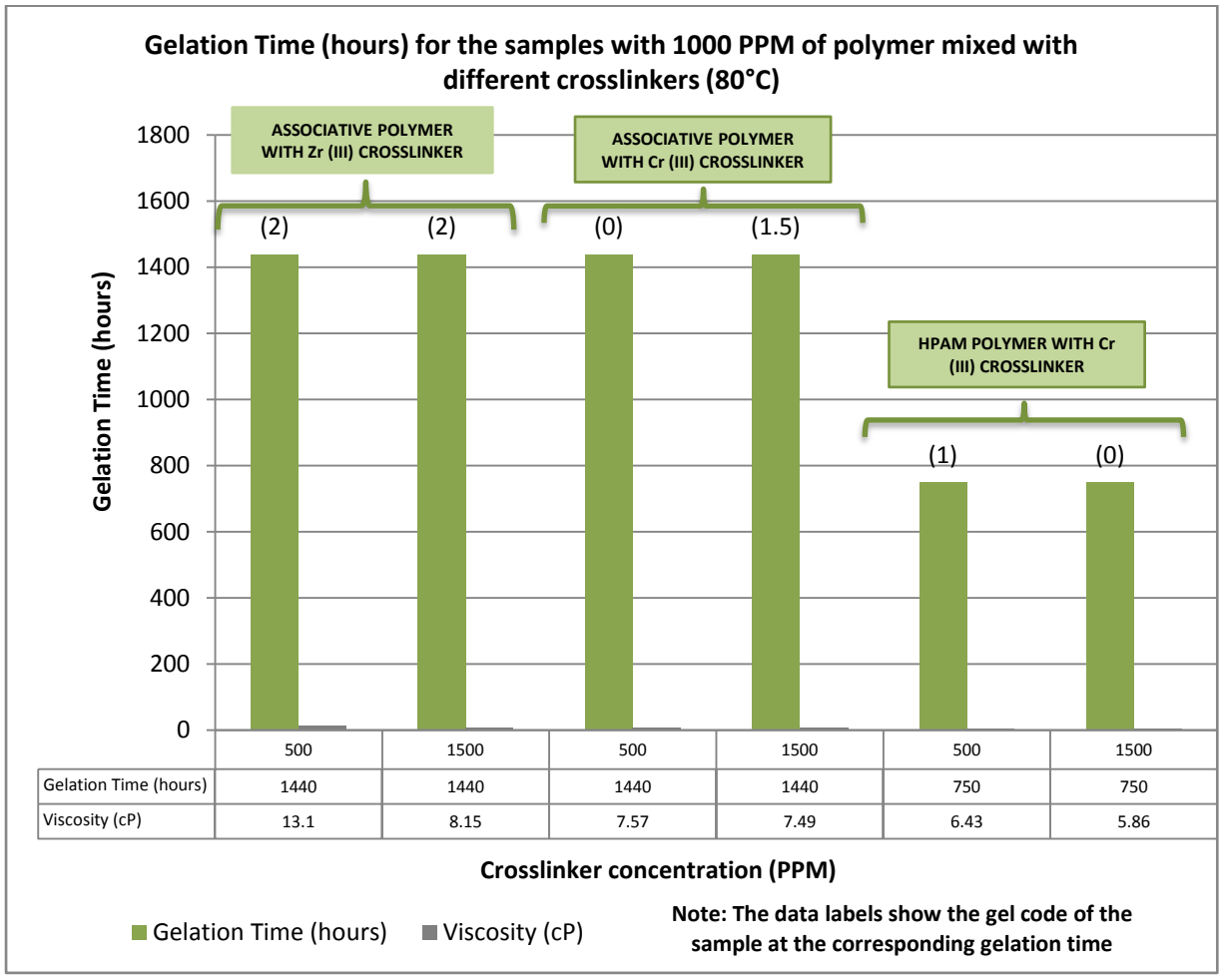

Figure 31: Gelation time for the samples with 1000 PPM of polymer mixed with different crosslinkers as a function of the corresponding crosslinker concentration (80°C)

This plot shows that as the polymer concentration is reduced below 1000 PPM, associative polymers take a very long time to form a gel but they still form a weak gel. At the same time, however, no polymer was able to form a gel with Cr (III) crosslinker when the concentration of polymer was 1000 PPM.

The above plots show that associative polymers have the capability of forming strong gels with Zr (III) crosslinker at concentrations ranging from 1000 PPM to 4000 PPM and have shown good results for viscosity measurements at a concentration of 2000 PPM, which are favourable for polymer gel treatments in real field scenarios. As compared to the associative polymers, HPAM polymers also form strong gels for high concentrations of polymer with low-to-medium concentrations of crosslinker, especially Cr (III), but show larger gel syneresis than the associative polymers. They are also not recommended for polymer gel treatments as they do not form a gel at the favourable viscosity values formed by mixing the Cr (III) crosslinker with a low concentration of HPAM polymer.

5.4. EFFECT OF SHEAR RATE ON THE RHEOLOGICAL PROPERTIES OF THE POLYMER-CROSSLINKER MIXTURES

The main use of polymers is to viscosify the water and hence reduce its mobility and improve the macroscopic sweep efficiency. The effect of shear rate on the viscosity of the polymer-crosslinker mixtures was studied for this work. Figure 32 shows the rheograms of 2000 PPM of associative polymer mixed with zirconium (III) crosslinker at different concentrations.

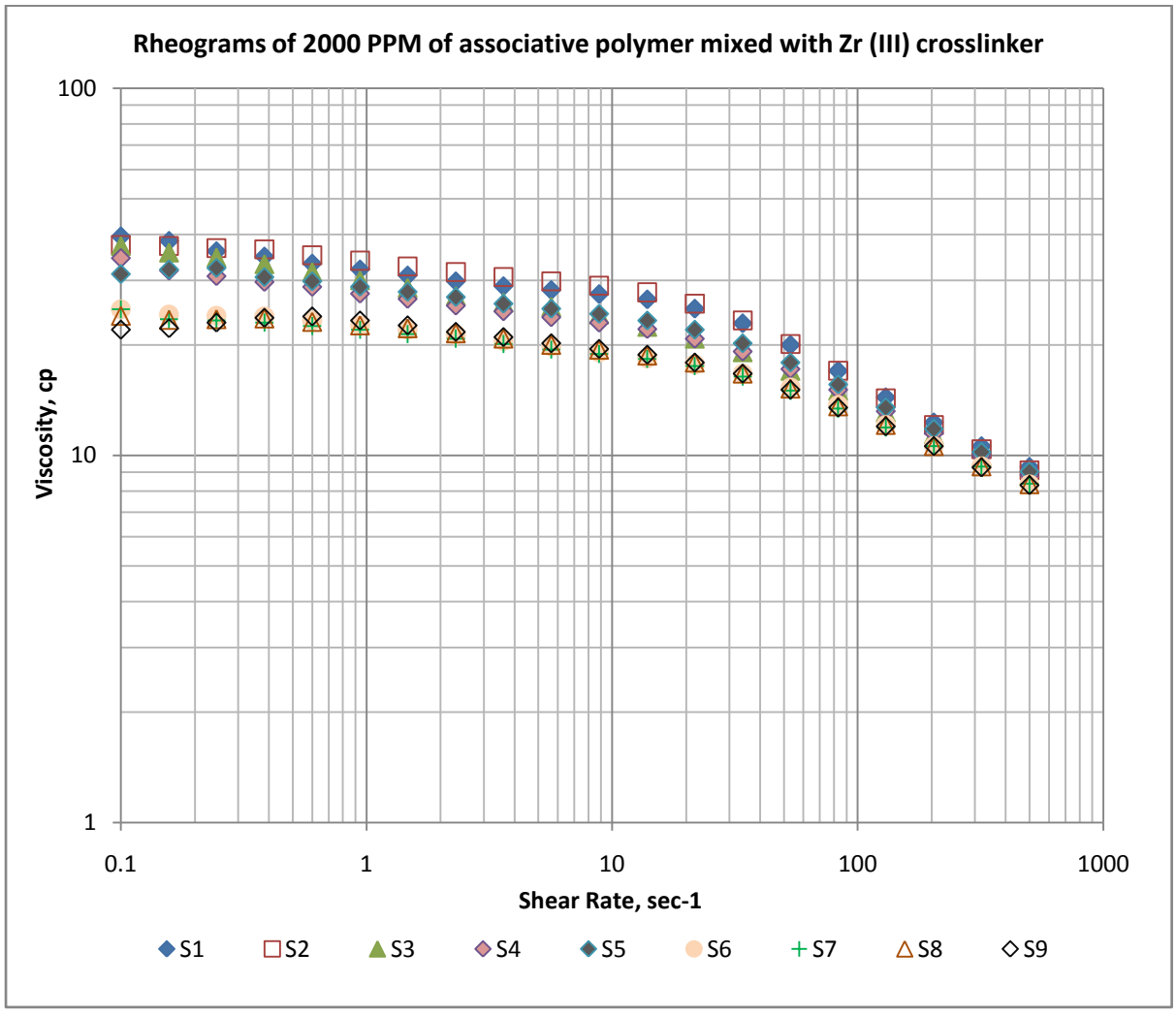

Figure 32: Rheograms of 2000 PPM of associative polymer mixed with zirconium (III) crosslinker

In this plot S1 to S9 denote the sample numbers with different concentrations of crosslinker as summarised in table 37.

Sample number	Concentration of Zr (III) crosslinker (PPM)	Sample number	Concentration of Zr (III) crosslinker (PPM)	Sample number	Concentration of Zr (III) crosslinker (PPM)
S1	10000	S4	1250	S7	500
S2	4000	S5	1000	S8	250
S3	2000	S6	750	S9	100

Table 37: Concentration of crosslinker in different samples with 2000PPM of associative polymer

The viscosity measurements were conducted very shortly (within 15 minutes) after the preparation of the mixtures. The gelation times were found to be more than 80 hours for all the samples at high temperatures. Therefore, there was no scope of microgels being formed in that short span of time at room temperature, which could have affected the viscosity measurements.

It is obvious from figure 32 that for the samples with low concentrations of crosslinker, there is a large transition period from Newtonian behaviour to shear-thinning behaviour, but for the samples with high concentrations of crosslinker, this transition period is small. At low shear rates, the shear-thinning index is more gentle, but at high shear rates, the shinning-thinning index is more steep.

One important point to be noted here is that polymers also exhibit shear thickening behaviour. For a given shear rate, it is not uncommon for the polymers to exhibit shear thinning or upper Newtonian regimes in bulk rheological tests while exhibiting shear thickening or degradation in a core experiment (Norris, 2011, p. 5). Polyacrylamide polymer molecules are better described as flexible coils that take on random configuration (Green & Willhite, 1998). The flexible nature of the coil structure of polyacrylamide molecules lends to their ability to produce viscoelastic responses in high shear environments (Hirasaki & Pope, 1974; Heemskerk, Rosmalen, Janssen-van, Holtslag & Teeuw, 1984; Southwick & Manke, 1988; Green & Willhite, 1998; Norris, 2011, p. 6).

5.5. ADVANTAGES OF ASSOCIATIVE POLYMERS OVER POLYACRYLAMIDES

Reichenbach-Klinke et al. (2013) have reported that hydrophobically modified associative polymers offer significant advantages in polymer injection over anionic polyacrylamides.

Associative polymers increase the viscosity of water not only due to the thickening effect by their molecular weight but also due to the hydrophobic interactions between different polymer chains. They form an intermolecular polymer network in aqueous solution due to the interaction between different hydrophobic groups on the polymer backbone. The

viscosity of this polymer network is significantly larger than the viscosity of one of the independent, individual polymer chains. Therefore, the associative polymers deliver superior viscosities compared to polyacrylamides at similar levels of molecular weights (Reichenbach-Klinke et al., 2013).

Moreover the viscosity of this type of polymer is not as sensitive to salinity as the viscosity of polyacrylamides. There is no negative influence on the interaction between the hydrophobic groups when salt is added. Indeed the hydrophobic interactions will be even stronger in more polar environments like salt-containing aqueous solutions which yields in a higher viscosity (Reichenbach-Klinke et al., 2013).

The associative polymers are also more shear stable than other synthetic EOR polymers. When the shear forces are applied by injecting the polymer solution into the formation, the comparatively weak intermolecular network is broken up but the polymer backbone still remains intact. When the polymer solution is already flowing in the reservoir, the shear will substantially decrease and the associative polymer network is reformed and the viscosity is built up to its original level (Reichenbach-Klinke et al., 2013).

Taylor and Nasr-El-Din (1998) reported that associative polymers show greater resistance and residual resistance factors than conventional polyacrylamides.

Despite these advantages for associative polymers over the conventional polyacrylamides, associative polymers have not been used in the field so far. The most likely reasons for the associative polymers not being used extensively are that their behaviour in the porous medium and the mechanism of oil recovery are still not well understood and are an ongoing debate in the literature.

6. EXPERIMENTAL WORK - CORE FLOODING EXPERIMENT

One core flooding experiment was performed on the Berea sandstone core to establish any potential DPR effects when associative polymer was injected through it. This section deals with the results of this experiment.

6.1. OBJECTIVE

To investigate the single-phase associative polymer DPR effect on the Berea sandstone core to understand its effectiveness for conformance-improvement purposes.

6.2. EXPERIMENTAL SETUP

A schematic of the experimental setup is given in figure 33.

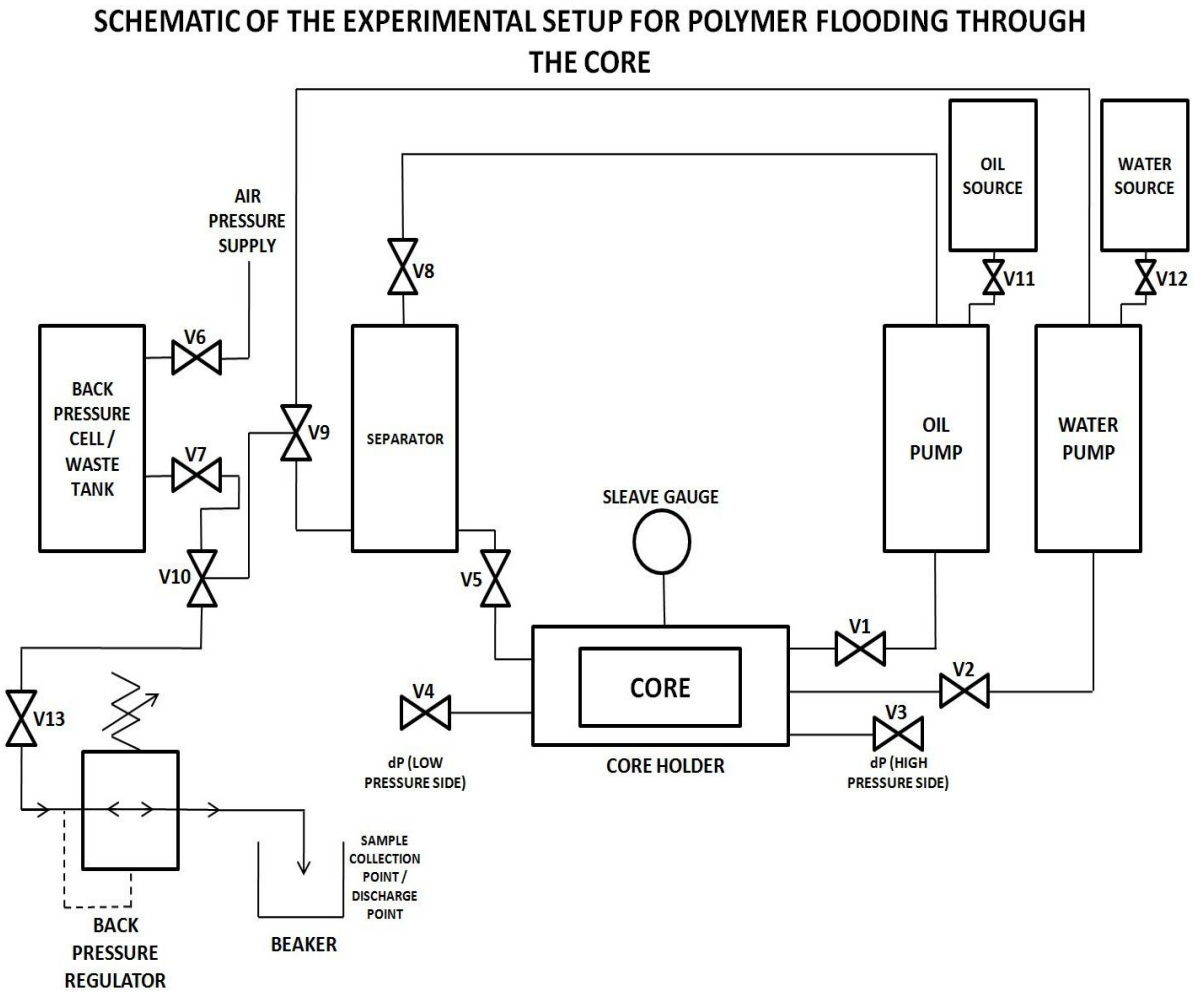

Figure 33: Schematic of the experimental setup used for the single-phase polymer DPR core flood experiment on water-wet core.

In figure 33, V1 to V13 denote the different valves used in the system. The valves were kept open or closed depending on the phase injected into the core and whether that phase was re-circulated in the system or not.

6.3. EXPERIMENTAL PROCEDURE

Single-phase associative polymer DPR core flood experiment on water-wet core was performed. A simplified experimental procedure applied for this experiment is given below:

1. Mount the core with overburden pressure (40 bar).
2. Inject single-phase brine for pore volume and absolute permeability measurement.
3. Inject single-phase oil (Isopar H), and establish S_{wi}, and measure k_o (S_{wi}).
4. Inject brine to establish S_{or}.
5. Inject single-phase polymer solution until the pressure (dP) becomes stabilised.
    a) Calculate Resistance Factor (RF)
6. Stop injecting polymer solution and clean the flow lines.
7. Inject single-phase brine at constant flow rate (equal to the flow rate used for treatment flooding with polymer).
    a) Re-circulate the brine and observe the pressure changes
    b) Obtain Residual Resistance Factor for water
8. Inject single-phase oil at constant flow rate.
    a) Monitor saturation changes in the core (water production should be monitored)
    b) Obtain Residual Resistance Factor for oil

The above-mentioned experimental procedure has been divided into three broad categories: pre-treatment flooding, treatment flooding and post-treatment flooding, to describe every step in detail.

6.3.1. PRE-TREATMENT FLOODING

The various steps performed prior to the treatment of core with polymer are described below.

6.3.1.1. SAMPLE PREPARATION

The experiment was performed on a Berea sandstone core. The sample was cleaned properly from the outside by using air pressure from a pressurised air gun. The length and diameter of the core sample were then measured, and the bulk volume of the core was calculated, and is given in table 38.

BEREA SANDSTONE CORE					
Length of the core, L	Diameter of the core, d	Cross-sectional area of the core, A	Bulk volume of the core, V_b	Volume of the spiral grooves, V_{sg}	Volume of the steel screen used on the core, V_{ss}
		$A = \pi d^2/4$	$V_b = A*L$		
cm	cm	cm^2	cm^3	cm^3	cm^3
9.564	3.776	11.198	107.101	0.1	0.2

Table 38: Length, diameter and bulk volume of the Berea sandstone core used for core flooding experiment

The core sample was then mounted into a core holder and the whole system was vacuumed using a vacuum pump.

6.3.1.2.CALCULATION OF PORE VOLUME

The core holder under vacuum condition was weighed. A 0.5 litre transfer vessel was filled with brine (0.1M NaCl) and connected to the water pump through the valve V12 and to the core holder through the valve V2. After connecting all the inlet and the outlet valves to the core holder and preparing the core sample for the experiment, the brine inside the transfer vessel was pressurised to a desired reference pressure (here 7.058 bar) using water pump. The overburden pressure of 40 bar was applied using oil. After making sure that the system was leak tight and that the reference pressure had stabilised, valve V2 was opened, whereby the core sample was allowed to saturate with brine. At the same time, the water pump was turned on at constant rate mode. The injection was continued until the pressure inside the core holder reached the reference pressure of 7.058 bars. The cumulative volume of the brine used to saturate the core sample V_1 was noted down. The flow rate was turned down to 0 ml/min for 3 minutes during which the core was tested for any leakage (through any drop in the pressure inside the core holder). After three minutes, a small flow rate was applied to let the brine saturate the core sample again to the reference pressure (the pressure drop is due to possible minor unseen leakages). After noting down the new cumulative volume V_2, these two volume readings were used to calculate the total brine volume injected at the reference pressure, which in turn was used to calculate the pore volume by volume method and porosity. After saturating the core sample with brine, the weight of the saturated core sample (with the core holder) was measured. The dry weight and the saturated weight of the core sample were used to calculate the pore volume by weight method and the porosity.

The dry weight and the saturated weight of the core sample and the pore volume and porosity evaluation by weight method are given in table 39.

POROSITY MEASUREMENT BY WEIGHT METHOD				
Dry weight of the core sample, W_d	Saturated weight of the core sample, W_s	Brine density, δ_w	Total brine volume used to saturate the core, V_{btsc} $V_{btsc} = (W_s-W_d)/\delta w$	Tubing length, L_t
g	g	g/cm^3	ml	cm
7719.3	7746.8	1	27.5	110

Tube volume per unit length, V_t/L_t	Tubing and valve volume, V_{tv} $V_{tv} = L_t*(V_t/L_t)$	Pore volume, V_p $V_p = V_{btsc}-V_{tv}-V_{sg}-V_{ss}$	Porosity, ϕ $\phi = V_p/V_b$
cm3/cm	cm^3	cm^3	fraction
0.0156	1.716	25.484	0.237943681

Table 39: Pore volume and porosity evaluation by weight method

The two volume readings at the reference pressure of 7.058 bars, and the pore volume and porosity evaluation by volume method are given in table 40.

POROSITY MEASUREMENT BY VOLUME METHOD (liquid injection at reference pressure)				
Tubing length, L_t	Tube volume per unit length, V_t/L_t	Reference pressure, P_{ref}	Volume 1 at reference pressure, $V_{1,ref}$	Volume 2 at reference pressure, $V_{2,ref}$
cm	cm3/cm	bar	ml	ml
110	0.0156	7.058	27.595	27.62

Total brine volume, V_{bt} $V_{bt} = 2*V_{1,ref} - V_{2,ref}$	Tubing and valve volume, V_{tv} $V_{tv} = L_t*(V_t/L_t)$	Pore volume, V_p $V_p = V_{bt}-V_{tv}-V_{sg}-V_{ss}$	Porosity, ϕ $\phi = V_p/V_b$
ml	cm^3	cm^3	fraction
27.570	1.716	25.554	0.2386

Table 40: Pore volume and porosity evaluation by volume method

As can be seen from the tables 39 and 40, the pore volume calculated through the weight method and the volume method are very close to each other. Therefore, a pore volume of 25.484 cm^3 calculated through the weight method has been used for all of the further calculations.

6.3.1.3. MEASUREMENT OF ABSOLUTE PERMEABILITY AND EFFECTIVE PERMEABILITY TO OIL AT S_{wi}

The separator was joined to the system. Back pressure was applied to the core using the back pressure cell, which was divided into two portions using a piston. The lower part was filled with brine and the upper part with air.

The separator was calibrated in such a way that one point change in the separator reading corresponded to 1 cm^3 change in the fluid volume. The initial level in the separator was set to 40 ml with oil on the top and water at the bottom and the circulation was started by turning the pumps on. The oil was supplied directly from the source through valve V11. The water pump was run at different flow rates and the corresponding differential pressures were measured which were then used to calculate the absolute permeability using the Darcy equation. The results are given in table 41.

ABSOLUTE PERMEABILITY MEASUREMENT							
Brine viscosity, μ_w	Brine rate, $q_{w,cc/min}$	Brine rate, $q_{w,cc/sec}$	Differential pressure, dP_{mbar}	dP at q=0, $dP_{q=0, mbar}$	Corrected dP, $dP_{corrected,mbar}$	Differential pressure in atm, dP_{atm}	Absolute permeabiity , K_{abs}
		$q_{w,cc/sec} = q_{w,cc/min}/60$			$dP_{corrected, mbar} = dP_{mbar} - dP_{q=0,mbar}$	$dP_{atm} = 0.000986923 16*dP_{corrected, mbar}$	$K_{abs} = q_{w,cc/sec}*\mu_w* L/(dP_{atm}*A)$
cP	cc/min	cc/sec	mbar	mbar	mbar	Atm	D
1	7	0.1167	159	-5.2	164.2	0.1621	0.6149
1	5	0.0833	112	-5.2	117.2	0.1157	0.6153
1	3	0.0500	66	-5.2	71.2	0.0703	0.6077
1	2	0.0333	43	-5.2	48.2	0.0476	0.5985
1	1	0.0167	20	-5.2	25.2	0.0249	0.5723

Table 41: Absolute permeability measurement from the Darcy equation

The average absolute permeability of the core was found to be 0.6017. The effective permeability to oil was calculated in a similar manner. The oil pump was run at different flow rates and the corresponding differential pressures were measured, which were then used to calculate the effective permeability to oil using the Darcy equation. The results are given in table 42.

EFFECTIVE PERMEABILITY TO OIL (AT S_{wi})MEASUREMENT							
Oil viscosity, μ_o	Oil rate, $q_{o,cc/min}$	Oil rate, $q_{o,cc/sec}$	Differential pressure, dP_{mbar}	dP at q=0, $dP_{q=0,mbar}$	Corrected dP, $dP_{corrected,\ mbar}$	Differential pressure in atm, dP_{atm}	Effective permeabiity to oil, K_o (S_{wi})
		$q_{w,cc/sec} = q_{w,cc/min}/60$			$dP_{corrected,\ mbar} = dP_{mbar} - dP_{q=0,mbar}$	$dP_{atm} = 0.00098692316 * dP_{corrected,mbar}$	$K_o = q_{o,cc/sec} * \mu_o * L / (dP_{atm}) * A$
cP	cc/min	cc/sec	mbar	mbar	mbar	atm	D
1.29	2	0.0333	54	-5.2	59.2	0.0584	0.6286
1.29	7	0.1167	201	-5.2	206.2	0.2035	0.6316
1.29	5	0.0833	141	-5.2	146.2	0.1443	0.6363
1.29	3	0.0500	84.5	-5.2	89.7	0.0885	0.6223
1.29	1	0.0167	24.9	-5.2	30.1	0.0297	0.6181

Table 42: Effective permeability measurement from the Darcy equation

The average effective permeability to oil (K_o at S_{wi}) in the core was found to be 0.6274.

6.3.1.4. MEASUREMENT OF IRREDUCIBLE WATER SATURATION BEFORE TREATMENT WITH POLYMER ($S_{wi,before}$)

Pre-treatment flooding was done with oil to establish S_{wi}. Oil was injected into the core at two different flow rates and the oil produced from the other side of the core was re-injected into the core. The separator level readings were taken at frequent time intervals and the differential pressure readings (dP) between the inlet (high pressure side) and the outlet (low pressure side) of the core were noted down at the same time. Pump cylinder volume changes with time, due to re-circulation of oil in the system, were taken into account in the calculations to estimate the volume of oil in the core at each time reading. The volume of oil in the core at a particular time divided by the pore volume of the core gives the saturation of oil at that time. The noted dP values were used to calculate the effective permeability to oil in the core ($K_{o,before}$) at those time readings using the Darcy equation. The table summarising the readings of separator level taken at different times and the cumulative oil volume injected into the core at those times are given in Appendix D as well as the values estimated for saturation of oil and effective permeability to oil in the core at the same time.

Figure 34 shows the oil saturation in the core as a function of pore volumes of oil injected during the pre-treatment flooding to establish S_{wi}.

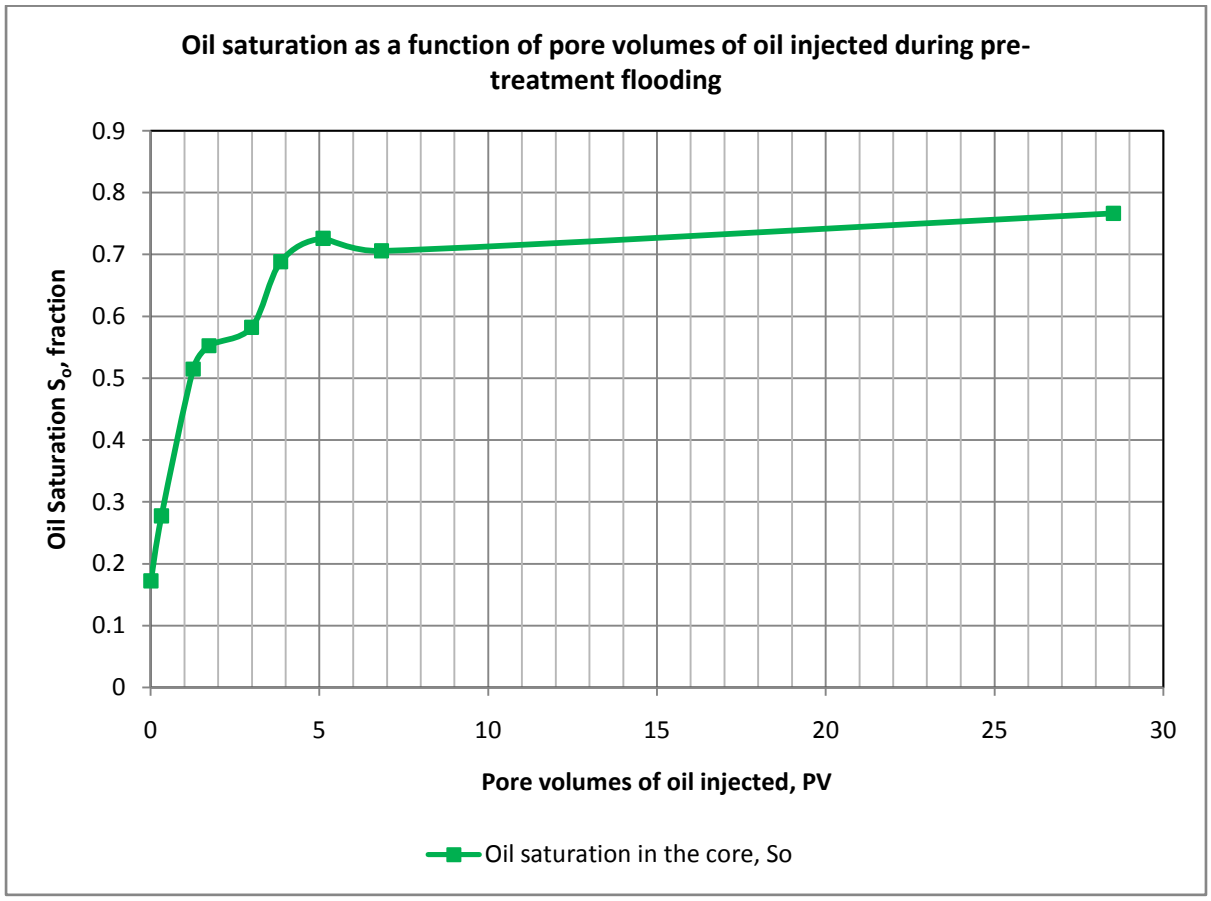

Figure 34: Oil saturation as a function of pore volumes of oil injected during pre-treatment flooding with oil to establish S_{wi}

The core was saturated with brine before the pre-treatment flooding with oil. It is evident from the plot that as the volume of oil injected into the core is increasing, the oil saturation is increasing. This increase in the oil saturation is due to the fact that as more and more volumes of oil are being injected into the core, more volumes of water are pushed out from the pore spaces and that space is taken up by the oil until a point is reached when oil can no longer push any more water out of the pore spaces. This water remains trapped in these pore spaces. This gives the irreducible water saturation, i.e. the maximum water saturation that the formation can retain without producing water. These pore spaces resulting in irreducible water saturation exist as isolated pore spaces (non-effective porosity) or sometimes, they are so small in diameter (4 µm or less) that they trap and hold water immobile through capillary action (microporosity).

The value of irreducible water saturation ($S_{wi,before}$) for the core was found to be 0.23324.

6.3.1.5. MEASUREMENT OF RESIDUAL OIL SATURATION BEFORE TREATMENT WITH POLYMER ($S_{or,before}$)

After the pre-treatment flooding with oil, pre-treatment flooding was carried out with 0.1M brine to establish S_{or}. Brine was injected into the core at four different flow rates and the oil produced from the other end of the core was collected in a waste tank. The separator level readings were taken at frequent time intervals and the differential pressure readings (dP) between the inlet (high pressure side) and the outlet (low pressure side) of the core were noted down at the same time. Water saturation was calculated at these times by taking into account the change in the level in the separator. $S_{or,before}$ was calculated from the final water saturation value and was found to be 0.4485. The table summarising the readings of separator level taken at different times and the cumulative water volume injected into the core at those times are given in Appendix D as well as the values estimated for saturation of water at the same time.

Figure 35 shows the water saturation in the core as a function of pore volumes of brine injected during the pre-treatment flooding to establish S_{or}.

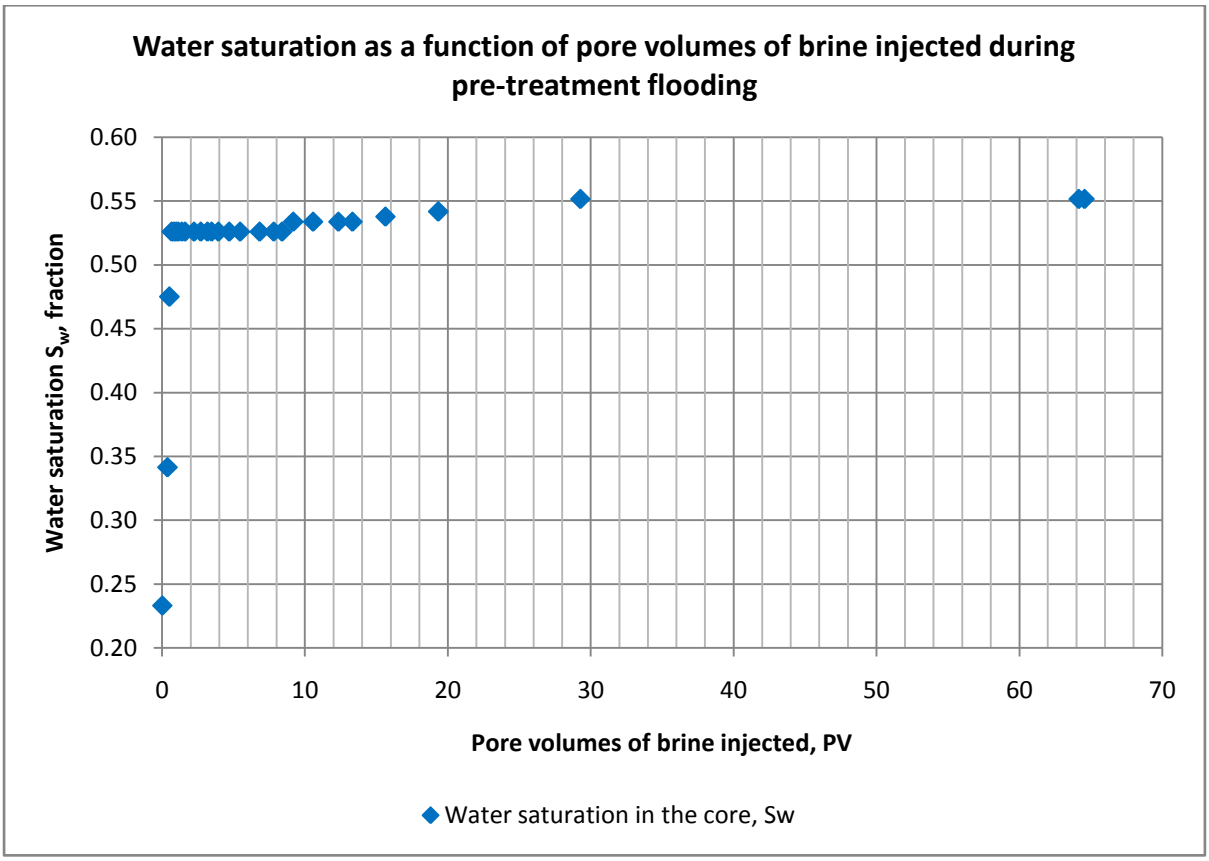

Figure 35: Water saturation as a function of pore volumes of brine injected during pre-treatment flooding

An increase in the water saturation in the core is observed from figure 35 as the volume of brine injected into the core is increasing.

Figure 36 shows the differential pressure (dP) between the high pressure side and low pressure side of the core as a function of pore volumes of brine injected during the pre-treatment flooding.

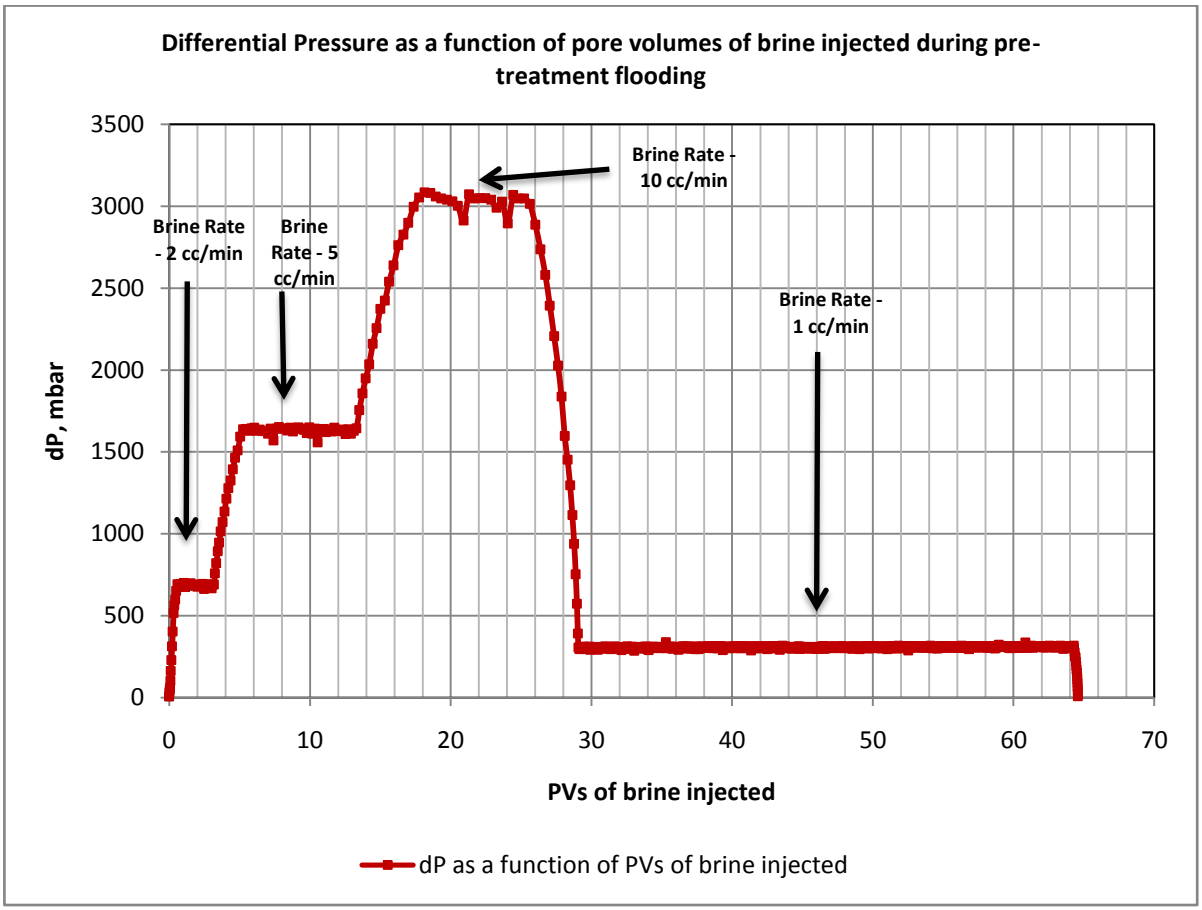

Figure 36: Differential pressure as a function of pore volumes of brine injected during pre-treatment flooding

It is evident from figure 36 that the increase in the brine rate resulted in an increase in the differential pressure between the two ends of the core. The stabilised dP values at each brine rate were used to calculate the effective permeability to water in the core ($K_{w,before}$) using the Darcy equation. The calculated values for the effective permeability to water in the core are also given in the table in Appendix D.

6.3.2. TREATMENT FLOODING

The description for the polymer treatment flooding is given below.

6.3.2.1. POLYMER INJECTION

The associative polymer with a concentration of 1000 PPM was injected into the core. The viscosity of the injected associative polymer at shear rate of 8.85s^{-1} (a shear rate that is corresponding to a typical velocity in the reservoir) was measured and found to be 6.67 cP.

The polymer was injected at a rate of 0.1 ml/min. The separator level readings were taken at frequent time intervals and the differential pressure readings (dP) between the inlet (high pressure side) and the outlet (low pressure side) of the core were noted down at the same time. A total of 12.183 PVs of polymer were injected when the injection was stopped. The pressure did not stabilise perfectly but in the last one hour of injection, the average dP was found to be 5131.63 mbar. Figure 37 shows the differential pressure (dP) between the high pressure side and low pressure side of the core as a function of pore volumes of polymer injected during treatment.

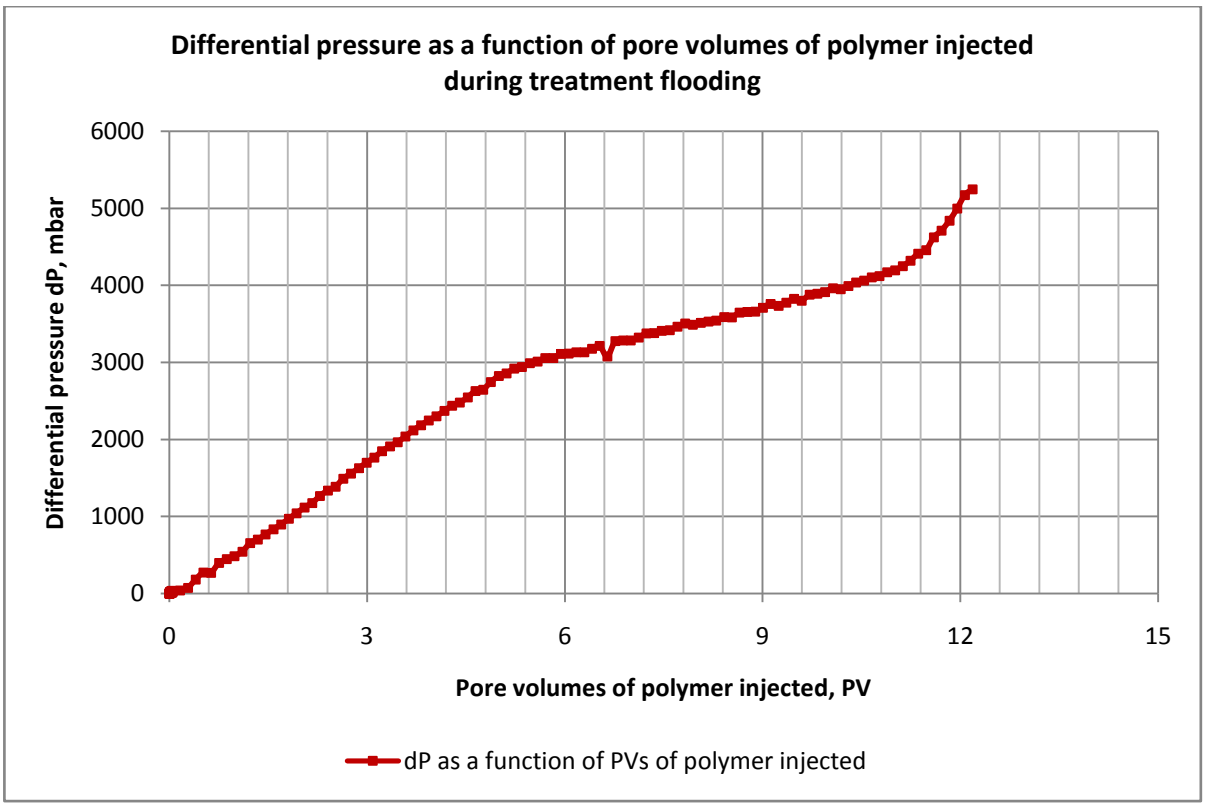

Figure 37: Differential pressure as a function of pore volumes of polymer injected during treatment

The corresponding change in the separator level was observed to be very small. Change in the saturation of water corresponding to this change in the separator level was calculated and added to the water saturation at the end of pre-treatment flooding with brine to estimate the water saturation at the end of polymer injection. Hence the value of residual oil saturation at the end of polymer injection (S_{orp}) was determined. The value of S_{orp} was found to be 0.4223.

From the values calculated for dP/q for polymer injection, the resistance factor (RF) was calculated by dividing these values by the average dP/q value of 331 mbar.min/ml calculated during pre-treatment brine flooding. The table summarising the initial and final reading of separator level including the calculations for S_{orp} and the calculated values of RF is given in Appendix D.

The plot of the resistance factor as a function of pore volumes of polymer injected is given in figure 38.

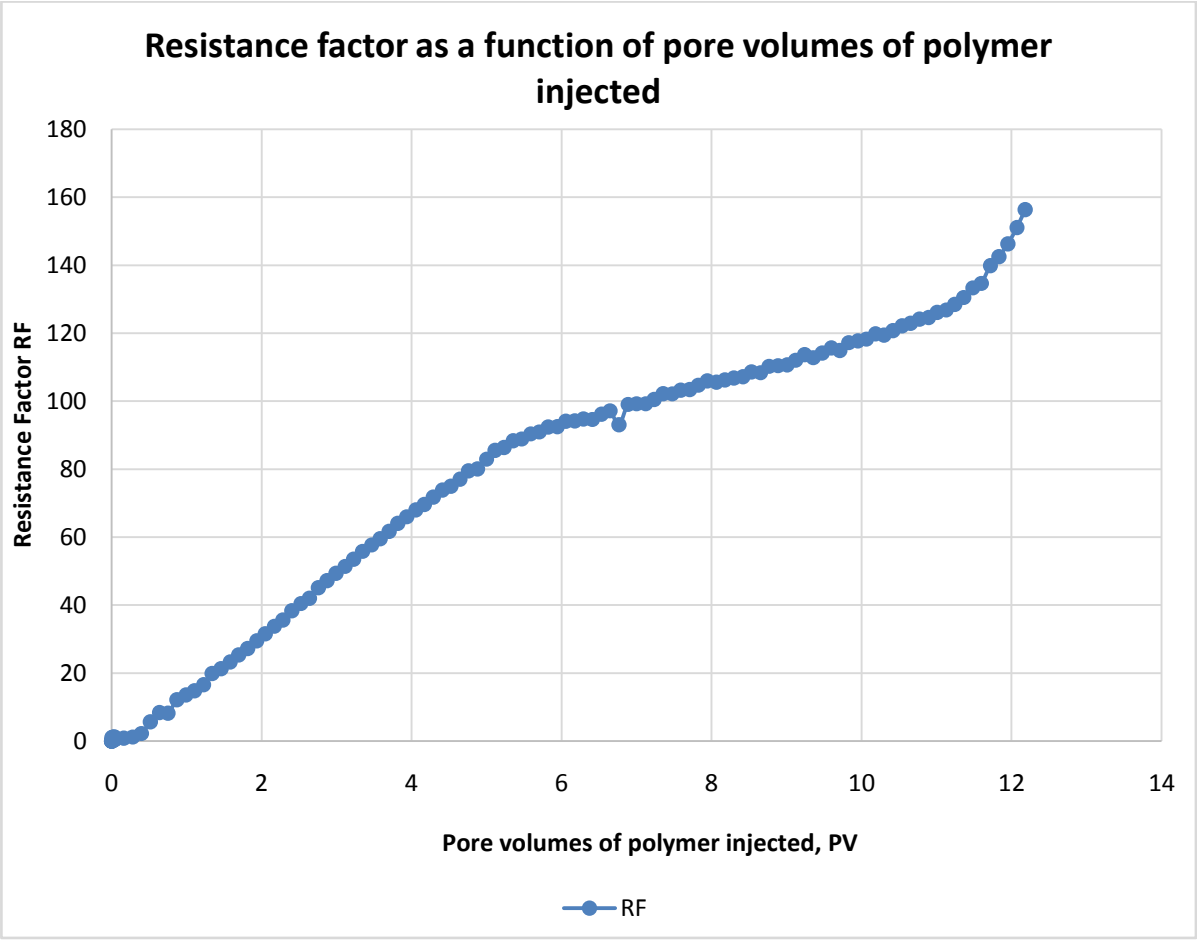

Figure 38: Resistance factor as a function of pore volumes of polymer injected

It is clear from figure 38 that as the volume of polymer injected into the core is increasing, the resistance factor is increasing. In other words, the polymer mobility in the core decreases with volume of the polymer injected. For the core considered in this work, the mobility of polymer became 160 fold less than the mobility of brine before polymer treatment as is observed from the plot. This mobility reduction can be due to polymer retention in porous media and reduction in the absolute permeability of the core because of creation of Inaccessible Pore Volume (IPV) by polymer injection.

6.3.3. POST-TREATMENT FLOODING

Post-treatment flooding was conducted to evaluate the effectiveness of associative polymer for any DPR effect in the core.

6.3.3.1. WATER INJECTION

The polymer molecules get adsorbed onto the rock during polymer injection and cause a resistance to the post-flood water flow and ultimately lead to an increase in the viscosity of

water. Some of the adsorbed molecules desorb during the post-flood water treatment and go into the solution and result in an increase in the sweep efficiency for a post-flood water compared to the pre-flood water (Littmann, 1988).

A post-treatment flooding with water was conducted to establish the new value of effective permeability to water after polymer injection. 1M NaCl brine was injected at a rate of 0.1 ml/min. The differential pressure readings (dP) between the inlet (high pressure side) and the outlet (low pressure side) of the core were noted down at frequent time intervals. Fresh brine was continuously injected into the system; no change in the separator level was observed. In this case, the water saturation at the end will be equal to that at the start of the post-treatment flooding. Hence, the residual oil saturation after treatment with polymer ($S_{or,after}$) is equal to S_{orp} = 0.4223. The dP was found to have stabilised at an average value of 1730 mbar after the injection of 21.31 PVs of brine. Figure 39 shows the differential pressure as a function of pore volumes of brine injected during post-treatment flooding.

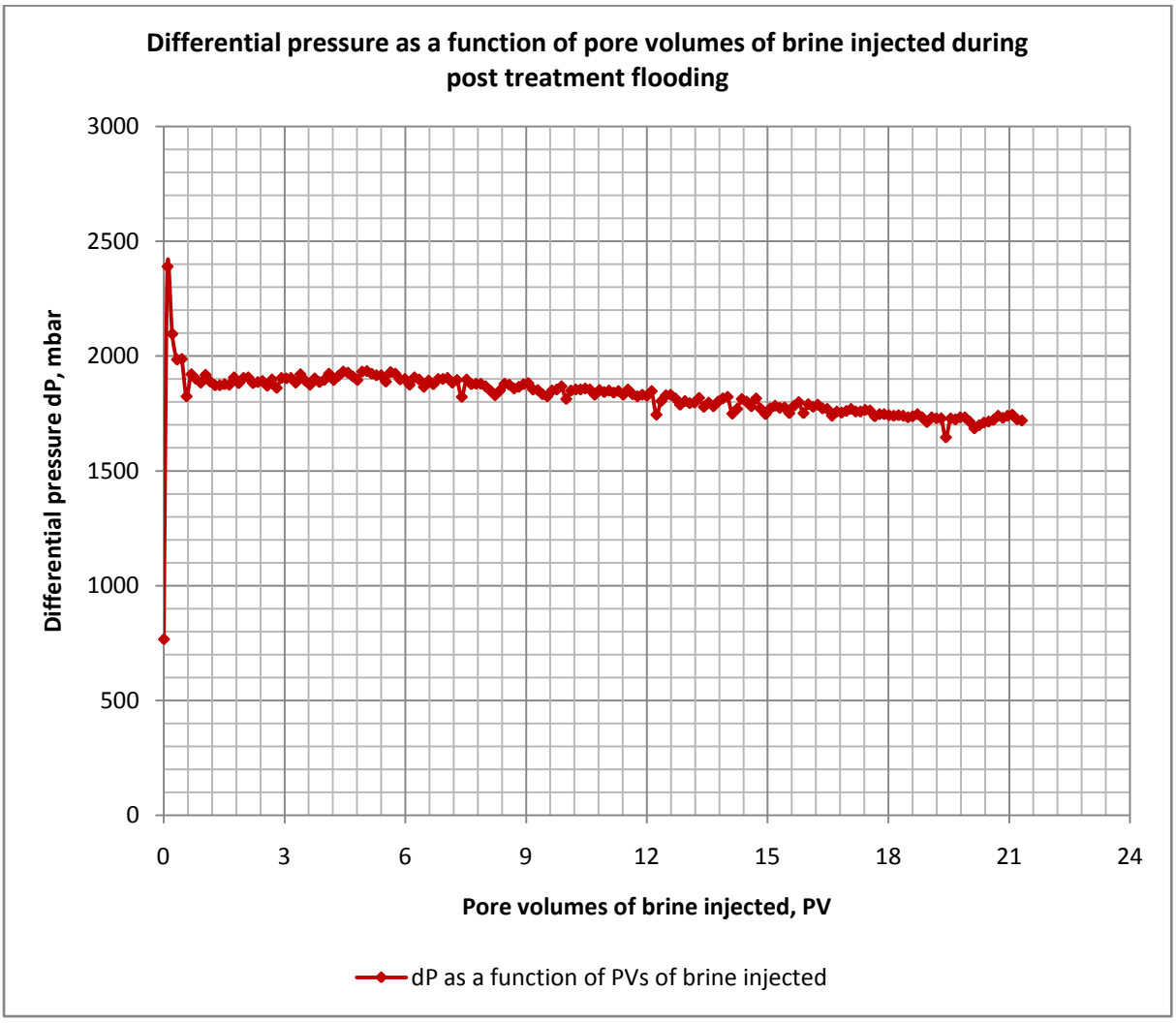

Figure 39: Differential pressure as a function of pore volumes of brine injected during post-treatment brine flooding

The values for effective permeability to water ($K_{w,after}$) in the core after treatment were calculated using the Darcy equation. The final $K_{w,after}$ value was used in conjunction with the final $K_{w,before}$ value to calculate the residual resistance factor for water (RRF_w). The table summarising the calculated values of $K_{w,after}$ and RRF is given in Appendix D.

6.3.3.2. OIL INJECTION

After post-treatment water flooding, oil flooding was performed to establish the new S_{wi} value and the effective permeability to oil in the core. Oil was injected into the core at three different rates of 0.1 ml/min, 0.2 ml/min and 0.5 ml/min. The separator level readings were taken at frequent time intervals and the differential pressure readings (dP) between the inlet (high pressure side) and the outlet (low pressure side) of the core were noted down at the same time. Oil saturation was calculated at these times by taking into account the change in the level in the separator. The new S_{wi} value ($S_{wi,after}$) was calculated from the final oil saturation value and was found to be 0.35905.

Figure 40 shows the oil saturation in the core as a function of pore volumes of oil injected during the post-treatment flooding to establish the new value of S_{wi}.

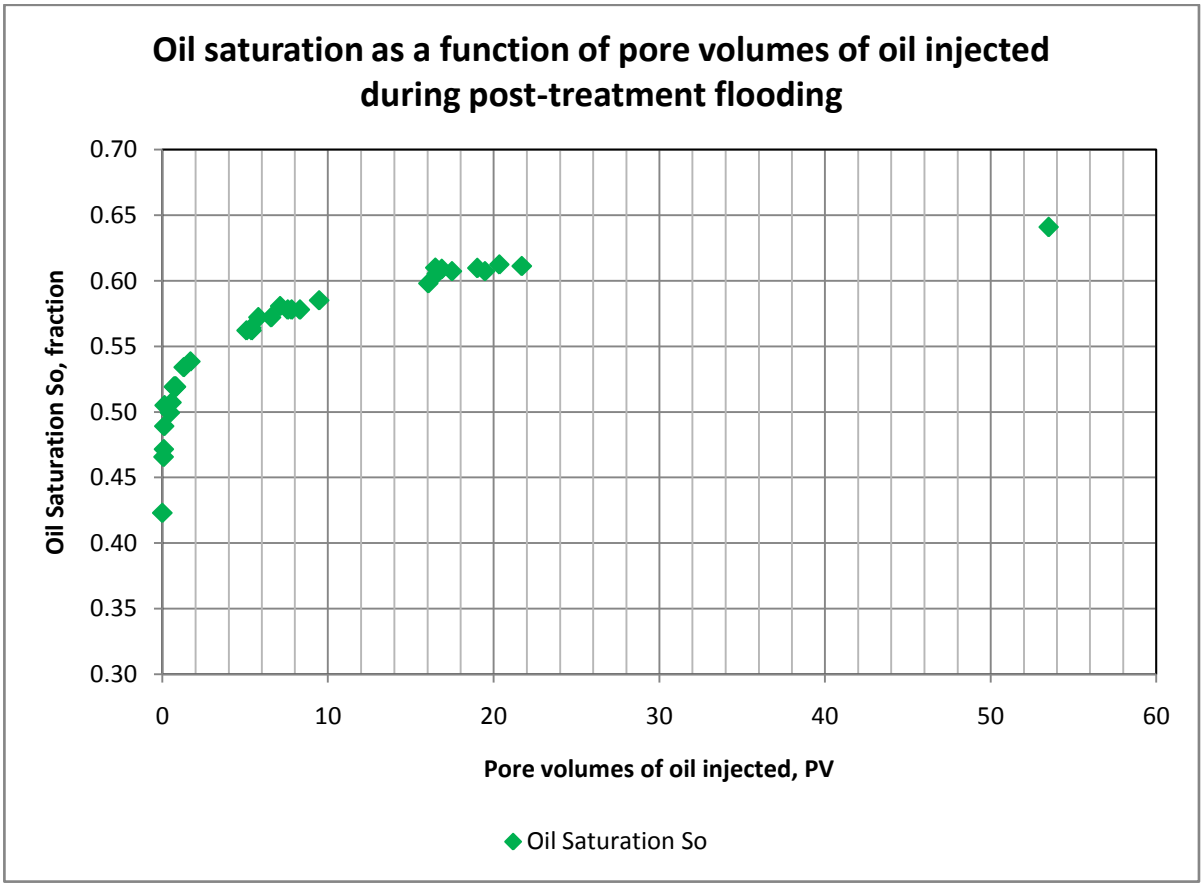

Figure 40: Oil saturation as a function of pore volumes of oil injected during post-treatment flooding

The values for effective permeability to oil ($K_{o,after}$) in the core after treatment were calculated using the Darcy equation. The final $K_{o,after}$ value was used in conjunction with the

final $K_{o,before}$ value to calculate the residual resistance factor for oil (RRF_o). The table summarising the calculated values of saturation of oil and $K_{o,after}$ and RRF is given in Appendix D.

The values found for RRF_o and RRF_w are given in table 43.

Parameter	Value
RRF_w	55.26543
RRF_o	15.50236

Table 43: Values for RRF_w and RRF_o

The residual resistance factor (RRF) gives the polymer-induced permeability reduction. Hence, from table 43, it is obvious that the effective permeability for water after treatment with polymer is reduced by a factor of 55.3, while it is only reduced by a factor of 15.5 for oil (please note that this RRF value for oil has been calculated using the values of effective permeability of oil before and after treatment at the same water saturation value $S_{wi,after}$). This shows that although effective permeability reduction to oil was high, the effective permeability to water is reduced more significantly than the reduction observed in the effective permeability to oil.

Effective permeability to oil and water in the core before and after treatment with polymer is plotted as a function of water saturation. This plot is given in figure 41.

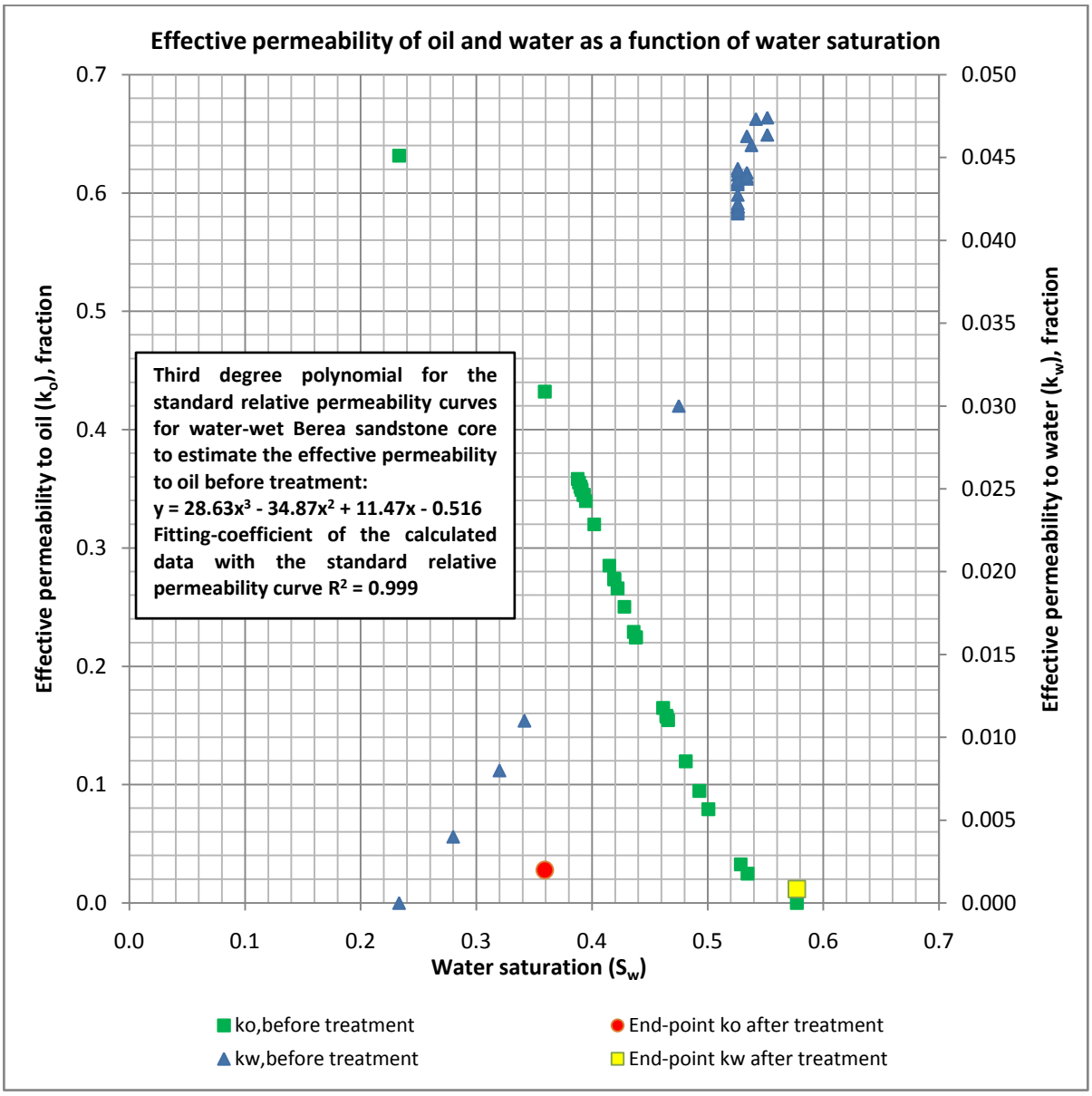

Figure 41: Effective permeability to oil and water before and after treatment with polymer as a function of water saturation

In figure 41, the effective permeability to oil before and after treatment is depicted on primary y-axis and the effective permeability to water on secondary y-axis. The green-squared points give the calculated values for effective permeability to oil before treatment and the blue-triangled points give the calculated values for effective permeability to water before treatment. The red-circled dot gives the estimated end-point k_o after treatment and the yellow-squared dot gives the estimated end-point k_w after treatment. The third degree polynomial equation (given in figure 41), for the standard experimental relative permeability curves for water-wet Berea sandstone core, is used to calculate the values for effective permeability to oil in the core before treatment with polymer at the same water saturation

readings to compare the effective permeability to oil before and after treatment. As can be observed from figure 41, there is a decrease in the effective permeability to oil in the core after polymer treatment. This decrease is quantified by the residual resistance factor for oil which, as mentioned before, has been estimated to be equal to 15.5. This value is high for oil but, compared to the RRF value for water (55.3), it still looks reasonable. Both these values prove that there is a potential DPR effect observed due to the injection of associative polymer into the core. The standard experimental values of relative permeability curves for water-wet Berea core and the calculated values for RRF_w and RRF_o are given in Appendix D.

Figure 42 gives the residual resistance factor of oil as a function of pore volumes of oil injected during post-treatment flooding.

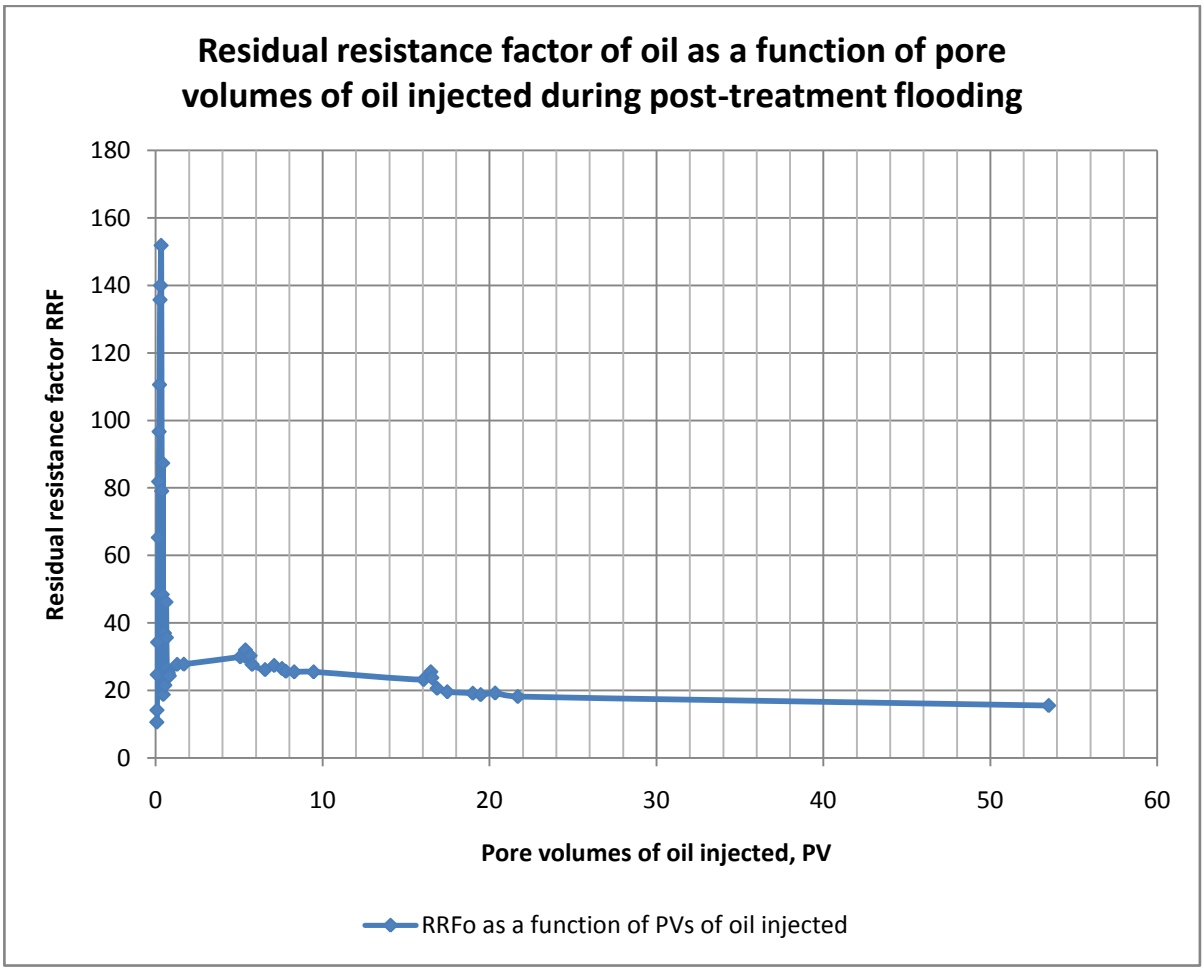

Figure 42: Residual resistance factor of oil as a function of pore volumes of oil injected during post-treatment flooding

This figure shows that as the volume of injected oil is increasing, the residual resistance factor is decreasing. This means that the effective permeability to oil in the core is increasing as increased volumes of post-flood oil are injected into the core. In addition, changing to higher rates caused minor improvements in the effective oil permeability.

Table 44 gives the initial and final saturation of water in the core until this step.

	Pre-treatment			Treatment	Post-treatment	
	Brine injection	Oil injection	Brine injection	Polymer injection	Brine injection	Oil injection
Initial S_w	0	1	0.2332	0.5515	0.5770	0.5770
Final S_w	1	0.2332	0.5515	0.5770	0.5770	0.3590

Table 44: Initial and final saturations of water in the core at different steps

6.3.3.3. TWO PHASE (OIL AND WATER) FLOODING

After the post-treatment with oil, two-phase flooding with oil and water was carried out at different fractional flows of 0.22, 0.5 and 0.78 but due to the high dead volumes (mainly outlet tubings from the core to the separator) and erroneous values from oil pump cylinders, the results obtained were not as expected. Therefore, in order to determine the water content of the core at the last stage of the two-phase flow (at the fractional flow of 0.78 for two-phase flooding), it is recommended to carry out water flooding again with a different composition (for example with nitrate ions) to remove all the previous brine water from the core. The determined water content is used to obtain the real residual oil saturation. Then, through an ion analysis of the effluent samples which are taken at frequent time intervals, the true volume of the original brine (sodium chloride) in the core will be obtained. It is probable that very large volumes of water with the new composition have to be injected to completely remove the brine water from the core. Based on the new true value for residual oil saturation in the core, the two-phase flooding saturation results can be adjusted.

7. CONCLUSIONS AND RECOMMENDATIONS

In this section the overall summary and conclusions from this study are presented and the recommendations for the future works are suggested.

7.1. CONCLUSIONS

The main conclusions drawn from the laboratory evaluation carried out for silicates and polymers are given below:

1. Gelation time, gel strength and post-gelation behaviour (mainly shrinkage) are the major factors that affect the application of a gel for DPR/RPM water-shutoff treatments.
2. The sodium silicate system is found to form a gel faster than the potassium silicate system at temperatures below or equal to 60°C, whereas the potassium silicate system is found to form a gel faster at temperatures above 60°C than the sodium silicate system.
3. An appropriate silicate system can be chosen for conformance-improvement treatment depending on the depth of the reservoir, reservoir temperature, gelation time required, capacities of the injection pumps and the time required to inject and place the gelant system at the designated areas in the reservoir.
4. Gelation time is reduced with increasing temperature.
5. The higher the number of acids used as activators in the system, the shorter is the gelation time at constant salt concentration.
6. $CaCl_2$ has a catalytic effect on gelation time.
7. Hydrochloric acid (HCl) has been found to form hard residue on the walls of the bob and cup assembly of the rheometer with the sodium silicate system without formation of gels for up to 12 hours.
8. The effects of EDTA, $CaCl_2$ and temperature on the sodium silicate and the potassium silicate systems have been investigated and defined through a unified sol-gel transition time correlation.
9. Associative polymer with concentrations of more than 1500 PPM are found to form strong gels with zirconium (III) crosslinker (concentration varying from 250 PPM to 1500 PPM) at 80°C and 60°C at pH values ranging from 5 to 7.
10. The viscosity values for 2000 PPM of associative polymer with any concentration of crosslinker are found to be in the favourable range of 20 to 30 cP, which is suitable for injectivity purposes.

11. An increasing trend of the gelation time has been observed at 80°C when 2000 PPM of associative polymer is mixed with concentrations of zirconium (III) crosslinker increasing from 250 PPM to 1500 PPM. For crosslinker concentrations lower than 250 PPM, no gel is formed and for crosslinker concentrations higher than 1750 PPM, gel seems to form after very long durations of time (found to be more than 1500 hours).
12. A slight shrinkage was observed in the samples with associative polymer crosslinked to zirconium (III) samples at 80°C. This fact has to be taken into account while planning the conformance-improvement treatment with associative polymers.
13. The gelation times for associative polymers with chitosan (1.5 wt%) are very long (more than 1000 hours) and the samples have shown syneresis and shrank to as much as 97% of their original volumes.
14. Chromium (III) is not found to be a good crosslinker for associative polymers.
15. Acrylamido-Methyl-Propane Sulfonate (AMPS) polymers gel instantaneously with zirconium (III) crosslinker at room temperature.
16. Anionic hydrolysed polyacrylamides (HPAM) does not form gel with very high concentrations of chromium (III) crosslinker. The ones with lower concentrations of crosslinker that formed a gel at 80°C showed severe shrinkage.
17. Polyethylenimine (PEI - 1 wt%) is not found to be a good crosslinker for any of the three polymers tested.
18. The core flooding experiment on the Berea sandstone core has shown that associative polymers do show potential DPR effects when injected into the porous medium.
19. Calculated values for oil and water residual resistance factors have shown that even though the reduction in the effective permeability to oil was high after the injection of associative polymer, the reduction in effective permeability to water was significantly higher.
20. Associative polymer is retained when injected in porous media which causes a reduction in the mobility of polymer.
21. The reduction in absolute permeability of the core after the injection of associative polymer, due to the creation of Inaccessible Pore Volume (IPV) by polymer injection, also leads to a reduction in the mobility of polymer.

7.2. RECOMMENDATIONS FOR FUTURE WORK

This work has produced very interesting outcomes that are worth looking into in the future. My recommendations for future work that can be performed to enhance our knowledge and strengthen our stand on the use of silicates and polymers for DPR in the oil reservoirs are given below:

1. A reservoir pilot test is recommended to better understand the advantages and pitfalls of using silicate systems for conformance-improvement treatments and any risks associated with their application in real field scenarios.
2. The silicate samples should be kept for longer periods of time with the Dynamic-Mechanical (DMA) mode running after the sol-gel transition time so that a high apparent viscosity value is attained where it is expected that a stronger gel is formed before starting the Amplitude Sweep (AS) mode for carrying out strength test.
3. More tests for silicates with high concentrations of calcium ions or EDTA should be designed and performed to observe the trend of the gel strengths beyond the tested concentrations to get a better picture of how the samples are behaving after sol-gel transition times for high concentrations of divalent ions or EDTA.
4. More detailed laboratory tests should be planned for associative polymers to better understand their rheological properties and to get a more accurate estimate of their gelation times with zirconium (III) crosslinker.
5. More core flooding experiments should be designed and performed with associative polymers to better perceive their behaviour in the porous media and their effect on the oil recovery. A different approach can be to crosslink the associative polymer with zirconium (III) and carry out core flooding experiments on different kinds of cores.
6. Numerical simulations with sensitivity analysis should be carried out based on the data obtained from the associative polymer core flooding experiment to upscale from the pore-scale and visualise the DPR effects on a reservoir-scale.

REFERENCES

Bailey, B., Crabtree, M., Tyrie, J., Elphick, J., Kuchuk, F., Romano, C., and Roodhart, L. 2000. Water Control. *Oilfield Review*.

Barnes H.A. 2000. *A Handbook of Elementary Rheology*. Aberystwyth: The University of Wales Institute of Non-Newtonian Fluid Mechanics.

Bedaiwi, E., Al-Anazi, B.D., Al-Anazi, A.F., and Paiaman, A.M. 2009. Polymer Injection for Water Production Control through Permeability Alteration in Fractured Reservoir. *NAFTA* **60** (4): 221-231.

Botermans, C.W., Van Batenburg, D.W., and Bruining, J. 2001. Relative Permeability Modifiers: Myth or Reality?. Paper SPE 68973 presented at the SPE European Formation Damage Conference, The Hague, Netherlands, 21-22 May.

Bowers, B.E., Brownlee, R.F., and Schrenkel, P.J. 1998. Development of a Downhole Oil/Water Separation and Reinjection System for Offshore Application. Paper SPE 8865 presented at the Offshore Technology Conference, Houston, Texas, 4-7 May.

Brinker, C.J. and Scherer, G.W. 1990. *Sol-Gel Science: The Physics and Chemistry of Sol-Gel Processing*. San Diego, California: Academic Press Inc.

Bryant, S.L., Rabaioli, M.R., and Lockhart, T.P. 1996. Influence of Syneresis on Permeability Reduction by Polymer Gels. *SPE Production & Facilities* **11** (04): 209–215, November. SPE-35446-PA.

Bøye, B., Rygg, A., Jodal, C., and Klungland, I. 2011. Development and Evaluation of a New Environmentally Acceptable Conformance Sealant. Paper SPE 142417 presented at the SPE European Formation Damage Conference, Noordwijk, Netherlands, 7-10 June.

Chitosan. 2012, June 18. Retrieved March 15, 2015, from Sigma-Aldrich http://www.sigmaaldrich.com/catalog/product/aldrich/417963?lang=en&region=NO

Chromium (III) Acetate Hydroxide. 2014, February 12. Retrieved March 15, 2015, from Sigma-Aldrich http://www.sigmaaldrich.com/catalog/product/aldrich/318108?lang=en&region=NO

Conformance Improvement Gel Treatment Design. 2015, February 11. Retrieved May 20, 2015, from PetroWiki http://petrowiki.org/Conformance_improvement_gel_treatment_design

Dunlap, D.D., Boles, J.L., and Novotny, R.J. 1986. Method for Improving Hydrocarbon/Water Ratios in Producing Wells. Paper SPE 4822 presented at the SPE Formation Damage Control Symposium, Lafayette, Louisiana, 26-27 February.

Green, D.W. and Willhite, G.P. (1998). *Enhanced Oil Recovery*. Richardson, Texas: Society of Petroleum Engineers

Hamouda, A.A. and Akhlaghi Amiri, H.A. 2014. Factors Affecting Alkaline Sodium Silicate Gelation for In-Depth Reservoir Profile Modification. *Energies* **7** (2): 568-590.

Hatzignatiou, D.G., Askarinezhad, R., Giske, N.H., and Stavland, A. 2015. Laboratory Testing of Environmentally Friendly Chemicals for Water Management. Paper SPE 173853 presented at the SPE one day seminar, Bergen, Norway, 22 April.

Hatzignatiou, D.G. and Olsen, T. 1999. Innovative Production Enhancement Interventions through Existing Wellbores. Paper SPE 54632 presented at the SPE Western Regional Meeting, Anchorage, Alaska, 26-27 May.

Heemskerk, J., Rosmalen, R., Janssen-van, R., Holtslag, R. J., and Teeuw, D. 1984. Quantification of Viscoelastic Effects of Polyacrylamide Solutions. Paper SPE 12652 presented at the SPE Enhanced Oil Recovery Symposium, Tulsa, Oklahoma, 15-18 April.

Hirasaki, G.J. and Pope, G.A. 1974. Analysis of Factors Influencing Mobility and Adsorption in the Flow of Polymer Solution Through Porous Media. *Society of Petroleum Engineers Journal* **14** (4): 337–346, August.

Iler, R.K. 1979. *The Chemistry of Silica: Solubility, Polymerization, Colloid and Surface Properties and Biochemistry*. New York City: John Wiley & Sons/Wiley-Interscience.

Instruction Manual MCR Series. 2011. Ostfildern: Anton Paar Germany GmbH

Jurinak, J.J. and Summers, L.E. 1991. Oilfield Applications of Colloidal Silica Gel. *SPE Production Engineering* **6** (4): 406–412. SPE-18505-PA.

Jurinak, J.J. and Summers, L.E. 1991. Laboratory Testing of Colloidal Silica Gel for Oilfield Applications (Supplement to SPE 18505). Paper SPE 23581 available from SPE, Richardson, Texas, USA.

Kafil, V. and Omidi, Y. 2011. Cytotoxic Impacts of Linear and branched Polyethylenimine Nanostructures in A431 Cells. *BioImpacts* **1** (1): 23-30, June.

Kalfayan, L.J. and Dawson, J.C. 2004. Successful Implementation of Resurgent Relative Permeability Modifier (RPM) Technology in Well Treatments Requires Realistic Expectations. Paper SPE 90430 presented at the SPE Annual Technical Conference and Exhibition, Houston, Texas, 26-29 September.

Krumrine, P.H. and Boyce, S.D. 1985. Profile Modification and Water Control with Silica Gels. In Proceedings of the SPE International Symposium on Oilfield and Geothermal Chemistry, Phoenix, AZ, USA, 9–11 April.

Lakatos, I., Lakatos-Szabo, J., Tiszai, Gy., Palasthy, Gy., Kosztin, B., Tromboczky, S., Bodola, M. and Patterman-Farkas, Gy. 1999. Application of Silicate-Based Well Treatment Techniques at the Hungarian Oil Fields. Paper SPE 56739 presented at the SPE Annual Technical Conference and Exhibition, Houston, Texas, 3-6 October.

Lane, R.H. and Seright, R.S. 2000. Gel Water Shutoff in Fractured or Faulted Horizontal Wells. Paper SPE 65527 presented at the 2000 SPE/PS-CIM International Conference on Horizontal Well Technology, Calgary, Alberta, Canada, 6-8 November.

Littmann, W. 1988. *Polymer Flooding*. Amsterdam: Elsevier Science Publishers B.V.

Mennella, A., Chiappa, L., Lockhart, T.P., and Burrafato, G. 2001. Candidate and Chemical Selection Guidelines for Relative Permeability Modification (RPM) Treatments. *SPE Production & Facilities* **16** (03): 181-188, August. SPE-72056-PA.

Meyers, M.A. and Chawla, K.K. 1998. *Mechanical Behavior of Materials*. Upper Saddle River, New Jersey: Prentice-Hall.

Mezger, T.G. 2011. *The Rheology Handbook, 3rd Revised Edition*. Hanover: Vincentz Network.

Norris, U.L. 2011. *Core-Scale Simulation of Polymer Flow Through Porous Media*. Master Thesis. U.L. Norris, Stavanger.

Perez D., Fragachan F.E., Ramirez, A., and Ferraud J.P. 2001. Applications of Polymer Gel for Establishing Zonal Isolations and Water Shutoff in Carbonate Formations. *SPE Drilling & Completion* **16** (3): 182–189, September.

Pham, L.T. and Hatzignatiou, D.G. 2015. *Rheological Evaluation of Sodium Silicate Gel for Water Management in Mature, Naturally-Fractured Oilfields.* Paper submitted for publication.

Polyethylenimine. 2008. Retrieved March 18, 2015, from Chemical Book: http://www.chemicalbook.com/ProductChemicalPropertiesCB5499238_EN.htm

Polyethylenimine, ethylenediamine branched. 2014, December 1. Retrieved March 15, 2015, from Sigma-Aldrich http://www.sigmaaldrich.com/catalog/product/aldrich/408719?lang=en&region=NO

Poly(ethyleneimine) solution. 2013, July 4. Retrieved March 15, 2015, from Sigma-Aldrich https://www.sigmaaldrich.com/catalog/product/fluka/03880?lang=en&region=NO

Reddy, B.R., Eoff, L., Dalrymple, E.D., Black, K., Brown, D., and Rietjens, M. 2003. A Natural Polymer-Based Cross-Linker System for Conformance Gel Systems. *SPE Journal* **8** (2): 99-106, June. SPE-84937-PA.

Reichenbach-Klinke, R., Stavland, A., Langlotz, B., Wenzke, B., & Brodt, G. 2013. New Insights into the Mechanism of Mobility Reduction by Associative Type Copolymers. Paper SPE 165225 presented at the SPE Enhanced Oil Recovery Conference, Kuala Lumpur, Malaysia, 2-4 July.

Reichenbach-Klinke, R., Stavland, A., Zimmermann, T., Bittner, C. and Brodt, G. 2015. Associative Copolymers for Polymer Flooding - Structure-Performance Relationships in Porous Media. Paper presented at the IOR 2015 - 18th European Symposium on Improved Oil Recovery, Dresden, Germany, 14-16 April.

Rheology. 1998. Retrieved April 20, 2015, from http://www.uio.no/studier/emner/matnat/kjemi/KJM3100/v07/undervisningsmateriale/Lecture%202.pdf

Sandiford, B.B. 1964. Laboratory and Field Studies of Water Floods Using Polymer Solutions to Increase Oil Recovery. *Journal of Petroleum Technology,* 917-922, August. SPE-844-PA.

Seright, R.S., Lane, R.H., and Sydansk, R.D. 2001. A Strategy for Attacking Excess Water Production. Paper SPE 70067 presented at the SPE Permian Basin Oil and Gas Recovery Conference, Midland, Texas, 15-17 May.

Seright, R.S., Lane, R.H., and Sydansk, R.D. 2003. A Strategy for Attacking Excess Water Production. SPE-84966-PA. *SPE Production & Facilities* **18** (3): 158-169.

Simjoo, M., Vafaie Sefti, M., Dadvand, A., Hasheminasab, R., and Sajjadian, V.A. 2007. Polyacrylamide Gel Polymer as Water Shut-off System**:** Preparation and Investigation of Physical and Chemical Properties in One of the Iranian Oil Reservoir Conditions. *Iranian Journal of Chemistry & Chemical Engineering* **26** (4): 99-108.

Skrettingland, K. Giske, N.H., Johnsen, J.H. and Stavland, A. 2012. Snorre In-depth Water Diversion Using Sodium Silicate - Single Well Injection Pilot. Paper SPE 154004 presented at the SPE Improved Oil Recovery Symposium, Tulsa, Oklahoma, 14-18 April.

Sodium and Potassium Silicates: Versatile compounds for your applications, PQ Europe. 2004, October. Retrieved April 15, 2015 from http://www.pqcorp.com/Portals/1/docs/Sodium%20and%20Potassium%20silicates%20brochure%20ENG%20oct%202004.pdf

Southwick, J.G. and Manke, C.W. 1988. Molecular Degradation, Injectivity, and Elastic Properties of Polymer Solutions. *SPE Reservoir Engineering* **3** (4): 1193-1201, November.

Sparlin, D.D. 1976. An Evaluation of Polyacrylamides for Reducing Water Production (includes associated papers 6561 and 6562). *Journal of Petroleum Technology* **28** (8): 906-914. SPE-5610-PA.

Stavland, A. and Nilsson, S. 2001. Segregated Flow Is the Governing Mechanism of Disproportionate Permeability Reduction in Water and Gas Shutoff. Paper SPE 71510 presented at the 2001 SPE Annual Technical Conference and Exhibition, New Orleans, Louisiana, 30 September - 3 October.

Stavland, A., Jonsbråten, H.C., Vikane, O., Skrettingland, K. and Fischer, H. 2011. In-depth water diversion using sodium silicate - Preparation for single well field pilot on Snorre. Paper presented at the 16th European Symposium on Improved Oil Recovery, Cambridge, UK, 12-14 April.

Sydansk, R.D. 1990. A Newly Developed Chromium(III) Gel Technology. *SPE Reservoir Engineering* **5** (3): 346-352. SPE-19308-PA.

Sydansk, R.D. and Romero-Zeron, L. 2011. *Reservoir Conformance Improvement.* Richardson, Texas: Society of Petroleum Engineers

Sydansk, R.D. and Seright, S.S. 2006. When and Where Relative Permeability Modification Water-Shutoff Treatments can be Successfully Applied. Paper SPE 99371 presented at the SPE/DOE Symposium on Improved Oil Recovery, Tulsa, Oklahoma, 22-26 April.

Sydansk, R.D. and Southwell, G.P. 2000. More Than 12 Years of Experience with a Successful Conformance-Control Polymer Gel Technology. *SPE Production & Facilities* **15** (4): 270. SPE-66558-PA.

Taylor, K.C. and Nasr-El-Din, H.A. 1998. Water-Soluble Hydrophobically Associating Polymers for Improved Oil Recovery: A Literature Review. *Journal of Petroleum Science and Engineering* **19**: 265-280.

Usaitis, V. 2011. *Laboratory Evaluation of Sodium Silicate for Zonal Isolation.* Master Thesis. V. Usaitis, Stavanger.

VanLandingham, J.V. 1979. Laboratory & Field Development of Dispersed Phase Polymer Systems for Water Control. Paper SPE 8423 presented at the SPE Annual Technical Conference and Exhibition, Las Vegas, Nevada, 23–26 September.

Vinot, B., Schechter, R.S., and Lake, L.W. 1989. Formation of Water Soluble Silicate Gels by the Hydrolysis of Diester of Dicarboxylic Acid Solubilized as Microemulsions. *SPE Reservoir Engineering* **4** (3): 391-397, August. SPE-14236-PA.

Weaver, J.D. 1978. A New Water-Oil Ratio Improvement Material. Paper SPE 7574 presented at the SPE Annual Fall Technical Conference and Exhibition, Houston, Texas, 1–3 October.

White, J.L., Goddard, J.E., and Phillips, H.M. 1973. Use of Polymers to Control Water Production in Oil Wells. *Journal of Petroleum Technology* **25** (2): 143–150. SPE-3672-PA.

Zaitoun, A., Kohler, N., Bossie-Codreanu, D., and Denys, K. 1999. Water Shutoff by Relative Permeability Modifiers: Lessons from Several Field Applications. Paper SPE 56740 presented at the SPE Annual Technical Conference and Exhibition, Houston Texas, 3-6 October.

APPENDIX A

This appendix presents an example showing the plots obtained for Dynamic-Mechanical (DMA) measuring mode applied on a sample to measure the gel point.

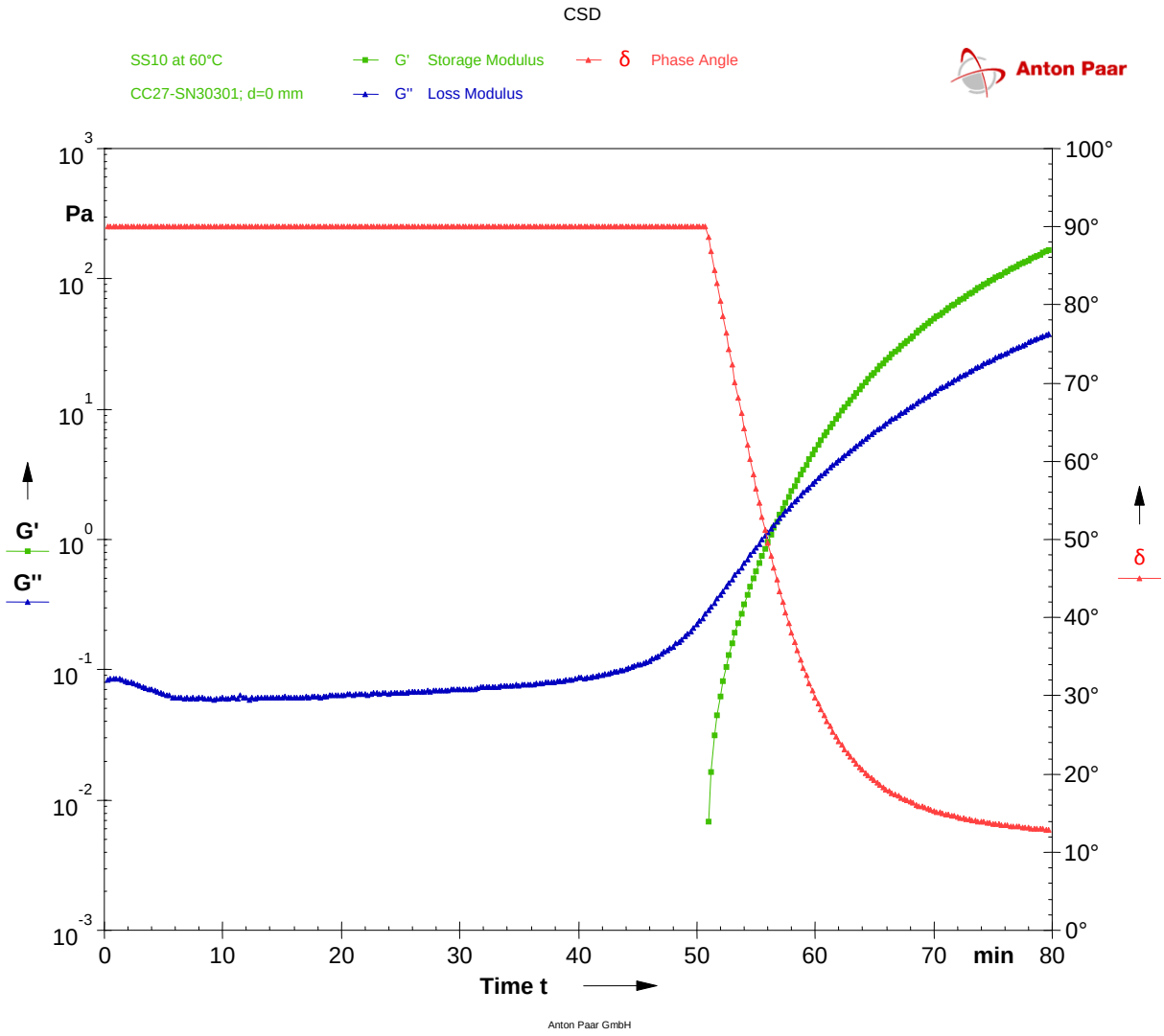

Figure A1: Plot of loss and storage modulus, and phase angle with time for SS10 case at 60°C

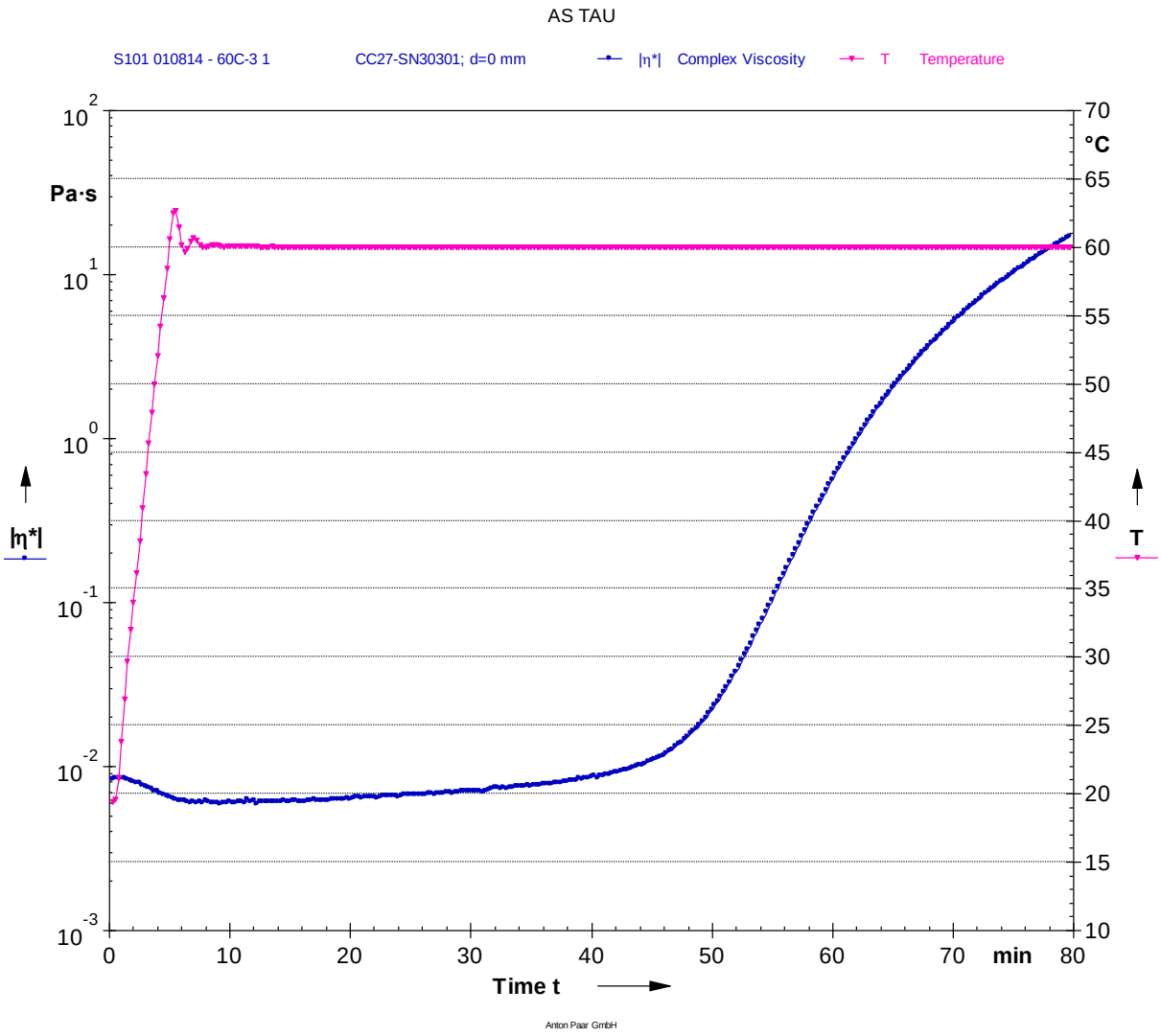

Figure A2: Plot of apparent viscosity as a function of time for SS10 case at 60°C

APPENDIX B

This appendix gives the gel points at different temperatures when the silicates are mixed with the different activator systems, with the correlations used to establish the relationship between gel points and percentage of $CaCl_2$/EDTA concentration for deriving the unified sol-gel transition time correlation.

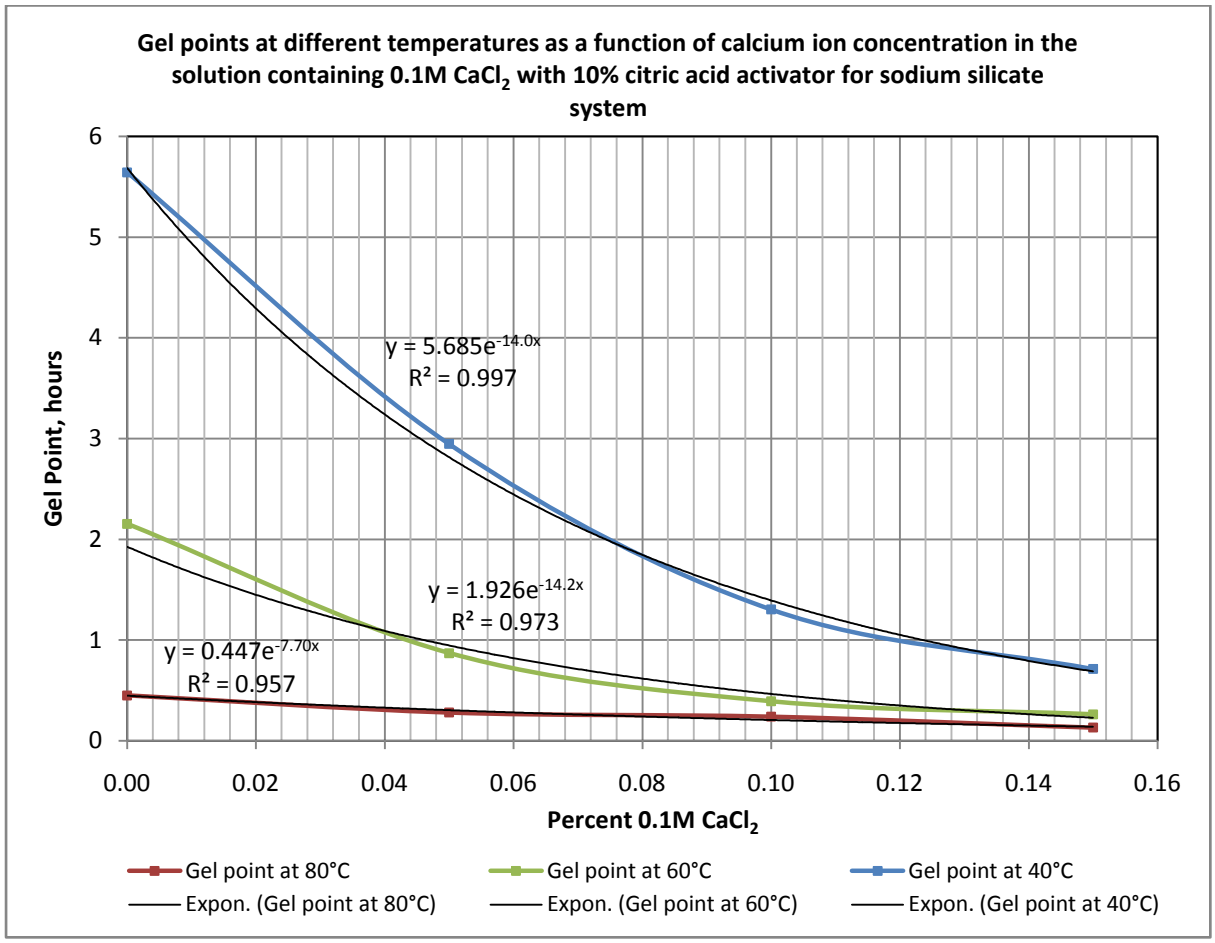

Figure B1: Gel points at different temperatures as a function of calcium ion concentration in the solution containing 0.1M $CaCl_2$ with 10% citric acid activator for the sodium silicate system

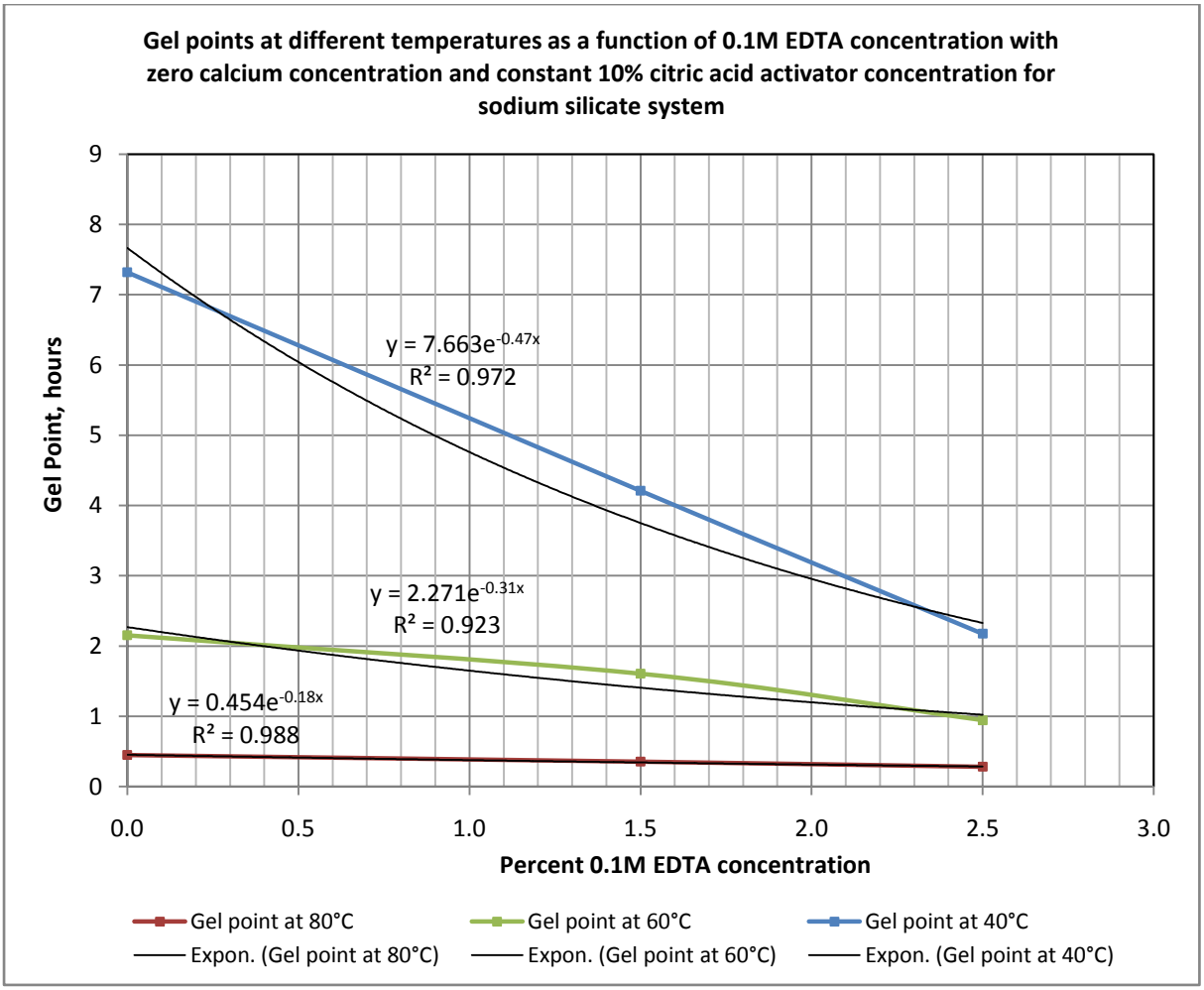

Figure B2: Gel points at different temperatures as a function of 0.1M EDTA concentration with zero calcium concentration and constant 10% citric acid activator for the sodium silicate system

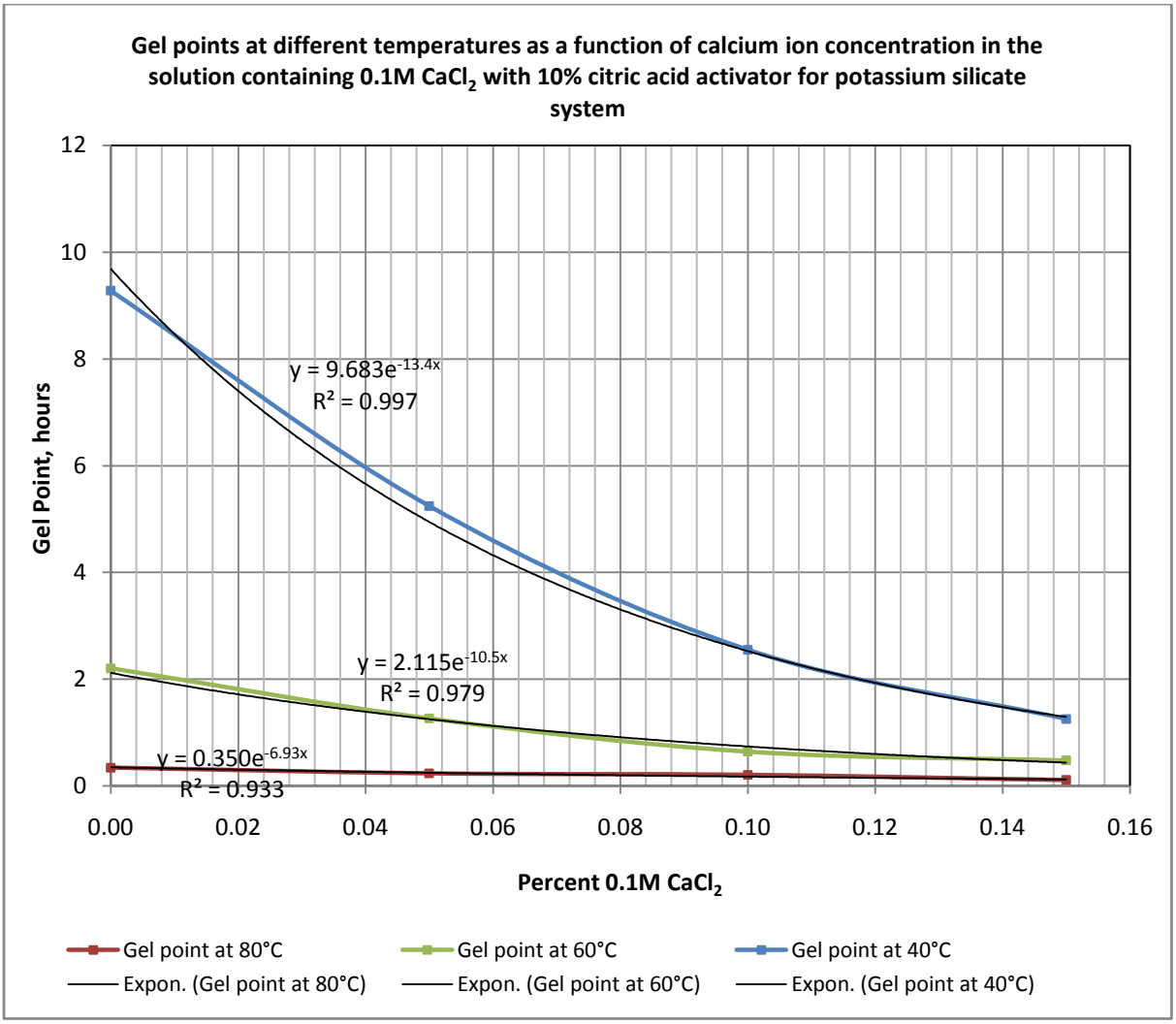

Figure B3: Gel points at different temperatures as a function of calcium ion concentration in the solution containing 0.1M $CaCl_2$ with 10% citric acid activator for the potassium silicate system

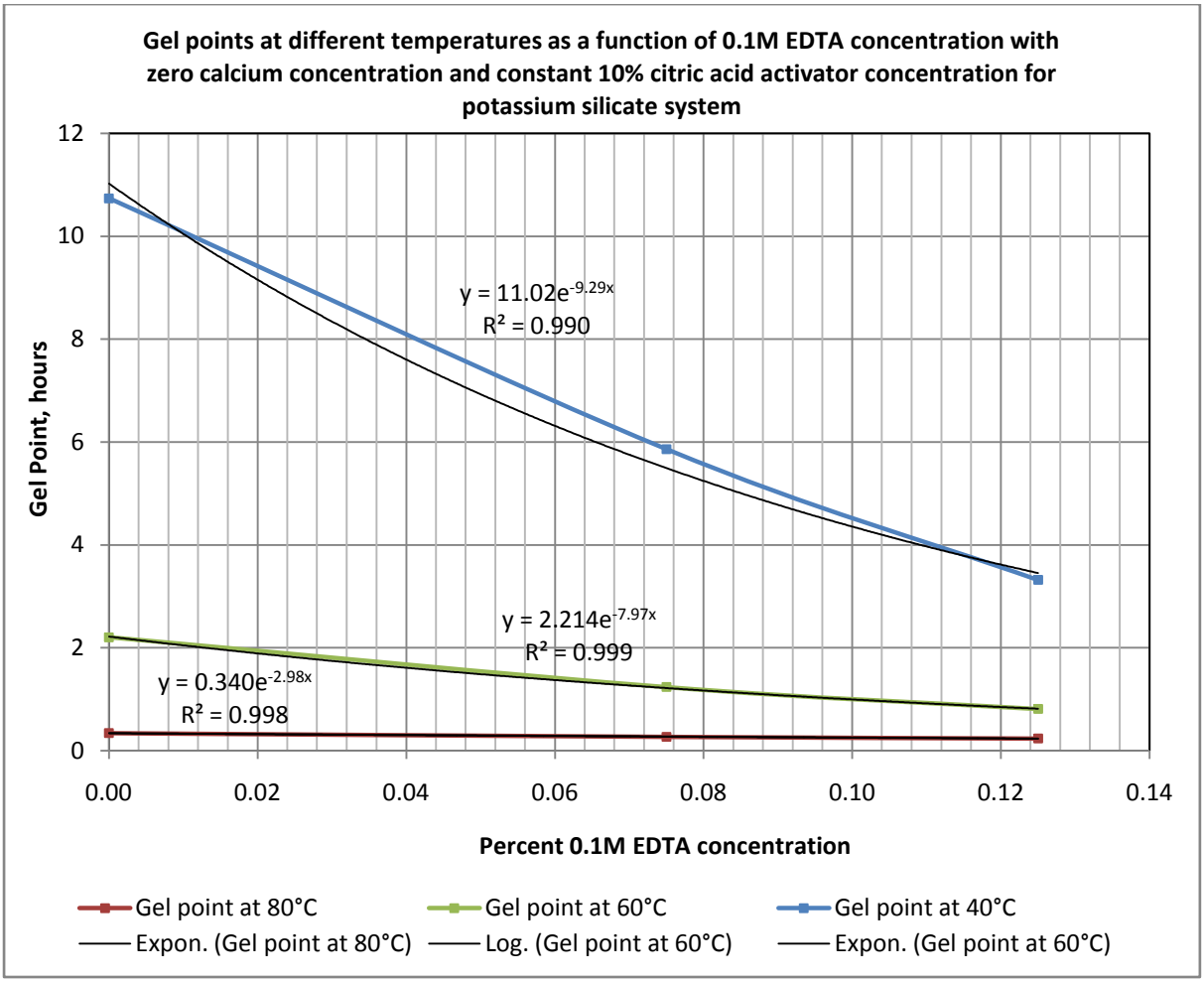

Figure B4: Gel points at different temperatures as a function of 0.1M EDTA concentration with zero calcium concentration and constant 10% citric acid activator concentration for the potassium silicate system

APPENDIX C

This appendix presents the plots of gelation time as a function of inverse absolute temperature, with the correlations and the fitting coefficients used to find the value of activation energy to derive the unified sol-gel transition time correlation for the silicate systems.

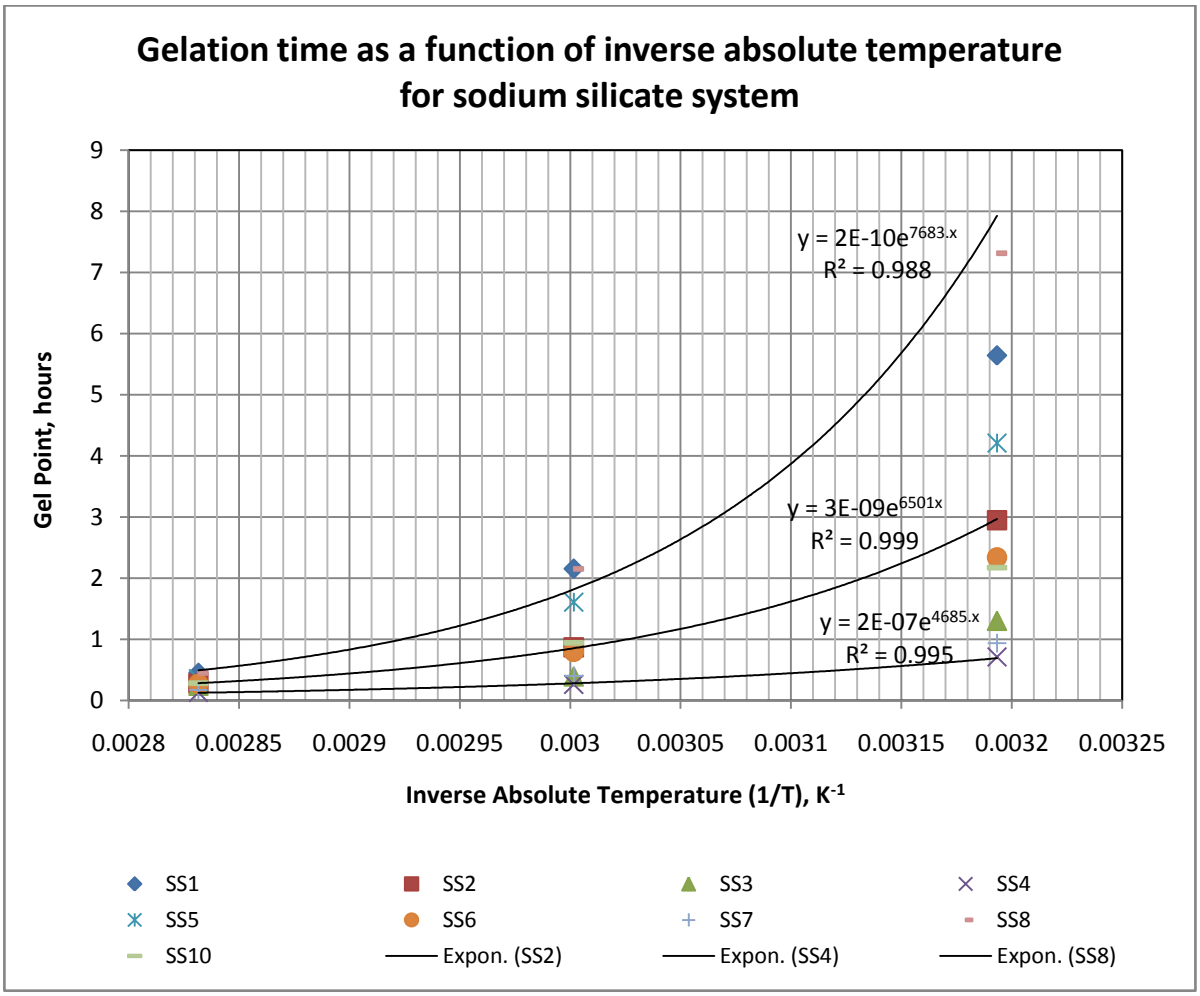

Figure C1: Gelation time as a function of inverse absolute temperature for the sodium silicate system with the correlations used to find the value of activation energy

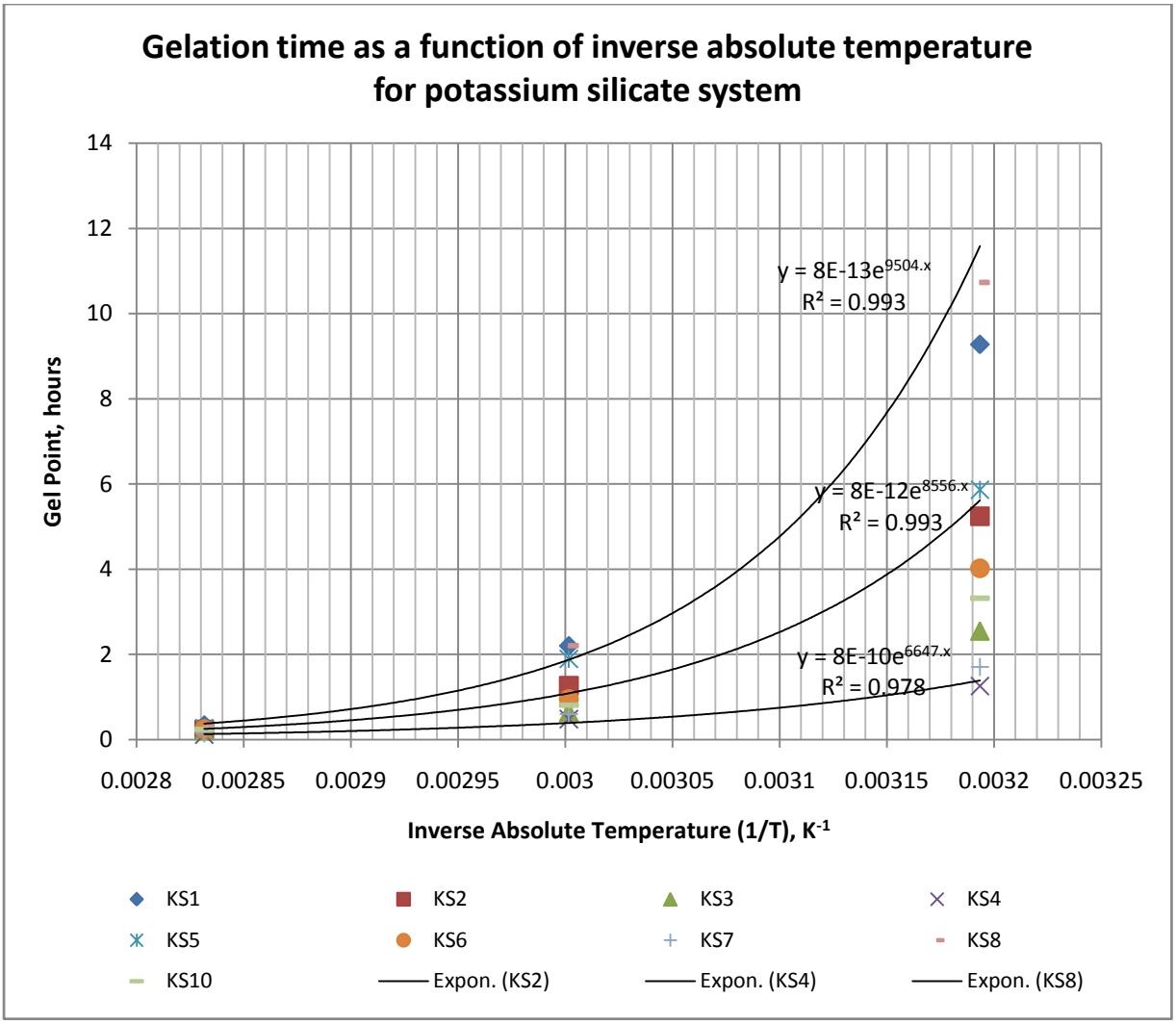

Figure C2: Gelation time as a function of inverse absolute temperature for the potassium silicate system with the correlations used to find the value of activation energy

APPENDIX D

This appendix gives the various tables with the results obtained from various steps of core flooding experiment performed on Berea sandstone core.

Parameters	Abbreviations	Units	Values
Length of core	L	cm	9.564
Diameter of core	d	cm	3.776
Cross-sectional area	A	sq. Cm	11.1983
Pore volume	PV	cc	25.484
Volume of spiral grooves	Vsg	cc	0.1
Volume of steel screen	Vss	cc	0.2
Total inlet tubing length	$L_{t,i}$	cm	60
Total outlet tubing length	$L_{t,o}$	cm	50
Tube Volume per unit length	V_t/L_t	cc/cm	0.0156
Inlet tubing volume	$V_{t,i}$	cc	0.936
Outlet tubing volume	$V_{t,o}$	cc	0.78
Viscosity of brine	μ_w	cp	1
Viscosity of oil	μ_o	cp	1.29
Oil/water inlet tubing length per tubing	$L_{t,i/t}$	cm	20
Oil/water inlet tubing volume per tubing	$V_{t,i/t}$	cc	0.312
Oil/water outlet tubing length per tubing	$L_{t,o/t}$	cm	25
Oil/water outlet tubing volume per tubing	$V_{t,o/t}$	cc	0.39
Outlet line to the separator inlet volume	$V_{o,s}$	cc	2.4
Separator - Rig, from inlet upto tip of the inner tube volume	$V_{si,ri}$	cc	0.316
Plastic pipe outlet from core volume	$V_{pp,c}$	cc	3.433
Total volume of the pipes from the outlet of core to the inlet of separator	$V_{s,r}$	cc	6.539

Table D1: General parameters for the core and the rig used in the core flooding experiment, and the viscosities for oil and water

In the following tables, the subscript 'n' denotes the n^{th} time reading and 'n+1' denotes the $(n+1)^{th}$ time reading. As an example, $S_{l,n}$ denotes the separator level at the nth time reading.

PRE-TREATMENT FLOODING WITH OIL TO ESTABLISH $S_{wi,before}$

Day	Oil injection rate, $q_{o,cc/min}$	Oil injection rate, $q_{o,cc/sec}$	Exact time	Separator level, S_l	Change in the separator level, ΔS_l	Cylinder 1A volume, V_{cyl1A}	Cylinder 1B volume, V_{cyl1B}	Approximate watercut in outlet tubings, WC	Oil volume in the core, $V_{o,c}$	Oil saturation, So	Differential pressure, dP_{mbar}	dP at q=0, $dP_{q=0,mbar}$	Corrected dP, $dP_{corrected,mbar}$	Differential pressure in atm, dP_{atm}	ΔP/q	Effective Permeability to Oil, K_o	Cumulative Volume of Oil Injected	Pore volumes of oil injected
					$\Delta S_{l,n} = S_{l,1} - S_{l,n}$			$WC = (S_{l,n} - S_{l,n+1})/(V_{cum,o,n+1} - V_{cum,o,n})$	$V_{o,c,n} = \Delta S_{l,n} - V_{sc} - V_{ss} - V_{t,i/t} - ((1-WC_n)*V_{s,r}) + ((V_{cyl1A,1} + V_{cyl1B,1}) - (V_{cyl1A,n} + V_{cyl1B,n})$				$dP_{corrected,mbar} = dP_{mbar} - dP_{q=0,mbar}$	$dP_{atm} = 0.00098692326*dP_{corrected,mbar}$	$\Delta P/q = dP_{corrected,mbar}/q_{o,cc/min}$	$K_o = q_{o,cc/sec}*\mu_o*L/(dP_{atm})*A$	$V_{cum,o}$	$PV_o = V_{cum,o}/PV$
	cc/min	cc/sec	hr:min:sec		-	ml	ml	fraction	ml	$S_o = V_{o,c}/PV$	mbar	mbar	mbar	atm	mbar.min/ml	D	ml	PV
Day 1	0	0.00000	14:10:34	39.6	0	-0.72376	0.82477	-	-		-5.2	-5.2	0	0.000	-	-	0	0.000
Day 1	0.1961	0.00327	14:12:34	37.1	2.5	-0.62749	-1.56533	-	4.38183	0.17194	-	-5.2	0	0.000	-	-	0.097	0.004
Day 1	0.5984	0.00997	14:14:34	32.3	7.3	0.17274	-6.50119	-	13.31746	0.52258	-	-5.2	0	0.000	-	-	0.897	0.035
Day 1	0.9973	0.01662	14:16:34	32	7.6	1.76629	-6.65131	0.18832	12.17403	0.47771	-	-5.2	0	0.000	-	-	2.49	0.098
Day 1	1.3996	0.02333	14:18:34	32	7.6	4.18082	-6.65160	0.00000	9.75980	0.38298	-	-5.2	0	0.000	-	-	4.905	0.192
Day 1	1.7986	0.02998	14:20:34	31.5	8.1	7.37482	-6.65036	0.15654	7.06455	0.27721	-	-5.2	0	0.000	-	-	8.099	0.318
Day 1	2	0.03333	14:22:34	26.9	12.7	2.42517	-2.74761	1.00000	12.71145	0.49880	54	-5.2	59.2	0.058	29.6	0.628563	12.004	0.471
Day 1	2	0.03333	14:24:34	21.9	17.7	-2.55156	1.26138	1.00000	18.47919	0.72513	54	-5.2	59.2	0.058	29.6	0.628563	16.013	0.628
Day 1	2	0.03333	14:26:34	19.8	19.8	-3.56900	4.12432	0.52356	15.61825	0.61286	54	-5.2	59.2	0.058	29.6	0.628563	20.024	0.786
Day 1	2	0.03333	14:28:34	18.5	21.1	0.43635	-0.84897	0.32459	16.58516	0.65081	54	-5.2	59.2	0.058	29.6	0.628563	24.029	0.943
Day 1	2	0.03333	14:30:34	17.3	22.3	4.44636	-5.82810	0.29925	18.58856	0.72942	54	-5.2	59.2	0.058	29.6	0.628563	28.039	1.100
Day 1	2	0.03333	14:32:34	19	20.6	5.96386	-5.53072	0.00000	13.11687	0.51471	54	-5.2	59.2	0.058	29.6	0.628563	32.044	1.257
Day 1	2	0.03333	14:34:34	17.75	21.85	0.98295	-1.52238	0.31188	17.37880	0.68195	54	-5.2	59.2	0.058	29.6	0.628563	36.052	1.415
Day 1	2	0.03333	14:36:34	16.7	22.9	-3.96009	2.45552	0.26395	19.08057	0.74873	54	-5.2	59.2	0.058	29.6	0.628563	40.03	1.571
Day 1	2	0.03333	14:38:34	18.2	21.4	-2.38333	2.65252	0.00000	14.08083	0.55254	54	-5.2	59.2	0.058	29.6	0.628563	44.038	1.728
Day 1	2	0.03333	14:40:34	17.3	22.3	1.62580	-2.32698	0.22449	17.41916	0.68353	54	-5.2	59.2	0.058	29.6	0.628563	48.047	1.885
Day 1	2	0.03333	14:42:34	17	22.6	5.63396	-6.64679	0.07485	17.05229	0.66914	54	-5.2	59.2	0.058	29.6	0.628563	52.055	2.043
Day 1	2	0.03333	14:44:34	18	21.6	4.48115	-4.33744	0.00000	14.40630	0.56531	54	-5.2	59.2	0.058	29.6	0.628563	56.062	2.200
Day 1	2	0.03333	14:46:34	16.9	22.7	-0.49675	-0.33070	0.27452	18.27254	0.71702	54	-5.2	59.2	0.058	29.6	0.628563	60.069	2.357

Day 1	2	0.03333	14:49:34	18	21.6	-3.16592	3.62436	0.00000	14.09157	0.55296	54	-5.2	59.2	0.058	29.6	0.628563	66.082	2.593
Day 1	2	0.03333	14:52:34	16.5	23.1	2.84287	-3.83901	0.24967	18.67873	0.73296	54	-5.2	59.2	0.058	29.6	0.628563	72.09	2.829
Day 1	2	0.03333	14:54:34	17.5	22.1	6.85552	-6.64573	0.00000	14.84022	0.58233	54	-5.2	59.2	0.058	29.6	0.628563	76.103	2.986
Day 1	2	0.03333	14:57:34	16.5	23.1	0.47385	-1.11144	0.16633	17.77526	0.69751	54	-5.2	59.2	0.058	29.6	0.628563	82.115	3.222
Day 1	2	0.03333	15:00:34	17.9	21.7	-3.95026	4.59965	0.00000	14.00062	0.54939	54	-5.2	59.2	0.058	29.6	0.628563	88.123	3.458
Day 1	2	0.03333	15:05:34	16.5	23.1	6.06621	-6.64634	0.13976	17.54404	0.68843	54	-5.2	59.2	0.058	29.6	0.628563	98.14	3.851
Day 1	2	0.03333	15:10:34	15.6	24	-3.52375	2.10402	0.08987	18.95736	0.74389	54	-5.2	59.2	0.058	29.6	0.628563	108.155	4.244
Day 1	2	0.03333	15:11:34	17	22.6	-4.09010	4.10822	0.00000	15.53189	0.60948	54	-5.2	59.2	0.058	29.6	0.628563	110.159	4.323
Day 1	2	0.03333	15:21:34	15.7	23.9	-2.55421	1.32303	0.06486	18.50533	0.72615	54	-5.2	59.2	0.058	29.6	0.628563	130.201	5.109
Day 1	2	0.03333	15:23:34	17.5	22.1	-3.51819	4.06170	0.00000	14.50650	0.56924	54	-5.2	59.2	0.058	29.6	0.628563	134.207	5.266
Day 1	2	0.03333	15:43:34	15.7	23.9	-0.56992	-0.27606	0.04494	17.98988	0.70593	54	-5.2	59.2	0.058	29.6	0.628563	174.256	6.838
Day 1	7	0.11667	17:10:34	14	25.6	-3.25698	2.28711	0.00308	19.53999	0.76676	201	-5.2	206.2	0.204	29.45714	0.631612	726.88	28.523

$S_{wi,before}$	**0.23324**

Table D2: Results from pre-treatment flooding with oil to establish $S_{wi,before}$

Cumulative volume of oil injected when the first drop of oil was observed in the separator	ml	20.024
Outlet tubing volumes up to the tip of inner tube in separator	ml	6.539
Cumulative volume of oil injected when oil breakthrough occurred from the core	ml	13.485
Time corresponding to the oil breakthrough from datalog	Day 1	14:23:10
Pore volumes injected at oil breakthrough	PV	0.529156

Table D3: Calculation of pore volumes injected at oil breakthrough during pre-treatment flooding with oil

PRE-TREATMENT FLOODING WITH 0.1M NaCl BRINE TO ESTABLISH $S_{or,before}$													
Day	Brine injection rate, $q_{w,cc/min}$	Brine injection rate, $q_{w,cc/sec}$	Exact time	Separator level, S_l	Water saturation in the core, Sw	Differential pressure, dP_{mbar}	dP at q=0, $dP_{q=0,mbar}$	Corrected dP, $dP_{corrected,mbar}$	Differential pressure in atm, dP_{atm}	ΔP/q	Effective Permeability to Water, K_w	Cumulative Volume of Water Injected	Pore volumes of Water Injected
					$S_{w,n} = (S_{l,n}-S_{l,1}-V_{sg}-V_{t,i/t})/PV$			$dP_{corrected,mbar} = dP_{mbar} - dP_{q=0,mbar}$	$dP_{atm} = 0.00098692326 * dP_{corrected,mbar}$	$\Delta P/q = dP_{corrected,mbar} / q_{w,cc/min}$	$K_w = q_{w,cc/sec} * \mu_w * L / (dP_{atm}) * A$	$V_{cum,w}$	$PV_w = V_{cum,w}/PV$
	cc/min	cc/sec	hr:min:sec		fraction	mbar	mbar	mbar	atm	mbar.min/ml	D	ml	PV
Day 1	0.1274	0.00212	14:41:55	25.0	0.2332	-0.3	-7	6.7	0.007	52.590	0.000	0.060	0.002
Day 1	0.7945	0.01324	14:46:55	27.1	-	95.9	-7	102.9	0.102	129.515	0.004	2.367	0.093
Day 1	1.3264	0.02211	14:50:55	31.6	-	395.7	-7	402.7	0.397	303.604	0.008	6.602	0.259
Day 1	1.5946	0.02658	14:52:55	34.6	0.3416	555.9	-7	562.9	0.556	353.004	0.011	9.543	0.374
Day 1	1.8606	0.03101	14:54:55	38.0	0.4750	645.1	-7	652.1	0.644	350.478	0.030	12.993	0.510
Day 1	2	0.03333	14:56:55	39.3	0.5260	681.8	-7	688.8	0.680	344.400	0.042	16.925	0.664
Day 1	2	0.03333	14:58:55	39.3	0.5260	686.3	-7	693.3	0.684	346.650	0.042	20.932	0.821
Day 1	2	0.03333	15:00:55	39.3	0.5260	679.5	-7	686.5	0.678	343.250	0.042	24.939	0.979
Day 1	2	0.03333	15:02:55	39.3	0.5260	668.0	-7	675.0	0.666	337.500	0.043	28.946	1.136
Day 1	2	0.03333	15:05:55	39.3	0.5260	684.0	-7	691.0	0.682	345.500	0.042	34.960	1.372
Day 1	2	0.03333	15:08:55	39.3	0.5260	679.5	-7	686.5	0.678	343.250	0.042	40.970	1.608
Day 1	2	0.03333	15:16:55	39.3	0.5260	679.5	-7	686.5	0.678	343.250	0.042	57.003	2.237
Day 1	2	0.03333	15:22:55	39.3	0.5260	679.5	-7	686.5	0.678	343.250	0.042	68.990	2.707
Day 1	2	0.03333	15:28:55	39.3	0.5260	684.0	-7	691.0	0.682	345.500	0.042	81.014	3.179
Day 1	2.6187	0.04365	15:31:55	39.3	0.5260	887.7	-7	894.7	0.883	341.658	0.042	87.995	3.453
Day 1	3.42	0.05700	15:35:55	39.3	0.5260	1130.3	-7	1137.3	1.122	332.544	0.043	100.105	3.928
Day 1	4.4173	0.07362	15:40:55	39.3	0.5260	1457.6	-7	1464.6	1.445	331.560	0.043	119.669	4.696
Day 1	5	0.08333	15:44:55	39.3	0.5260	1633.8	-7	1640.8	1.619	328.160	0.044	138.887	5.450
Day 1	5	0.08333	15:51:55	39.3	0.5260	1620.1	-7	1627.1	1.606	325.420	0.044	173.957	6.826
Day 1	5	0.08333	15:56:55	39.3	0.5260	1645.3	-7	1652.3	1.631	330.460	0.044	198.995	7.809
Day 1	5	0.08333	15:59:55	39.3	0.5260	1624.7	-7	1631.7	1.610	326.340	0.044	214.027	8.398

Day 1	5	0.08333	16:03:55	39.5	0.5339	1643.0	-7	1650.0	1.628	330.000	0.044	233.993	9.182
Day 1	5	0.08333	16:10:55	39.5	0.5339	1551.4	-7	1558.4	1.538	311.680	0.046	269.056	10.558
Day 1	5	0.08333	16:19:55	39.5	0.5339	1629.3	-7	1636.3	1.615	327.260	0.044	314.146	12.327
Day 1	5	0.08333	16:24:55	39.5	0.5339	1638.4	-7	1645.4	1.624	329.080	0.044	339.190	13.310
Day 1	8.0541	0.13424	16:33:55	39.6	0.5378	2533.3	-7	2540.3	2.507	315.405	0.046	398.323	15.630
Day 1	10	0.16667	16:43:55	39.7	0.5417	3041.4	-7	3048.4	3.009	304.840	0.047	492.751	19.336
Day 1	1	0.01667	17:20:55	40.0	0.5515	297.3	-7	304.3	0.300	304.300	0.047	745.973	29.272
Day 2	1	0.01667	08:09:55	40.0	0.5515	304.1	-7	311.1	0.307	311.100	0.04636	1635.346	64.171

$S_{or,before}$	**0.4485**

Table D4: Results from pre-treatment flooding with brine to establish $S_{or,before}$

TREATMENT FLOODING WITH 1000 PPM ASSOCIATIVE POLYMER

Day	Polymer injection rate, $q_{p,cc/min}$	Polymer injection rate, $q_{p,cc/sec}$	Exact time	Differential pressure, dP_{mbar}	dP at q=0, $dP_{q=0,mbar}$	Corrected dP, $dP_{corrected,mbar}$	Differential pressure in atm, dP_{atm}	dP/q for polymer, $(dP/q)_p$	Cumulative volume of polymer injected	Pore volumes of polymer injected	dP/q for brine (pre-treatment), $(dP/q)_b$	Resistance Factor, RF
						$dP_{corrected,mbar} = dP_{mbar} - dP_{q=0,mbar}$	$dP_{atm} = 0.00098692326 * dP_{corrected,mbar}$	$(dP/q)_p = dP_{corrected,mbar}/q_{o,cc/min}$	$V_{cum,o}$	$PV_o = V_{cum,o}/PV$		$RF = (dP/q)_p / (dP/q)_b$
	cc/min	cc/sec	hr:min:sec	mbar	mbar	mbar	atm	mbar.min/ ml	ml	PV	mbar.min/ml	-
Day 1	0.0015	0.00003	11:01:12	-9.4	-9.4	0	0.000		0.000	0.000	331	0.0000
Day 1	0.0082	0.00014	11:02:12	-9.4	-9.4	0	0.000		0.004	0.000		0.0000
Day 1	0.0148	0.00025	11:03:12	-9.4	-9.4	0	0.000		0.016	0.001		0.0000
Day 1	0.0216	0.00036	11:04:12	-7.1	-9.4	2.3	0.002		0.034	0.001		0.0000
Day 1	0.0282	0.00047	11:05:12	-14	-9.4	-4.6	-0.005		0.059	0.002		0.0000
Day 1	0.0349	0.00058	11:06:12	2	-9.4	11.4	0.011	326.648	0.091	0.004		0.9869
Day 1	0.0415	0.00069	11:07:12	-0.3	-9.4	9.1	0.009	219.277	0.129	0.005		0.6625
Day 1	0.0482	0.00080	11:08:12	-0.3	-9.4	9.1	0.009	188.797	0.174	0.007		0.5704
Day 1	0.0548	0.00091	11:09:12	8.9	-9.4	18.3	0.018	333.942	0.225	0.009		1.0089
Day 1	0.0616	0.00103	11:10:12	6.6	-9.4	16	0.016	259.740	0.284	0.011		0.7847
Day 1	0.0682	0.00114	11:11:12	11.2	-9.4	20.6	0.020	302.053	0.349	0.014		0.9125
Day 1	0.0749	0.00125	11:12:12	15.8	-9.4	25.2	0.025	336.449	0.420	0.016		1.0165
Day 1	0.0801	0.00134	11:12:59	13.5	-9.4	22.9	0.023	285.893	0.481	0.019		0.8637
Day 1	0.0812	0.00135	11:13:09	15.8	-9.4	25.2	0.025	310.345	0.494	0.019		0.9376
Day 1	0.0823	0.00137	11:13:19	15.8	-9.4	25.2	0.025	306.197	0.508	0.020		0.9251
Day 1	0.0834	0.00139	11:13:29	18	-9.4	27.4	0.027	328.537	0.522	0.020		0.9926
Day 1	0.0846	0.00141	11:13:39	11.2	-9.4	20.6	0.020	243.499	0.536	0.021		0.7356
Day 1	0.0857	0.00143	11:13:49	8.9	-9.4	18.3	0.018	213.536	0.551	0.022		0.6451
Day 1	0.0868	0.00145	11:13:59	15.8	-9.4	25.2	0.025	290.323	0.565	0.022		0.8771
Day 1	0.0878	0.00146	11:14:09	8.9	-9.4	18.3	0.018	208.428	0.579	0.023		0.6297
Day 1	0.089	0.00148	11:14:19	13.5	-9.4	22.9	0.023	257.303	0.594	0.023		0.7774
Day 1	0.0901	0.00150	11:14:29	13.5	-9.4	22.9	0.023	254.162	0.609	0.024		0.7679
Day 1	0.0912	0.00152	11:14:39	13.5	-9.4	22.9	0.023	251.096	0.624	0.024		0.7586
Day 1	0.0924	0.00154	11:14:49	13.5	-9.4	22.9	0.023	247.835	0.640	0.025		0.7487
Day 1	0.0934	0.00156	11:14:59	18	-9.4	27.4	0.027	293.362	0.655	0.026		0.8863
Day 1	0.0945	0.00158	11:15:09	13.5	-9.4	22.9	0.023	242.328	0.671	0.026		0.7321

Day 1	0.0957	0.00160	11:15:19	13.5	-9.4	22.9	0.023	239.289	0.687	0.027		0.7229
Day 1	0.0968	0.00161	11:15:29	15.8	-9.4	25.2	0.025	260.331	0.703	0.028		0.7865
Day 1	0.0979	0.00163	11:15:39	13.5	-9.4	22.9	0.023	233.912	0.719	0.028		0.7067
Day 1	0.0991	0.00165	11:15:49	13.5	-9.4	22.9	0.023	231.080	0.736	0.029		0.6981
Day 1	0.1	0.00167	11:15:59	15.8	-9.4	25.2	0.025	252	0.751	0.029		0.7613
Day 1	0.1	0.00167	11:16:09	13.5	-9.4	22.9	0.023	229	0.768	0.030		0.6918
Day 1	0.1	0.00167	11:16:19	15.8	-9.4	25.2	0.025	252	0.785	0.031		0.7613
Day 1	0.1	0.00167	11:16:29	18	-9.4	27.4	0.027	274	0.801	0.031		0.8278
Day 1	0.1	0.00167	11:16:39	22.6	-9.4	32	0.032	320	0.818	0.032		0.9668
Day 1	0.1	0.00167	11:16:49	18	-9.4	27.4	0.027	274	0.835	0.033		0.8278
Day 1	0.1	0.00167	11:16:59	29.5	-9.4	38.9	0.038	389	0.851	0.033		1.1752
Day 1	0.1	0.00167	11:17:09	24.9	-9.4	34.3	0.034	343	0.868	0.034		1.0363
Day 1	0.1	0.00167	11:17:19	6.6	-9.4	16	0.016	160	0.885	0.035		0.4834
Day 1	0.1	0.00167	11:17:29	6.6	-9.4	16	0.016	160	0.902	0.035		0.4834
Day 1	0.1	0.00167	11:17:39	13.5	-9.4	22.9	0.023	229	0.918	0.036		0.6918
Day 1	0.1	0.00167	11:17:49	6.6	-9.4	16	0.016	160	0.935	0.037		0.4834
Day 1	0.1	0.00167	11:17:59	15.8	-9.4	25.2	0.025	252	0.952	0.037		0.7613
Day 1	0.1	0.00167	11:18:09	11.2	-9.4	20.6	0.020	206	0.968	0.038		0.6224
Day 1	0.1	0.00167	11:18:19	11.2	-9.4	20.6	0.020	206	0.985	0.039		0.6224
Day 1	0.1	0.00167	11:18:29	11.2	-9.4	20.6	0.020	206	1.002	0.039		0.6224
Day 1	0.1	0.00167	11:18:39	11.2	-9.4	20.6	0.020	206	1.018	0.040		0.6224
Day 1	0.1	0.00167	11:18:49	13.5	-9.4	22.9	0.023	229	1.035	0.041		0.6918
Day 1	0.1	0.00167	11:18:59	8.9	-9.4	18.3	0.018	183	1.052	0.041		0.5529
Day 1	0.1	0.00167	11:19:09	15.8	-9.4	25.2	0.025	252	1.069	0.042		0.7613
Day 1	0.1	0.00167	11:19:19	15.8	-9.4	25.2	0.025	252	1.085	0.043		0.7613
Day 1	0.1	0.00167	11:19:29	18	-9.4	27.4	0.027	274	1.102	0.043		0.8278
Day 1	0.1	0.00167	11:19:39	6.6	-9.4	16	0.016	160	1.119	0.044		0.4834
Day 1	0.1	0.00167	11:19:49	20.3	-9.4	29.7	0.029	297	1.135	0.045		0.8973
Day 1	0.1	0.00167	11:19:59	18	-9.4	27.4	0.027	274	1.152	0.045		0.8278
Day 1	0.1	0.00167	11:50:01	31.8	-9.4	41.2	0.041	412	4.159	0.163		1.2447
Day 1	0.1	0.00167	12:20:02	66.1	-9.4	75.5	0.075	755	7.166	0.281		2.2810
Day 1	0.1	0.00167	12:50:04	176	-9.4	185.4	0.183	1854	10.172	0.399		5.6012
Day 1	0.1	0.00167	13:20:05	267.5	-9.4	276.9	0.273	2769	13.179	0.517		8.3656
Day 1	0.1	0.00167	13:50:07	260.6	-9.4	270	0.266	2700	16.185	0.635		8.1571
Day 1	0.1	0.00167	14:20:08	391.1	-9.4	400.5	0.395	4005	19.191	0.753		12.0997
Day 1	0.1	0.00167	14:50:00	439.2	-9.4	448.6	0.443	4486	22.181	0.870		13.5529
Day 1	0.1	0.00167	15:20:01	478.1	-9.4	487.5	0.481	4875	25.188	0.988		14.7281
Day 1	0.1	0.00167	15:50:03	537.6	-9.4	547	0.540	5470	28.193	1.106		16.5257
Day 1	0.1	0.00167	16:20:04	647.4	-9.4	656.8	0.648	6568	31.200	1.224		19.8429

Day 1	0.1	0.00167	16:50:06	693.2	-9.4	702.6	0.693	7026	34.207	1.342		21.2266
Day 1	0.1	0.00167	17:20:07	759.6	-9.4	769	0.759	7690	37.214	1.460		23.2326
Day 1	0.1	0.00167	17:49:59	828.2	-9.4	837.6	0.827	8376	40.202	1.578		25.3051
Day 1	0.1	0.00167	18:20:00	890	-9.4	899.4	0.888	8994	43.209	1.696		27.1722
Day 1	0.1	0.00167	18:50:02	965.5	-9.4	974.9	0.962	9749	46.215	1.813		29.4532
Day 1	0.1	0.00167	19:20:03	1034.2	-9.4	1043.6	1.030	10436	49.222	1.931		31.5287
Day 1	0.1	0.00167	19:50:05	1109.7	-9.4	1119.1	1.104	11191	52.228	2.049		33.8097
Day 1	0.1	0.00167	20:20:06	1167	-9.4	1176.4	1.161	11764	55.234	2.167		35.5408
Day 1	0.1	0.00167	20:50:08	1258.5	-9.4	1267.9	1.251	12679	58.240	2.285		38.3051
Day 1	0.1	0.00167	21:19:59	1331.7	-9.4	1341.1	1.324	13411	61.230	2.403		40.5166
Day 1	0.1	0.00167	21:50:01	1379.8	-9.4	1389.2	1.371	13892	64.236	2.521		41.9698
Day 1	0.1	0.00167	22:20:02	1482.8	-9.4	1492.2	1.473	14922	67.242	2.639		45.0816
Day 1	0.1	0.00167	22:50:04	1551.4	-9.4	1560.8	1.540	15608	70.249	2.757		47.1541
Day 1	0.1	0.00167	23:20:05	1622.4	-9.4	1631.8	1.610	16318	73.255	2.875		49.2991
Day 1	0.1	0.00167	23:50:07	1693.3	-9.4	1702.7	1.680	17027	76.261	2.993		51.4411
Day 2	0.1	0.00167	00:19:59	1759.7	-9.4	1769.1	1.746	17691	79.250	3.110		53.4471
Day 2	0.1	0.00167	00:50:00	1839.8	-9.4	1849.2	1.825	18492	82.258	3.228		55.8671
Day 2	0.1	0.00167	01:20:02	1901.6	-9.4	1911	1.886	19110	85.263	3.346		57.7341
Day 2	0.1	0.00167	01:50:03	1958.8	-9.4	1968.2	1.942	19682	88.270	3.464		59.4622
Day 2	0.1	0.00167	02:20:05	2032.1	-9.4	2041.5	2.015	20415	91.277	3.582		61.6767
Day 2	0.1	0.00167	02:50:06	2109.9	-9.4	2119.3	2.092	21193	94.284	3.700		64.0272
Day 2	0.1	0.00167	03:20:08	2176.2	-9.4	2185.6	2.157	21856	97.290	3.818		66.0302
Day 2	0.1	0.00167	03:49:59	2240.3	-9.4	2249.7	2.220	22497	100.279	3.935		67.9668
Day 2	0.1	0.00167	04:20:01	2293	-9.4	2302.4	2.272	23024	103.285	4.053		69.5589
Day 2	0.1	0.00167	04:50:02	2363.9	-9.4	2373.3	2.342	23733	106.293	4.171		71.7009
Day 2	0.1	0.00167	05:20:04	2432.6	-9.4	2442	2.410	24420	109.298	4.289		73.7764
Day 2	0.1	0.00167	05:50:05	2471.5	-9.4	2480.9	2.448	24809	112.305	4.407		74.9517
Day 2	0.1	0.00167	06:20:07	2540.1	-9.4	2549.5	2.516	25495	115.312	4.525		77.0242
Day 2	0.1	0.00167	06:50:08	2620.2	-9.4	2629.6	2.595	26296	118.317	4.643		79.4441
Day 2	0.1	0.00167	07:20:00	2638.6	-9.4	2648	2.613	26480	121.307	4.760		80.0000
Day 2	0.1	0.00167	07:50:01	2737	-9.4	2746.4	2.710	27464	124.314	4.878		82.9728
Day 2	0.1	0.00167	08:20:03	2819.4	-9.4	2828.8	2.792	28288	127.320	4.996		85.4622
Day 2	0.1	0.00167	08:50:04	2849.1	-9.4	2858.5	2.821	28585	130.327	5.114		86.3595
Day 2	0.1	0.00167	09:20:06	2913.2	-9.4	2922.6	2.884	29226	133.332	5.232		88.2961
Day 2	0.1	0.00167	09:50:07	2933.8	-9.4	2943.2	2.905	29432	136.339	5.350		88.9184
Day 2	0.1	0.00167	10:19:59	2984.1	-9.4	2993.5	2.954	29935	139.329	5.467		90.4381
Day 2	0.1	0.00167	10:50:00	3002.4	-9.4	3011.8	2.972	30118	142.334	5.585		90.9909
Day 2	0.1	0.00167	11:20:02	3048.2	-9.4	3057.6	3.018	30576	145.341	5.703		92.3746
Day 2	0.1	0.00167	11:50:03	3050.5	-9.4	3059.9	3.020	30599	148.348	5.821		92.4441

Day 2	0.1	0.00167	12:20:05	3103.1	-9.4	3112.5	3.072	31125	151.353	5.939		94.0332
Day 2	0.1	0.00167	12:50:06	3107.7	-9.4	3117.1	3.076	31171	154.361	6.057		94.1722
Day 2	0.1	0.00167	13:20:08	3126	-9.4	3135.4	3.094	31354	157.367	6.175		94.7251
Day 2	0.1	0.00167	13:49:59	3123.7	-9.4	3133.1	3.092	31331	160.356	6.292		94.6556
Day 2	0.1	0.00167	14:20:01	3171.8	-9.4	3181.2	3.140	31812	163.364	6.410		96.1088
Day 2	0.1	0.00167	14:50:02	3208.4	-9.4	3217.8	3.176	32178	166.369	6.528		97.2145
Day 2	0.1	0.00167	15:20:04	3068.8	-9.4	3078.2	3.038	30782	169.375	6.646		92.9970
Day 2	0.1	0.00167	15:50:05	3270.2	-9.4	3279.6	3.237	32796	172.382	6.764		99.0816
Day 2	0.1	0.00167	16:20:07	3277.1	-9.4	3286.5	3.244	32865	175.388	6.882		99.2900
Day 2	0.1	0.00167	16:50:08	3277.1	-9.4	3286.5	3.244	32865	178.394	7.000		99.2900
Day 2	0.1	0.00167	17:20:00	3316	-9.4	3325.4	3.282	33254	181.383	7.118		100.4653
Day 2	0.1	0.00167	17:50:01	3370.9	-9.4	3380.3	3.336	33803	184.390	7.236		102.1239
Day 2	0.1	0.00167	18:20:03	3373.2	-9.4	3382.6	3.338	33826	187.397	7.354		102.1934
Day 2	0.1	0.00167	18:50:04	3405.2	-9.4	3414.6	3.370	34146	190.403	7.471		103.1601
Day 2	0.1	0.00167	19:20:06	3412.1	-9.4	3421.5	3.377	34215	193.410	7.589		103.3686
Day 2	0.1	0.00167	19:50:07	3457.9	-9.4	3467.3	3.422	34673	196.416	7.707		104.7523
Day 2	0.1	0.00167	20:19:59	3496.8	-9.4	3506.2	3.460	35062	199.405	7.825		105.9275
Day 2	0.1	0.00167	20:50:00	3483.1	-9.4	3492.5	3.447	34925	202.413	7.943		105.5136
Day 2	0.1	0.00167	21:20:02	3505.9	-9.4	3515.3	3.469	35153	205.418	8.061		106.2024
Day 2	0.1	0.00167	21:50:03	3524.3	-9.4	3533.7	3.487	35337	208.425	8.179		106.7583
Day 2	0.1	0.00167	22:20:05	3538	-9.4	3547.4	3.501	35474	211.432	8.297		107.1722
Day 2	0.1	0.00167	22:50:06	3583.8	-9.4	3593.2	3.546	35932	214.438	8.415		108.5559
Day 2	0.1	0.00167	23:20:08	3579.2	-9.4	3588.6	3.542	35886	217.445	8.533		108.4169
Day 2	0.1	0.00167	23:49:59	3641	-9.4	3650.4	3.603	36504	220.433	8.650		110.2840
Day 3	0.1	0.00167	00:20:01	3647.8	-9.4	3657.2	3.609	36572	223.441	8.768		110.4894
Day 3	0.1	0.00167	00:50:03	3652.4	-9.4	3661.8	3.614	36618	226.447	8.886		110.6284
Day 3	0.1	0.00167	01:20:04	3700.5	-9.4	3709.9	3.661	37099	229.452	9.004		112.0816
Day 3	0.1	0.00167	01:50:06	3753.1	-9.4	3762.5	3.713	37625	232.459	9.122		113.6707
Day 3	0.1	0.00167	02:20:07	3725.7	-9.4	3735.1	3.686	37351	235.465	9.240		112.8429
Day 3	0.1	0.00167	02:49:59	3766.9	-9.4	3776.3	3.727	37763	238.456	9.357		114.0876
Day 3	0.1	0.00167	03:20:00	3817.2	-9.4	3826.6	3.777	38266	241.463	9.475		115.6073
Day 3	0.1	0.00167	03:50:02	3792	-9.4	3801.4	3.752	38014	244.468	9.593		114.8459
Day 3	0.1	0.00167	04:20:03	3872.1	-9.4	3881.5	3.831	38815	247.474	9.711		117.2659
Day 3	0.1	0.00167	04:50:05	3885.9	-9.4	3895.3	3.844	38953	250.480	9.829		117.6828
Day 3	0.1	0.00167	05:20:06	3906.5	-9.4	3915.9	3.865	39159	253.487	9.947		118.3051
Day 3	0.1	0.00167	05:50:08	3954.5	-9.4	3963.9	3.912	39639	256.493	10.065		119.7553
Day 3	0.1	0.00167	06:19:59	3943.1	-9.4	3952.5	3.901	39525	259.483	10.182		119.4109
Day 3	0.1	0.00167	06:50:01	3986.6	-9.4	3996	3.944	39960	262.489	10.300		120.7251
Day 3	0.1	0.00167	07:20:02	4032.3	-9.4	4041.7	3.989	40417	265.496	10.418		122.1057

Day 3	0.1	0.00167	07:50:04	4057.5	-9.4	4066.9	4.014	40669	268.502	10.536		122.8671
Day 3	0.1	0.00167	08:20:05	4098.7	-9.4	4108.1	4.054	41081	271.509	10.654		124.1118
Day 3	0.1	0.00167	08:50:07	4114.7	-9.4	4124.1	4.070	41241	274.514	10.772		124.5952
Day 3	0.1	0.00167	09:20:08	4162.8	-9.4	4172.2	4.118	41722	277.521	10.890		126.0483
Day 3	0.1	0.00167	09:50:00	4190.3	-9.4	4199.7	4.145	41997	280.510	11.007		126.8792
Day 3	0.1	0.00167	10:20:01	4240.6	-9.4	4250	4.194	42500	283.517	11.125		128.3988
Day 3	0.1	0.00167	10:50:03	4311.6	-9.4	4321	4.264	43210	286.524	11.243		130.5438
Day 3	0.1	0.00167	11:20:04	4405.4	-9.4	4414.8	4.357	44148	289.530	11.361		133.3776
Day 3	0.1	0.00167	11:50:06	4448.9	-9.4	4458.3	4.400	44583	292.537	11.479		134.6918
Day 3	0.1	0.00167	12:20:07	4618.2	-9.4	4627.6	4.567	46276	295.543	11.597		139.8066
Day 3	0.1	0.00167	12:49:59	4705.2	-9.4	4714.6	4.653	47146	298.533	11.715		142.4350
Day 3	0.1	0.00167	13:20:00	4831.1	-9.4	4840.5	4.777	48405	301.539	11.832		146.2387
Day 3	0.1	0.00167	13:50:02	4989	-9.4	4998.4	4.933	49984	304.545	11.950		151.0091
Day 3	0.1	0.00167	14:20:03	5165.2	-9.4	5174.6	5.107	51746	307.552	12.068		156.3323
Day 3	0.1	0.00167	14:49:15	5240.7	-9.4	5250.1	5.181	52501	310.461	12.183		158.6133

S_{orp}	**0.4223**

Table D5: Results from treatment flooding with 1000 PPM of associative polymer

Parameters	Abbreviations	Units	Values
Viscosity of 1000 PPM polymer	μ_p	cp	6.67
Initial level in separator	$S_{l,i}$	ml	39.85
Final level in separator	$S_{l,f}$	ml	40.5
Volume change in separator	$V_{change} = S_{l,f} - S_{l,i}$	ml	0.65
Saturation change	$S_{change} = V_{change}/PV$	fraction	0.0255062
Residual oil saturation after polymer injection	$\mathbf{S_{orp} = S_{or} - S_{change}}$	**fraction**	**0.422970942**

Table D6: Calculation of residual oil saturation, S_{orp} after treatment with polymer

POST-TREATMENT FLOODING WITH 1M NaCl BRINE											
Day	Brine injection rate, $q_{w,cc/min}$	Brine injection rate, $q_{w,cc/sec}$	Exact time	Differential pressure, dP_{mbar}	dP at q=0, $dP_{q=0,mbar}$	Corrected dP, $dP_{corrected,mbar}$	Differential pressure in atm, dP_{atm}	ΔP/q	Effective Permeability to Water, K_w	Cumulative Volume of Water Injected	Pore volumes of Water Injected
						$dP_{corrected,mbar} = dP_{mbar} - dP_{q=0,mbar}$	$dP_{atm} = 0.00098692326*dP_{corrected,mbar}$	$\Delta P/q = dP_{corrected,mbar}/q_{w,cc/min}$	$K_w = q_{w,cc/sec}*\mu_w*L/(dP_{atm})*A$	$V_{cum,w}$	$PV_w = V_{cum,w}/PV$
	cc/min	cc/sec	hr:min:sec	mbar	mbar	mbar	atm	mbar.min/ml	D	ml	PV
Day 1	0.1	0.00167	15:55:28	-377.9	1.492	-379.39239	-0.374	-3793.9239	-0.003802	0.001	0.000
Day 1	0.1	0.00167	15:55:38	-377.9	1.492	-379.39239	-0.374	-3793.9239	-0.003802	0.002	0.000
Day 1	0.1	0.00167	15:55:48	-382.5	1.492	-383.99239	-0.379	-3839.9239	-0.003756	0.002	0.000
Day 1	0.1	0.00167	15:55:58	-377.9	1.492	-379.39239	-0.374	-3793.9239	-0.003802	0.002	0.000
Day 1	0.1	0.00167	15:56:08	-375.6	1.492	-377.09239	-0.372	-3770.9239	-0.003825	0.002	0.000
Day 1	0.1	0.00167	15:56:18	-375.6	1.492	-377.09239	-0.372	-3770.9239	-0.003825	0.002	0.000
Day 1	0.1	0.00167	15:56:28	3885.9	1.492	3884.40761	3.834	38844.0761	0.000371	0.002	0.000
Day 1	0.1	0.00167	15:56:38	2508.1	1.492	2506.60761	2.474	25066.0761	0.000575	0.002	0.000
Day 1	0.1	0.00167	15:56:48	1860.4	1.492	1858.90761	1.835	18589.0761	0.000776	0.002	0.000
Day 1	0.1	0.00167	15:56:58	1494.2	1.492	1492.70761	1.473	14927.0761	0.000966	0.002	0.000
Day 1	0.1	0.00167	15:57:08	1265.4	1.492	1263.90761	1.247	12639.0761	0.001141	0.016	0.001
Day 1	0.1	0.00167	15:57:18	1096	1.492	1094.50761	1.080	10945.0761	0.001318	0.104	0.004
Day 1	0.1	0.00167	15:57:28	970.1	1.492	968.60761	0.956	9686.0761	0.001489	0.104	0.004
Day 1	0.1	0.00167	15:57:38	997.6	1.492	996.10761	0.983	9961.0761	0.001448	0.104	0.004
Day 1	0.1	0.00167	15:57:48	828.2	1.492	826.70761	0.816	8267.0761	0.001745	0.104	0.004
Day 1	0.1	0.00167	15:57:58	800.8	1.492	799.30761	0.789	7993.0761	0.001804	0.105	0.004
Day 1	0.1	0.00167	15:58:08	768.7	1.492	767.20761	0.757	7672.0761	0.001880	0.105	0.004
Day 1	0.1	0.00167	16:28:00	2391.4	1.492	2389.90761	2.359	23899.0761	0.000603	2.379	0.093
Day 1	0.1	0.00167	16:58:01	2098.4	1.492	2096.90761	2.069	20969.0761	0.000688	5.385	0.211
Day 1	0.1	0.00167	17:28:03	1986.3	1.492	1984.80761	1.959	19848.0761	0.000727	8.391	0.329
Day 1	0.1	0.00167	17:58:04	1988.6	1.492	1987.10761	1.961	19871.0761	0.000726	11.398	0.447
Day 1	0.1	0.00167	18:28:06	1826.1	1.492	1824.60761	1.801	18246.0761	0.000790	14.404	0.565
Day 1	0.1	0.00167	18:58:07	1922.2	1.492	1920.70761	1.896	19207.0761	0.000751	17.411	0.683
Day 1	0.1	0.00167	19:27:59	1901.6	1.492	1900.10761	1.875	19001.0761	0.000759	20.4	0.801
Day 1	0.1	0.00167	19:58:00	1885.6	1.492	1884.10761	1.859	18841.0761	0.000766	23.408	0.919
Day 1	0.1	0.00167	20:28:02	1919.9	1.492	1918.40761	1.893	19184.0761	0.000752	26.412	1.036
Day 1	0.1	0.00167	20:58:03	1890.2	1.492	1888.70761	1.864	18887.0761	0.000764	29.42	1.154
Day 1	0.1	0.00167	21:28:05	1874.1	1.492	1872.60761	1.848	18726.0761	0.000770	32.426	1.272
Day 1	0.1	0.00167	21:58:06	1874.1	1.492	1872.60761	1.848	18726.0761	0.000770	35.432	1.390

Day 1	0.1	0.00167	22:27:58	1878.7	1.492	1877.20761	1.853	18772.0761	0.000768	38.42	1.508
Day 1	0.1	0.00167	22:57:59	1876.4	1.492	1874.90761	1.850	18749.0761	0.000769	41.427	1.626
Day 1	0.1	0.00167	23:28:01	1908.5	1.492	1907.00761	1.882	19070.0761	0.000756	44.434	1.744
Day 1	0.1	0.00167	23:58:02	1883.3	1.492	1881.80761	1.857	18818.0761	0.000766	47.44	1.862
Day 2	0.1	0.00167	00:28:04	1906.2	1.492	1904.70761	1.880	19047.0761	0.000757	50.447	1.980
Day 2	0.1	0.00167	00:58:05	1908.5	1.492	1907.00761	1.882	19070.0761	0.000756	53.454	2.098
Day 2	0.1	0.00167	01:28:07	1883.3	1.492	1881.80761	1.857	18818.0761	0.000766	56.459	2.215
Day 2	0.1	0.00167	01:58:08	1887.9	1.492	1886.40761	1.862	18864.0761	0.000765	59.467	2.334
Day 2	0.1	0.00167	02:28:00	1892.5	1.492	1891.00761	1.866	18910.0761	0.000763	62.455	2.451
Day 2	0.1	0.00167	02:58:01	1871.9	1.492	1870.40761	1.846	18704.0761	0.000771	65.462	2.569
Day 2	0.1	0.00167	03:28:03	1899.3	1.492	1897.80761	1.873	18978.0761	0.000760	68.467	2.687
Day 2	0.1	0.00167	03:58:04	1862.7	1.492	1861.20761	1.837	18612.0761	0.000775	71.473	2.805
Day 2	0.1	0.00167	04:28:06	1906.2	1.492	1904.70761	1.880	19047.0761	0.000757	74.48	2.923
Day 2	0.1	0.00167	04:58:07	1903.9	1.492	1902.40761	1.878	19024.0761	0.000758	77.487	3.041
Day 2	0.1	0.00167	05:27:59	1906.2	1.492	1904.70761	1.880	19047.0761	0.000757	80.476	3.158
Day 2	0.1	0.00167	05:58:00	1885.6	1.492	1884.10761	1.859	18841.0761	0.000766	83.482	3.276
Day 2	0.1	0.00167	06:28:02	1922.2	1.492	1920.70761	1.896	19207.0761	0.000751	86.489	3.394
Day 2	0.1	0.00167	06:58:04	1894.7	1.492	1893.20761	1.868	18932.0761	0.000762	89.495	3.512
Day 2	0.1	0.00167	07:28:05	1876.4	1.492	1874.90761	1.850	18749.0761	0.000769	92.502	3.630
Day 2	0.1	0.00167	07:58:07	1903.9	1.492	1902.40761	1.878	19024.0761	0.000758	95.508	3.748
Day 2	0.1	0.00167	08:28:08	1887.9	1.492	1886.40761	1.862	18864.0761	0.000765	98.513	3.866
Day 2	0.1	0.00167	08:58:00	1897	1.492	1895.50761	1.871	18955.0761	0.000761	101.504	3.983
Day 2	0.1	0.00167	09:28:01	1924.5	1.492	1923.00761	1.898	19230.0761	0.000750	104.51	4.101
Day 2	0.1	0.00167	09:58:03	1897	1.492	1895.50761	1.871	18955.0761	0.000761	107.515	4.219
Day 2	0.1	0.00167	10:28:04	1915.3	1.492	1913.80761	1.889	19138.0761	0.000754	110.523	4.337
Day 2	0.1	0.00167	10:58:06	1933.6	1.492	1932.10761	1.907	19321.0761	0.000746	113.529	4.455
Day 2	0.1	0.00167	11:28:07	1929.1	1.492	1927.60761	1.902	19276.0761	0.000748	116.536	4.573
Day 2	0.1	0.00167	11:57:59	1913	1.492	1911.50761	1.887	19115.0761	0.000755	119.524	4.690
Day 2	0.1	0.00167	12:28:00	1897	1.492	1895.50761	1.871	18955.0761	0.000761	122.531	4.808
Day 2	0.1	0.00167	12:58:02	1933.6	1.492	1932.10761	1.907	19321.0761	0.000746	125.537	4.926
Day 2	0.1	0.00167	13:28:03	1935.9	1.492	1934.40761	1.909	19344.0761	0.000746	128.545	5.044
Day 2	0.1	0.00167	13:58:05	1924.5	1.492	1923.00761	1.898	19230.0761	0.000750	131.55	5.162
Day 2	0.1	0.00167	14:28:06	1917.6	1.492	1916.10761	1.891	19161.0761	0.000753	134.557	5.280
Day 2	0.1	0.00167	14:58:08	1917.6	1.492	1916.10761	1.891	19161.0761	0.000753	137.563	5.398
Day 2	0.1	0.00167	15:27:59	1890.2	1.492	1888.70761	1.864	18887.0761	0.000764	140.552	5.515
Day 2	0.1	0.00167	15:58:01	1931.4	1.492	1929.90761	1.905	19299.0761	0.000747	143.558	5.633
Day 2	0.1	0.00167	16:28:02	1924.5	1.492	1923.00761	1.898	19230.0761	0.000750	146.565	5.751
Day 2	0.1	0.00167	16:58:04	1899.3	1.492	1897.80761	1.873	18978.0761	0.000760	149.57	5.869
Day 2	0.1	0.00167	17:28:05	1901.6	1.492	1900.10761	1.875	19001.0761	0.000759	152.578	5.987

Day 2	0.1	0.00167	17:58:07	1876.4	1.492	1874.90761	1.850	18749.0761	0.000769	155.584	6.105
Day 2	0.1	0.00167	18:28:08	1908.5	1.492	1907.00761	1.882	19070.0761	0.000756	158.59	6.223
Day 2	0.1	0.00167	18:58:00	1899.3	1.492	1897.80761	1.873	18978.0761	0.000760	161.58	6.340
Day 2	0.1	0.00167	19:28:01	1867.3	1.492	1865.80761	1.841	18658.0761	0.000773	164.585	6.458
Day 2	0.1	0.00167	19:58:03	1894.7	1.492	1893.20761	1.868	18932.0761	0.000762	167.592	6.576
Day 2	0.1	0.00167	20:28:04	1878.7	1.492	1877.20761	1.853	18772.0761	0.000768	170.599	6.694
Day 2	0.1	0.00167	20:58:06	1901.6	1.492	1900.10761	1.875	19001.0761	0.000759	173.604	6.812
Day 2	0.1	0.00167	21:28:07	1901.6	1.492	1900.10761	1.875	19001.0761	0.000759	176.61	6.930
Day 2	0.1	0.00167	21:57:59	1906.2	1.492	1904.70761	1.880	19047.0761	0.000757	179.601	7.048
Day 2	0.1	0.00167	22:28:00	1885.6	1.492	1884.10761	1.859	18841.0761	0.000766	182.607	7.166
Day 2	0.1	0.00167	22:58:02	1897	1.492	1895.50761	1.871	18955.0761	0.000761	185.614	7.284
Day 2	0.1	0.00167	23:28:03	1823.8	1.492	1822.30761	1.798	18223.0761	0.000791	188.619	7.401
Day 2	0.1	0.00167	23:58:05	1899.3	1.492	1897.80761	1.873	18978.0761	0.000760	191.626	7.519
Day 3	0.1	0.00167	00:28:06	1878.7	1.492	1877.20761	1.853	18772.0761	0.000768	194.633	7.637
Day 3	0.1	0.00167	00:58:08	1881	1.492	1879.50761	1.855	18795.0761	0.000767	197.64	7.755
Day 3	0.1	0.00167	01:27:59	1881	1.492	1879.50761	1.855	18795.0761	0.000767	200.629	7.873
Day 3	0.1	0.00167	01:58:01	1869.6	1.492	1868.10761	1.844	18681.0761	0.000772	203.635	7.991
Day 3	0.1	0.00167	02:28:02	1851.3	1.492	1849.80761	1.826	18498.0761	0.000780	206.642	8.109
Day 3	0.1	0.00167	02:58:04	1830.7	1.492	1829.20761	1.805	18292.0761	0.000788	209.648	8.227
Day 3	0.1	0.00167	03:28:05	1851.3	1.492	1849.80761	1.826	18498.0761	0.000780	212.655	8.345
Day 3	0.1	0.00167	03:58:07	1881	1.492	1879.50761	1.855	18795.0761	0.000767	215.66	8.463
Day 3	0.1	0.00167	04:28:08	1876.4	1.492	1874.90761	1.850	18749.0761	0.000769	218.667	8.581
Day 3	0.1	0.00167	04:58:00	1860.4	1.492	1858.90761	1.835	18589.0761	0.000776	221.656	8.698
Day 3	0.1	0.00167	05:28:01	1867.3	1.492	1865.80761	1.841	18658.0761	0.000773	224.663	8.816
Day 3	0.1	0.00167	05:58:03	1878.7	1.492	1877.20761	1.853	18772.0761	0.000768	227.67	8.934
Day 3	0.1	0.00167	06:28:04	1883.3	1.492	1881.80761	1.857	18818.0761	0.000766	230.676	9.052
Day 3	0.1	0.00167	06:58:06	1855.8	1.492	1854.30761	1.830	18543.0761	0.000778	233.683	9.170
Day 3	0.1	0.00167	07:28:08	1853.5	1.492	1852.00761	1.828	18520.0761	0.000779	236.688	9.288
Day 3	0.1	0.00167	07:57:59	1835.2	1.492	1833.70761	1.810	18337.0761	0.000787	239.678	9.405
Day 3	0.1	0.00167	08:28:01	1826.1	1.492	1824.60761	1.801	18246.0761	0.000790	242.685	9.523
Day 3	0.1	0.00167	08:58:02	1851.3	1.492	1849.80761	1.826	18498.0761	0.000780	245.69	9.641
Day 3	0.1	0.00167	09:28:04	1855.8	1.492	1854.30761	1.830	18543.0761	0.000778	248.698	9.759
Day 3	0.1	0.00167	09:58:05	1869.6	1.492	1868.10761	1.844	18681.0761	0.000772	251.703	9.877
Day 3	0.1	0.00167	10:28:07	1814.6	1.492	1813.10761	1.789	18131.0761	0.000795	254.711	9.995
Day 3	0.1	0.00167	10:58:08	1851.3	1.492	1849.80761	1.826	18498.0761	0.000780	257.716	10.113
Day 3	0.1	0.00167	11:28:00	1855.8	1.492	1854.30761	1.830	18543.0761	0.000778	260.706	10.230
Day 3	0.1	0.00167	11:58:01	1855.8	1.492	1854.30761	1.830	18543.0761	0.000778	263.713	10.348
Day 3	0.1	0.00167	12:28:03	1860.4	1.492	1858.90761	1.835	18589.0761	0.000776	266.718	10.466
Day 3	0.1	0.00167	12:58:04	1855.8	1.492	1854.30761	1.830	18543.0761	0.000778	269.724	10.584

Day 3	0.1	0.00167	13:28:06	1832.9	1.492	1831.40761	1.807	18314.0761	0.000788	272.732	10.702
Day 3	0.1	0.00167	13:58:07	1853.5	1.492	1852.00761	1.828	18520.0761	0.000779	275.738	10.820
Day 3	0.1	0.00167	14:27:59	1844.4	1.492	1842.90761	1.819	18429.0761	0.000783	278.727	10.937
Day 3	0.1	0.00167	14:58:00	1851.3	1.492	1849.80761	1.826	18498.0761	0.000780	281.734	11.055
Day 3	0.1	0.00167	15:28:02	1842.1	1.492	1840.60761	1.817	18406.0761	0.000784	284.739	11.173
Day 3	0.1	0.00167	15:58:03	1849	1.492	1847.50761	1.823	18475.0761	0.000781	287.745	11.291
Day 3	0.1	0.00167	16:28:05	1832.9	1.492	1831.40761	1.807	18314.0761	0.000788	290.751	11.409
Day 3	0.1	0.00167	16:58:06	1855.8	1.492	1854.30761	1.830	18543.0761	0.000778	293.759	11.527
Day 3	0.1	0.00167	17:28:08	1835.2	1.492	1833.70761	1.810	18337.0761	0.000787	296.764	11.645
Day 3	0.1	0.00167	17:57:59	1826.1	1.492	1824.60761	1.801	18246.0761	0.000790	299.755	11.762
Day 3	0.1	0.00167	18:28:01	1832.9	1.492	1831.40761	1.807	18314.0761	0.000788	302.759	11.880
Day 3	0.1	0.00167	18:58:02	1828.4	1.492	1826.90761	1.803	18269.0761	0.000789	305.767	11.998
Day 3	0.1	0.00167	19:28:04	1849	1.492	1847.50761	1.823	18475.0761	0.000781	308.773	12.116
Day 3	0.1	0.00167	19:58:05	1746	1.492	1744.50761	1.722	17445.0761	0.000827	311.78	12.234
Day 3	0.1	0.00167	20:28:07	1805.5	1.492	1804.00761	1.780	18040.0761	0.000799	314.785	12.352
Day 3	0.1	0.00167	20:58:08	1830.7	1.492	1829.20761	1.805	18292.0761	0.000788	317.792	12.470
Day 3	0.1	0.00167	21:28:00	1832.9	1.492	1831.40761	1.807	18314.0761	0.000788	320.782	12.588
Day 3	0.1	0.00167	21:58:01	1816.9	1.492	1815.40761	1.792	18154.0761	0.000794	323.788	12.706
Day 3	0.1	0.00167	22:28:03	1789.5	1.492	1788.00761	1.765	17880.0761	0.000807	326.794	12.823
Day 3	0.1	0.00167	22:58:04	1805.5	1.492	1804.00761	1.780	18040.0761	0.000799	329.801	12.941
Day 3	0.1	0.00167	23:28:06	1796.3	1.492	1794.80761	1.771	17948.0761	0.000804	332.807	13.059
Day 3	0.1	0.00167	23:58:07	1798.6	1.492	1797.10761	1.774	17971.0761	0.000803	335.814	13.177
Day 4	0.1	0.00167	00:27:59	1819.2	1.492	1817.70761	1.794	18177.0761	0.000793	338.802	13.295
Day 4	0.1	0.00167	00:58:00	1780.3	1.492	1778.80761	1.756	17788.0761	0.000811	341.81	13.413
Day 4	0.1	0.00167	01:28:02	1798.6	1.492	1797.10761	1.774	17971.0761	0.000803	344.816	13.531
Day 4	0.1	0.00167	01:58:03	1782.6	1.492	1781.10761	1.758	17811.0761	0.000810	347.823	13.649
Day 4	0.1	0.00167	02:28:05	1803.2	1.492	1801.70761	1.778	18017.0761	0.000801	350.828	13.767
Day 4	0.1	0.00167	02:58:06	1816.9	1.492	1815.40761	1.792	18154.0761	0.000794	353.835	13.885
Day 4	0.1	0.00167	03:28:08	1823.8	1.492	1822.30761	1.798	18223.0761	0.000791	356.841	14.003
Day 4	0.1	0.00167	03:57:59	1750.6	1.492	1749.10761	1.726	17491.0761	0.000825	359.83	14.120
Day 4	0.1	0.00167	04:28:01	1771.2	1.492	1769.70761	1.747	17697.0761	0.000815	362.837	14.238
Day 4	0.1	0.00167	04:58:02	1814.6	1.492	1813.10761	1.789	18131.0761	0.000795	365.844	14.356
Day 4	0.1	0.00167	05:28:04	1803.2	1.492	1801.70761	1.778	18017.0761	0.000801	368.85	14.474
Day 4	0.1	0.00167	05:58:05	1782.6	1.492	1781.10761	1.758	17811.0761	0.000810	371.856	14.592
Day 4	0.1	0.00167	06:28:07	1816.9	1.492	1815.40761	1.792	18154.0761	0.000794	374.862	14.710
Day 4	0.1	0.00167	06:58:08	1771.2	1.492	1769.70761	1.747	17697.0761	0.000815	377.869	14.828
Day 4	0.1	0.00167	07:28:00	1748.3	1.492	1746.80761	1.724	17468.0761	0.000826	380.858	14.945
Day 4	0.1	0.00167	07:58:01	1773.4	1.492	1771.90761	1.749	17719.0761	0.000814	383.865	15.063
Day 4	0.1	0.00167	08:28:03	1784.9	1.492	1783.40761	1.760	17834.0761	0.000809	386.872	15.181

Day 4	0.1	0.00167	08:58:05	1775.7	1.492	1774.20761	1.751	17742.0761	0.000813	389.878	15.299
Day 4	0.1	0.00167	09:28:06	1778	1.492	1776.50761	1.753	17765.0761	0.000812	392.883	15.417
Day 4	0.1	0.00167	09:58:08	1752.8	1.492	1751.30761	1.728	17513.0761	0.000824	395.89	15.535
Day 4	0.1	0.00167	10:27:59	1784.9	1.492	1783.40761	1.760	17834.0761	0.000809	398.88	15.652
Day 4	0.1	0.00167	10:58:01	1800.9	1.492	1799.40761	1.776	17994.0761	0.000802	401.886	15.770
Day 4	0.1	0.00167	11:28:02	1752.8	1.492	1751.30761	1.728	17513.0761	0.000824	404.892	15.888
Day 4	0.1	0.00167	11:58:04	1791.8	1.492	1790.30761	1.767	17903.0761	0.000806	407.899	16.006
Day 4	0.1	0.00167	12:28:05	1780.3	1.492	1778.80761	1.756	17788.0761	0.000811	410.905	16.124
Day 4	0.1	0.00167	12:58:07	1789.5	1.492	1788.00761	1.765	17880.0761	0.000807	413.912	16.242
Day 4	0.1	0.00167	13:28:08	1773.4	1.492	1771.90761	1.749	17719.0761	0.000814	416.918	16.360
Day 4	0.1	0.00167	13:58:00	1771.2	1.492	1769.70761	1.747	17697.0761	0.000815	419.908	16.477
Day 4	0.1	0.00167	14:28:01	1741.4	1.492	1739.90761	1.717	17399.0761	0.000829	422.914	16.595
Day 4	0.1	0.00167	14:58:03	1759.7	1.492	1758.20761	1.735	17582.0761	0.000820	425.921	16.713
Day 4	0.1	0.00167	15:28:04	1755.1	1.492	1753.60761	1.731	17536.0761	0.000822	428.928	16.831
Day 4	0.1	0.00167	15:58:06	1762	1.492	1760.50761	1.737	17605.0761	0.000819	431.933	16.949
Day 4	0.1	0.00167	16:28:07	1771.2	1.492	1769.70761	1.747	17697.0761	0.000815	434.94	17.067
Day 4	0.1	0.00167	16:57:59	1759.7	1.492	1758.20761	1.735	17582.0761	0.000820	437.93	17.185
Day 4	0.1	0.00167	17:28:00	1759.7	1.492	1758.20761	1.735	17582.0761	0.000820	440.936	17.302
Day 4	0.1	0.00167	17:58:02	1766.6	1.492	1765.10761	1.742	17651.0761	0.000817	443.943	17.420
Day 4	0.1	0.00167	18:28:03	1764.3	1.492	1762.80761	1.740	17628.0761	0.000818	446.948	17.538
Day 4	0.1	0.00167	18:58:05	1739.1	1.492	1737.60761	1.715	17376.0761	0.000830	449.954	17.656
Day 4	0.1	0.00167	19:28:06	1748.3	1.492	1746.80761	1.724	17468.0761	0.000826	452.962	17.774
Day 4	0.1	0.00167	19:58:08	1748.3	1.492	1746.80761	1.724	17468.0761	0.000826	455.968	17.892
Day 4	0.1	0.00167	20:27:59	1743.7	1.492	1742.20761	1.719	17422.0761	0.000828	458.958	18.010
Day 4	0.1	0.00167	20:58:01	1741.4	1.492	1739.90761	1.717	17399.0761	0.000829	461.964	18.128
Day 4	0.1	0.00167	21:28:02	1743.7	1.492	1742.20761	1.719	17422.0761	0.000828	464.97	18.246
Day 4	0.1	0.00167	21:58:04	1741.4	1.492	1739.90761	1.717	17399.0761	0.000829	467.977	18.364
Day 4	0.1	0.00167	22:28:05	1734.5	1.492	1733.00761	1.710	17330.0761	0.000832	470.982	18.481
Day 4	0.1	0.00167	22:58:07	1739.1	1.492	1737.60761	1.715	17376.0761	0.000830	473.988	18.599
Day 4	0.1	0.00167	23:28:08	1748.3	1.492	1746.80761	1.724	17468.0761	0.000826	476.995	18.717
Day 4	0.1	0.00167	23:58:00	1734.5	1.492	1733.00761	1.710	17330.0761	0.000832	479.985	18.835
Day 5	0.1	0.00167	00:28:01	1713.9	1.492	1712.40761	1.690	17124.0761	0.000842	482.991	18.953
Day 5	0.1	0.00167	00:58:03	1734.5	1.492	1733.00761	1.710	17330.0761	0.000832	485.997	19.071
Day 5	0.1	0.00167	01:28:04	1730	1.492	1728.50761	1.706	17285.0761	0.000834	489.004	19.189
Day 5	0.1	0.00167	01:58:06	1730	1.492	1728.50761	1.706	17285.0761	0.000834	492.01	19.307
Day 5	0.1	0.00167	02:28:07	1647.6	1.492	1646.10761	1.625	16461.0761	0.000876	495.017	19.425
Day 5	0.1	0.00167	02:57:59	1730	1.492	1728.50761	1.706	17285.0761	0.000834	498.006	19.542
Day 5	0.1	0.00167	03:28:00	1725.4	1.492	1723.90761	1.701	17239.0761	0.000837	501.013	19.660
Day 5	0.1	0.00167	03:58:02	1734.5	1.492	1733.00761	1.710	17330.0761	0.000832	504.019	19.778

Day 5	0.1	0.00167	04:28:03	1734.5	1.492	1733.00761	1.710	17330.0761	0.000832	507.025	19.896
Day 5	0.1	0.00167	04:58:05	1716.2	1.492	1714.70761	1.692	17147.0761	0.000841	510.032	20.014
Day 5	0.1	0.00167	05:28:06	1686.5	1.492	1685.00761	1.663	16850.0761	0.000856	513.039	20.132
Day 5	0.1	0.00167	05:58:08	1700.2	1.492	1698.70761	1.676	16987.0761	0.000849	516.045	20.250
Day 5	0.1	0.00167	06:27:59	1711.6	1.492	1710.10761	1.688	17101.0761	0.000843	519.035	20.367
Day 5	0.1	0.00167	06:58:01	1716.2	1.492	1714.70761	1.692	17147.0761	0.000841	522.041	20.485
Day 5	0.1	0.00167	07:28:02	1723.1	1.492	1721.60761	1.699	17216.0761	0.000838	525.046	20.603
Day 5	0.1	0.00167	07:58:04	1741.4	1.492	1739.90761	1.717	17399.0761	0.000829	528.053	20.721
Day 5	0.1	0.00167	08:28:05	1732.2	1.492	1730.70761	1.708	17307.0761	0.000833	531.06	20.839
Day 5	0.1	0.00167	08:58:07	1741.4	1.492	1739.90761	1.717	17399.0761	0.000829	534.066	20.957
Day 5	0.1	0.00167	09:27:59	1746	1.492	1744.50761	1.722	17445.0761	0.000827	537.055	21.074
Day 5	0.1	0.00167	09:58:00	1725.4	1.492	1723.90761	1.701	17239.0761	0.000837	540.063	21.192
Day 5	0.1	0.00167	10:28:02	1720.8	1.492	1719.30761	1.697	17193.0761	0.000839	543.068	21.310

$S_{or,after}$	**0.42297094**

Table D7: Results from post-treatment flooding with brine to establish $S_{or,after}$

POST-TREATMENT FLOODING WITH OIL

Day	Oil injection rate, $q_{o,cc/min}$	Oil injection rate, $q_{o,cc/sec}$	Exact time	Separator level, S_l	Approximate watercut in outlet tubings, WC	Oil volume in the core, $V_{o,c}$	Normalized oil saturation, $S_{o,norm}$	Actual oil saturation, So	Differential pressure, dP_{mbar}	dP at q=0, $dP_{q=0,mbar}$	Corrected dP, $dP_{corrected,mbar}$	Differential pressure in atm, dP_{atm}	ΔP/q	Effective Permeability to Oil, K_o	Cumulative Volume of Oil Injected	Pore volumes of Oil Injected
					$WC = (S_{l,n} - S_{l,n+1})/(V_{cum,o,n+1} - V_{cum,o,n})$	$V_{o,c,n} = Sl,1 - Sl,n - V_{sg} - V_{ss} - V_{t,i/t} - ((1-WC_n)*V_{s,r})$	$S_{o,norm} = Vo,c/PV$	$S_o = S_{or,post} + S_{o,norm}$			$dP_{corrected,mbar} = dP_{mbar} - dP_{q=0,mbar}$	$dP_{atm} = 0.000986923 26*dP_{corrected,mbar}$	$\Delta P/q = dP_{corrected,mbar}/q_{o,cc/min}$	$K_o = q_{o,cc/sec}*\mu_o*L/(dP_{atm})*A$	$V_{cum,o}$	$PV_o = V_{cum,o}/PV$
	cc/min	cc/sec	hr:min:sec		fraction	ml	fraction	fraction	mbar	mbar	mbar	atm	mbar.min/ml	D	ml	PV
Day 1	0.1	0.00167	12:12:47	39.6	-			0.42297	-2.5	0.219	-2.719	-0.003	-27.19	-0.684276	0	0.000
Day 1	0.1	0.00167	12:38:47	38.1	0.81213	1.0880	0.04269	0.46566	796.2	0.219	795.981	0.786	7959.81	0.002337	1.847	0.072
Day 1	0.1	0.00167	12:40:47	37.95	0.75000	1.2380	0.04858	0.47155	807.6	0.219	807.381	0.797	8073.81	0.002304	2.047	0.080
Day 1	0.1	0.00167	12:45:47	37.5	0.89820	1.6880	0.06624	0.48921	759.6	0.219	759.381	0.749	7593.81	0.002450	2.548	0.100
Day 1	0.1	0.00167	12:50:47	36.9	1.00000	2.0880	0.08193	0.50490	709.2	0.219	708.981	0.700	7089.81	0.002624	3.05	0.120
Day 1	0.1	0.00167	12:55:47	36.4	0.99800	2.5880	0.10155	0.52452	686.3	0.219	686.081	0.677	6860.81	0.002712	3.551	0.139
Day 1	0.1	0.00167	13:01:47	35.8	0.99834	3.1880	0.12510	0.54807	645.1	0.219	644.881	0.636	6448.81	0.002885	4.152	0.163
Day 1	0.1	0.00167	13:06:47	35.25	1.00000	3.7380	0.14668	0.56965	624.5	0.219	624.281	0.616	6242.81	0.002980	4.653	0.183
Day 1	0.1	0.00167	13:13:47	34.6	0.92593	4.3880	0.17219	0.59516	576.5	0.219	576.281	0.569	5762.81	0.003229	5.355	0.210
Day 1	0.1	0.00167	13:19:47	34	0.99834	4.9880	0.19573	0.61870	549	0.219	548.781	0.542	5487.81	0.003390	5.956	0.234
Day 1	0.1	0.00167	13:27:47	33.1	1.00000	5.8880	0.23105	0.65402	544.4	0.219	544.181	0.537	5441.81	0.003419	6.758	0.265
Day 1	0.1	0.00167	13:35:47	32.4	0.87500	6.5880	0.25852	0.68149	496.4	0.219	496.181	0.490	4961.81	0.003750	7.558	0.297
Day 1	0.1	0.00167	13:44:47	31.4	1.00000	7.5880	0.29776	0.72073	478.1	0.219	477.881	0.472	4778.81	0.003893	8.46	0.332
Day 1	0.1	0.00167	13:53:47	31	0.45198	4.4045	0.17283	0.59580	468.9	0.219	468.681	0.463	4686.81	0.003970	9.345	0.367
Day 1	0.1	0.00167	14:01:47	30.8	0.24420	3.2458	0.12737	0.55034	464.3	0.219	464.081	0.458	4640.81	0.004009	10.164	0.399
Day 1	0.1	0.00167	14:08:47	30.5	0.43860	4.8170	0.18902	0.61199	455.2	0.219	454.981	0.449	4549.81	0.004089	10.848	0.426
Day 1	0.1	0.00167	14:16:47	30.5	0.00000	1.9490	0.07648	0.49945	441.4	0.219	441.181	0.435	4411.81	0.004217	11.65	0.457
Day 1	0.1	0.00167	14:24:47	30.4	0.12453	2.8633	0.11236	0.53533	439.2	0.219	438.981	0.433	4389.81	0.004238	12.453	0.489
Day 1	0.1	0.00167	14:33:47	30.3	0.11086	2.8739	0.11277	0.53575	434.6	0.219	434.381	0.429	4343.81	0.004283	13.355	0.524
Day 1	0.1	0.00167	14:40:47	30.3	0.00000	2.1490	0.08433	0.50730	423.1	0.219	422.881	0.417	4228.81	0.004400	14.057	0.552
Day 1	0.1	0.00167	14:57:47	30.05	0.14680	3.3589	0.13181	0.55478	418.6	0.219	418.381	0.413	4183.81	0.004447	15.76	0.618

Day 1	0.1	0.00167	15:04:47	30	0.07133	2.9154	0.11440	0.53737	409.4	0.219	409.181	0.404	4091.81	0.004547	16.461	0.646
Day 1	0.1	0.00167	15:12:47	30	0.00000	2.4490	0.09610	0.51907	409.4	0.219	409.181	0.404	4091.81	0.004547	17.263	0.677
Day 1	0.1	0.00167	15:23:47	30	0.00000	2.4490	0.09610	0.51907	388.8	0.219	388.581	0.383	3885.81	0.004788	18.366	0.721
Day 1	0.1	0.00167	15:32:47	30	0.00000	2.4490	0.09610	0.51907	391.1	0.219	390.881	0.386	3908.81	0.004760	19.268	0.756
Day 1	0.1	0.00167	15:41:47	30	0.00000	2.4490	0.09610	0.51907	379.7	0.219	379.481	0.375	3794.81	0.004903	20.17	0.791
Day 1	0.1	0.00167	15:47:47	30	0.00000	2.4490	0.09610	0.51907	377.4	0.219	377.181	0.372	3771.81	0.004933	20.771	0.815
Day 1	0.1	0.00167	17:48:47	29.75	0.02065	2.8340	0.11121	0.53418	333.9	0.219	333.681	0.329	3336.81	0.005576	32.88	1.290
Day 1	0.1	0.00167	19:30:47	29.6	0.01468	2.9450	0.11556	0.53853	313.3	0.219	313.081	0.309	3130.81	0.005943	43.1	1.691
Day 2	0.1	0.00167	09:50:47	28.95	0.00755	3.5484	0.13924	0.56221	248.05	0.219	247.831	0.245	2478.31	0.007507	129.209	5.070
Day 2	0.1	0.00167	11:03:47	28.9	0.00684	3.5937	0.14102	0.56399	244.6	0.219	244.381	0.241	2443.81	0.007613	136.516	5.357
Day 2	0.1	0.00167	11:09:47	28.9	0.00000	3.5490	0.13926	0.56223	265.2	0.219	264.981	0.262	2649.81	0.007021	137.119	5.381
Day 2	0.2	0.00333	11:46:47	28.65	0.03466	4.0257	0.15797	0.58094	411.7	0.219	411.481	0.406	2057.41	0.009043	144.331	5.664
Day 2	0.2	0.00333	12:01:47	28.65	0.00000	3.7990	0.14907	0.57204	411.7	0.219	411.481	0.406	2057.41	0.009043	147.336	5.782
Day 2	0.2	0.00333	13:40:47	28.65	0.00000	3.7990	0.14907	0.57204	388.8	0.219	388.581	0.383	1942.91	0.009576	167.145	6.559
Day 2	0.2	0.00333	14:49:47	28.5	0.01085	4.0199	0.15774	0.58071	372.8	0.219	372.581	0.368	1862.91	0.009987	180.974	7.101
Day 2	0.2	0.00333	15:49:47	28.5	0.00000	3.9490	0.15496	0.57793	370.5	0.219	370.281	0.365	1851.41	0.010049	193	7.573
Day 2	0.2	0.00333	16:18:47	28.5	0.00000	3.9490	0.15496	0.57793	359.05	0.219	358.831	0.354	1794.16	0.010370	198.796	7.801
Day 2	0.2	0.00333	17:22:47	28.5	0.00000	3.9490	0.15496	0.57793	356.8	0.219	356.581	0.352	1782.91	0.010435	211.607	8.304
Day 2	0.2	0.00333	19:50:47	28.35	0.00506	4.1321	0.16214	0.58512	332.75	0.219	332.531	0.328	1662.66	0.011190	241.256	9.467
Day 3	0.2	0.00333	09:48:47	28	0.00209	4.4626	0.17512	0.59809	269.8	0.219	269.581	0.266	1347.91	0.013803	409.064	16.052
Day 3	0.2	0.00333	10:43:47	27.8	0.01814	4.7676	0.18708	0.61005	269.8	0.219	269.581	0.266	1347.91	0.013803	420.089	16.484
Day 3	0.2	0.00333	10:51:47	27.8	0.00000	4.6490	0.18243	0.60540	260.6	0.219	260.381	0.257	1301.91	0.014291	421.692	16.547
Day 3	0.5	0.00833	11:10:47	27.75	0.00620	4.7395	0.18598	0.60895	549	0.219	548.781	0.542	1097.56	0.016952	429.76	16.864
Day 3	0.5	0.00833	11:41:47	27.75	0.00000	4.6990	0.18439	0.60736	528.4	0.219	528.181	0.521	1056.36	0.017613	445.301	17.474
Day 3	0.5	0.00833	12:59:47	27.7	0.00128	4.7574	0.18668	0.60965	507.8	0.219	507.581	0.501	1015.16	0.018328	484.297	19.004
Day 3	0.5	0.00833	13:23:47	27.75	0.00000	4.6990	0.18439	0.60736	505.5	0.219	505.281	0.499	1010.56	0.018411	496.321	19.476
Day 3	0.5	0.00833	14:07:47	27.65	0.00454	4.8287	0.18948	0.61245	498.7	0.219	498.481	0.492	996.962	0.018662	518.37	20.341
Day 3	0.5	0.00833	15:16:47	27.65	0.00000	4.7990	0.18831	0.61129	475.8	0.219	475.581	0.469	951.162	0.019561	552.947	21.698
Day 4	0.5	0.00833	18:15:47	26.9	0.00093	5.5551	0.21798	0.64095	333.9	0.219	333.681	0.329	667.362	0.027879	1363.451	53.502

$S_{wi,after}$	0.35905

Table D8: Results from post-treatment flooding with oil to establish $S_{wi,after}$

Cumulative volume of oil injected when the first drop of oil was observed in the separator	ml	9.345
Outlet tubing volumes up to the tip of inner tube in separator	ml	6.539
Cumulative volume of oil injected when oil breakthrough occurred from the core	ml	2.806
Time corresponding to the oil breakthrough from datalog	Day 1	12:48:24
Pore volumes injected at oil breakthrough	PV	0.110108

Table D9: Calculation of pore volumes injected at oil breakthrough during post-treatment flooding with oil

CALCULATION OF RRF_o				
Values from post-treatment flooding of oil			Using experimental values of relative permeability for water-wet Berea core	
S_o	S_w	$k_{o,\ after}$	$k_{o,\ before}$	RRF_o
fraction	fraction	D	D	$k_{w,\ before}/k_{w,\ after}$
0.42297	0.577029	0.001000	-0.0072	-7.2253
0.46566	0.534336	0.002337	0.0247	10.5873
0.47155	0.528450	0.002304	0.0326	14.1504
0.48921	0.510791	0.002450	0.0604	24.6628
0.50490	0.495095	0.002624	0.0899	34.2553
0.52452	0.475475	0.002712	0.1320	48.6591
0.54807	0.451931	0.002885	0.1884	65.2946
0.56965	0.430349	0.002980	0.2440	81.8718
0.59516	0.404843	0.003229	0.3121	96.6738
0.61870	0.381298	0.003390	0.3749	110.5912
0.65402	0.345982	0.003419	0.4641	135.7331
0.68149	0.318514	0.003750	0.5249	139.9812
0.72073	0.279274	0.003893	0.5912	151.8581
0.59580	0.404196	0.003970	0.3139	79.0611
0.55034	0.449662	0.004009	0.1941	48.4114
0.61199	0.388009	0.004089	0.3572	87.3442
0.49945	0.500550	0.004217	0.0792	18.7786
0.53533	0.464671	0.004238	0.1572	37.0810
0.53575	0.464255	0.004283	0.1582	36.9254
0.50730	0.492702	0.004400	0.0947	21.5325
0.55478	0.445224	0.004447	0.2054	46.1779
0.53737	0.462628	0.004547	0.1621	35.6430
0.51907	0.480930	0.004547	0.1197	26.3352
0.51907	0.480930	0.004788	0.1197	25.0094
0.51907	0.480930	0.004760	0.1197	25.1574
0.51907	0.480930	0.004903	0.1197	24.4237
0.51907	0.480930	0.004933	0.1197	24.2757
0.53418	0.465822	0.005576	0.1544	27.6942
0.53853	0.461467	0.005943	0.1649	27.7438
0.56221	0.437790	0.007507	0.2245	29.9064
0.56399	0.436009	0.007613	0.2292	30.0993
0.56223	0.437765	0.007021	0.2246	31.9852
0.58094	0.419060	0.009043	0.2740	30.2970
0.57204	0.427955	0.009043	0.2503	27.6809
0.57204	0.427955	0.009576	0.2503	26.1404
0.58071	0.419286	0.009987	0.2734	27.3725
0.57793	0.422069	0.010049	0.2660	26.4646

0.57793	0.422069	0.010370	0.2660	25.6462
0.57793	0.422069	0.010435	0.2660	25.4854
0.58512	0.414885	0.011190	0.2852	25.4826
0.59809	0.401914	0.013803	0.3200	23.1817
0.61005	0.389946	0.013803	0.3520	25.5026
0.60540	0.394601	0.014291	0.3396	23.7625
0.60895	0.391049	0.016952	0.3491	20.5927
0.60736	0.392639	0.017613	0.3448	19.5787
0.60965	0.390348	0.018328	0.3509	19.1487
0.60736	0.392639	0.018411	0.3448	18.7298
0.61245	0.387551	0.018662	0.3584	19.2042
0.61129	0.388715	0.019561	0.3553	18.1638
0.64095	0.359047	0.027879	0.4322	15.5024

Table D10: Results from the calculation of RRF_o

CALCULATION OF RRF_w		
$K_{w,\ before}$	D	0.046361
$K_{w,\ after}$	D	0.000839
RRF_w	$K_{w,\ before}/K_{w,\ after}$	55.26543

Table D11: Results from the calculation of RRF_w

Experimental values of relative permeability for water-wet Berea core				
Reference Permeability Value			k_o(Swi)	0.631612
f_w	S_w	k_{rw}	k_{ro}	$k_o = k_{ro} * k_o$(Swi)
0	0.2360	0	0.9923	0.6268
0.008	0.3936	0.0034	0.5355	0.3382
0.06	0.4627	0.0140	0.2771	0.1750
0.22	0.5084	0.0251	0.1125	0.0711
0.5	0.5344	0.0296	0.0374	0.0236
0.78	0.5503	0.0306	0.0109	0.0069
0.94	0.5561	0.0288	0.0023	0.0015
0.992	0.5566	0.0295	0.0003	0.0002
1	0.5585	0.0290	0	0
1	0.5701	0.0351	0	0
1	0.5779	0.0376	0	0
1	0.5872	0.0398	0	0

Table D12: Experimental values of relative permeability for water-wet Berea core